The Dissertation Committee for Nathaniel Spencer Pope
certifies that this is the approved version of the following dissertation:

Genetic mark-recapture provides insights into bee movement and plant reproductive success

Committee:

Shalene Jha, Supervisor

Thomas Juenger

Timothy Keitt

Craig Linder

Peter Mueller

Genetic mark-recapture provides insights into bee movement and plant reproductive success

by

Nathaniel Spencer Pope,

DISSERTATION

Presented to the Faculty of the Graduate School of

The University of Texas at Austin

in Partial Fulfillment

of the Requirements

for the Degree of

DOCTOR OF PHILOSOPHY

THE UNIVERSITY OF TEXAS AT AUSTIN

May 2019

For Michael D. Pope and Rebecca S. Lemon.

Acknowledgments

I wish to thank my advisor Shalene Jha, who has provided me with innumerable opportunities and invaluable advice; while still allowing me the complete freedom to form my own line of scientific inquiry. Much of the research in this dissertation could not have occurred without the collaboration of Antonio R. Castilla and Rodolfo Jaffé, both talented scientists and wonderful friends. Nor could I have completed this work without the assistance and friendship of other graduate students in the Jha Lab at the University of Texas at Austin: Kim Ballare, Sarah Cusser, Nathan Leclear, and Megan O'Connell – thank you all. The National Science Foundation provided funding via a predoctoral fellowship, as did the Department of Integrative Biology, the Department of Statistics and Data Sciences, and the Graduate School at the University of Texas at Austin. The Texas Advanced Computing Center provided access to computing and technical resources, without which this research would have been infeasible. Most of all I wish to thank my parents, Michael D. Pope and Rebecca S. Lemon, and my extended family for the tremendous amount of support and encouragement they have given me over the years.

Genetic mark-recapture provides insights into bee movement and plant reproductive success

by

Nathaniel Spencer Pope, Ph.D.
The University of Texas at Austin, 2019

Supervisor: Shalene Jha

Genetic data offer a means of inferring the contemporary and historical movement of organisms, in study systems where direct observation is infeasible. However, the use of genetic markers as a proxy for the direct observation of movement presents its own challenges: the observed quantities (genotypes) are fundamentally stochastic. In many cases, movement can only be inferred from molecular markers by exploiting familial relationships among organisms. From a statistical perspective, this poses a unique challenge that requires linking ecological or behavioral hypotheses to an inherently noisy and constrained observation process. This thesis develops and applies statistical models to answer basic questions about movement in bees – a group of organisms that have tremendous ecological and commercial importance but are too small and too motile to track directly – by using molecular markers and exploiting family relationships among bees and among the plants they pollinate. Thematically, this thesis is organized into five chapters split across three sections. The first

section (chapters 1 and 2) concerns bee foraging movements in times of food scarcity, and employs as a study system a common species of bumble bee in the Californian chaparral. The second section (chapters 3 and 4) concerns the spatial context of plant reproductive success, and uses as a study system a widely distributed tropical understory tree that is pollinated by a functionally diverse bee community. The fifth chapter concerns constraints on dispersal movements, and develops a statistical methodology for inferring how environmental heterogeneity influences migration rates, given patterns of extant genetic variation.

Table of Contents

List of Tables

List of Figures

Chapter 1

Seasonal food scarcity prompts long-distance foraging by a wild social bee

The research in this chapter represents a collaboration between the author and Dr. Shalene Jha, and as of the time of writing has been published as [Pope and Jha, 2018].

Foraging is an essential process for mobile animals and its optimization serves as a foundational theory in ecology and evolution; however, drivers of foraging are rarely investigated across landscapes and seasons. Using a common bumble bee species from the Western US (*Bombus vosnesenskii*), we ask if seasonal decreases in food resources prompt changes in foraging behavior and space use. We employ a unique integration of population genetic tools and spatially-explicit foraging models to estimate foraging distances and rates of patch visitation for wild bumble bee colonies across three study regions and two seasons. By mapping the locations of 669 wild-caught individual foragers, we find substantial variation in colony-level foraging distances, often exhibiting a 60-fold difference within a study region. Our analysis of visitation rates indicates that foragers display a preference for high-cover destination patches and forage significantly further for these patches, but only in the summer,

when landscape-level resources are low. Overall, these results indicate that an increasing proportion of long-distance foraging bouts take place in the summer. As pollinators, the foraging dynamics of wild bees are of urgent concern given the potential impacts of global change on their movement and services. The behavioral shift towards long-distance foraging with seasonal declines in food resources suggests a novel phenologically-directed approach to landscape-level pollinator conservation and increased evaluation of late-season floral resources.

1.1 Introduction

Across the globe, pollinators are critical for the reproduction of more than 87% of wild plant species [Ollerton et al., 2011] and 60% of cultivated crop species [Klein et al., 2007], worth over $200 billion in enhanced crop yields [Gallai et al., 2009]. Bees, which consume pollen as larvae and have evolved a diverse array of pollen-collection strategies, are one of the most effective and ubiquitous groups of pollinators. Recent reviews have further revealed that "wild" bees (i.e., those species that are not intentionally bred and transported by humans) enhance the fruit set of crops, regardless of the presence of managed colonies of domesticated European honey bees [Garibaldi et al., 2013]. However, both managed and unmanaged bee species depend on pollen and nectar for survival and reproduction [Michener, 2000], and the availability of these floral resources is a function of the composition and phenological state of plant communities. Systematic changes in the presence, abundance, and reproductive phenology of pollen-producing plant species – for example,

due to shifting climatic conditions or human modification of landscapes – are therefore likely to have a strong influence on populations of bees. Recent work has highlighted the vulnerability of wild bees to urbanization [Jha, 2015], agricultural intensification [Kennedy et al., 2013], and climate change [Memmott et al., 2007], all forces that alter landscape floral cover and composition. To determine how these broad drivers of vegetation structure influence bees – and other animals that depend directly on floral rewards for survival and reproduction – it is essential to understand the relationship between the temporal and spatial availability of floral resources and the foraging patterns of wild pollinators.

Economic models of foraging provide a mechanistic basis for understanding how animals respond to heterogeneous resources in time and space, by describing the behaviors that are optimal with regards to the acquisition of a currency under a set of constraints [Stephens and Krebs, 1986]. At their most basic, economic foraging models weigh the time needed to travel to and exploit a geographically distinct set of resources (a "patch") against the energetic gains associated with doing so. The decision to visit a patch (and when to leave it) depends on the perceived utility of the patch to the animal, relative to the utility that could be realized by moving on [Stephens and Charnov, 1982]. Variation in utility presumably depends on temporal costs and energetic rewards: the shape of this function reflects a hypothesis about the deterministic currency that motivates foraging behavior [Bergman et al., 2001]. Animals that provision nests must both meet their own energetic needs

and collect a sufficient quantity of food for later use, and can only carry a finite amount of provisions during a single foraging bout. For these animals, the perceived utility of a patch at a given point in time depends not only on the amount of potential food it contains, but also on the energetic state of the individual, the energetic state of the nest, and the remaining capacity to carry provisions [McNamara and Houston, 1997]. The key assumption underlying these models is that the animal makes decisions so as to maximize utility over the course of a foraging bout.

Over the long term, a series of such decisions results in a spatial probability density that can be loosely conceived of as the frequency of occupancy (e.g. a home range or foraging kernel; [Moorcroft and Barnett, 2008]). At a given point in time, the spatial distribution of resources will influence decisions about visitation; temporal fluctuations in resource availability may therefore change the structure of the foraging kernel. For example, during periods when resources are abundant and relatively easy to locate, the utility of a given patch may depend strongly on its proximity to the nest site, and a relatively small spatial area may be utilized by the forager (Fig. 1.1, A). In contrast, during periods when resources are sparse, the demand for patches of sufficient quality may dominate constraints on the distance traveled (Fig. 1.1, E). Both possibilities are extremes of a behavioral gradient, with consequences for space use (Fig. 1.1, A-E). Essentially, when foraging decisions can be accurately described by an economic model, it is reasonable to assume that "optimal behavior" is dynamic and changes according to the needs of the animal and its

perception of resource availability at different spatial scales.

The ability to assess resources at multiple spatial scales and modulate foraging behavior based on current state may be particularly critical for animals that need to forage on resources that fluctuate over time and across landscapes, such as wild bees and other pollinators. Many food resources exhibit a seasonal peak and decline [Forrest and Miller-Rushing, 2010], including nectar and pollen biomass in terrestrial plant communities [Rathcke and Lacey, 1985]. The seasonal phenology of plant communities is not static across years: for example, the onset, end, and magnitude of the flowering period can shift independently and unpredictably with regional and local climate [CaraDonna et al., 2014]. The shapes of these phenological curves, and their consistency across space and between years, have implications for the population dynamics of herbivores, seed dispersers, pollinators, and a variety of organisms that depend on plant biomass (reviewed in [Elzinga et al., 2007]). For bees, the availability of food resources is determined by the abundance and phenological state of flowering plants, and can vary dramatically across short temporal and geographic distances (reviewed in [Goulson, 1999]). Because nectar and pollen collection are limited by pollinator crop size and external pollen storage space, many pollinators must make multiple foraging trips, which can be costly given the physiological challenges of foraging in a landscape (e.g. thermoregulation, reviewed in [Heinrich, 1975]). To efficiently locate and utilize resources across multiple trips, pollinators (like all foraging animals) must integrate and learn from environmental cues, as well as the behavior of competitors (and siblings

in the case of social insects; [Raine and Chittka, 2008], [Dawson and Chittka, 2012]). While foraging patterns across seasons and landscapes could provide insight into how variable environments influence the movements of wild pollinators, past studies have focused on small spatial scales [Biernaskie et al., 2009], simulated landscapes [Dreisig, 1995], or single time periods [Carvell et al., 2012, Jha and Kremen, 2013], largely due to methodological challenges and a historical emphasis on the theoretical aspects of optimal foraging. Thus, despite the potential to understand the spatial and temporal drivers of pollinator movement and service at large spatial and temporal scales, the foraging dynamics of wild pollinators at these scales remains unknown.

In this study, we examine the foraging patterns of the Yellow-faced bumble bee, *Bombus vosnesenskii* (Rad), across fluctuating resource landscapes that each span several kilometers in the chaparral of central California. Bumble bees are generalist central-place foragers and are among the most important pollinators contributing to the stability of plant-pollinator networks [Memmott et al., 2004]. They are also among the most effective native pollinators in temperate agroecosystems [Kremen et al., 2002] and have served as model systems in insect foraging ecology for decades [Heinrich, 1975], including a number of recent analyses that use molecular tools to examine foraging distance by sampling colonies along a series of sampling points [Knight et al., 2005, Carvell et al., 2012, Jha and Kremen, 2013, Redhead et al., 2016]. While molecular methods have shed light on wild bee foraging response to floral resources [Redhead et al., 2016], these approaches have never been employed

across phenological periods and multiple landscapes, and the statistical methods used to analyze these data have not accounted for spatial constraints imposed by sampling design. We use extensive field-based vegetation surveys, molecular tools, and bumble bee sib-ship identities to investigate if the distribution of foraging siblings in high- and low-resource periods is consistent with a temporal shift in foraging strategy. First, we ask if foraging bumble bees become more selective with regards to the amount of resources within patches and travel time, as the average density of floral resources in the landscape declines. We employ Bayesian inference and a spatially-explicit framework to model the density of foraging bees as a function of an unobserved utility that reflects the spatial distribution of colonies and floral resources. Second, we ask if foraging siblings travel further to reach patches with high floral cover during low-resource periods, as a consequence of increased patch selectivity. We use a combination of regression and simulation to compare the spatial dispersion of foraging siblings to a null model wherein bees forage without regard for spatial location or floral cover. Our results indicate that wild bumble bees modulate their foraging behavior and space-use across seasons, as evidenced by significantly longer foraging distances and significantly greater preferences for high density resource patches as landscape-level resources decline. By revealing the time periods and resource contexts wherein pollinators shift to long-distance movement, we highlight the late-season phenological period as particularly challenging for wild pollinator foraging and suggest a phenologically-targeted approach to floral restoration efforts.

1.2 Materials and Methods

Study system. The study was conducted within Napa County in central California (38.6801,-122.4130 NW corner, 38.5589,-122.2469 SE corner). Foraging bumble bees and flowering plant communities were sampled across three large transects that each spanned 3km and were separated by 7.03 km on average (± 4.37 km). Across all three study areas, the landscape is dominated by oak woodland and chaparral; past studies have indicated that these vegetation types provide high quality nesting habitat for bumble bees [Jha and Kremen, 2013]. In this region, the plant community exhibits a peak in flower density from March-May and then a marked reduction in flower density (by more than 50%) from June-July [Williams et al., 2012] (appendix section 1.5). Dominant flowering species include *Heteromeles arbutifolia* (Rosaceae), *Grindelia camporum* (Asteraceae), *Pickeringia montana* (Fabaceae), *Eschscholzia californica* (Papaveraceae), and *Acmispon glaber* (Fabaceae). The study animal, *B. vosnesenskii,* is a univoltine bumble bee species with colonies that are founded by a single queen and can eventually become as large as 100-300 workers. Past research in the region indicates that typical *B. vosnesenskii* colonies are close to peak size (in terms of mass) by late spring [Williams et al., 2012, Crone and Williams, 2016], allowing for the extensive forager sampling required in this study. In this region, *B. vosnesenskii* colonies actively forage from spring until mid-summer, and experience both high- and low- resource periods.

Pollinator sampling and molecular analysis. To measure the spatial distribution of foraging siblings across seasons, we collected foraging individuals and identified sibling relationships by molecular methods. We sampled 669 *B. vosnesenskii* worker bees for DNA across two time periods, from May-June (high bloom) and June-July of 2011 (low bloom). Along each 3km transect we established a series of seven sampling sites, consisting of five sites that were separated by 250m and two sites that were separated by 1km from either end (to capture long-distance foraging events; Fig. 1.2). Sites were sampled by collecting all *B. vosnesenskii* foragers within a 25m radius from the site center between 8am and 5pm and then storing these bees in ethanol for later DNA extraction. Each bee was assigned to the center of the site where she was collected. Thus, across the three transects, DNA was obtained from a mean of 15.92 ($\pm$ 1.03 SE) bees per site per time period (appendix section 1.5).

DNA was extracted from the tarsal segment of each bee sample and screened at 12 microsatellite loci, B96, B100, and B119 [Estoup et al., 1995] , and BT33, BT43, BT65, BT124, BT125, BT128, BT131, BT132, and BT136 [Stolle et al., 2009], which are located on 10 different chromosomes, based on the *B. terrestris* genome v1.1 [Stolle et al., 2011]. Multiplex polymerase chain reactions (PCRs) were performed in a final volume of 20μL, containing approximately 2ng of DNA, 2μL of 10x PCR buffer, 1.5mM MgCl2, 300μM of each dNTP, 1U of Taq Polymerase and 0.25μM of each primer. The thermal cycle began with a 5-min denaturation step at 95°C, and was followed by 37 cycles: 30s at 94°C, 60s at the locus-specific annealing temperature, and 30s at

72°C, followed by a final extension at 72°C for 20 min. One primer from each pair was labeled with 6-FAM, NED, VIC, or PET, and genotyped on an ABI 3730 Sequencer. Alleles were scored manually using GENEMARKER (Softgenetics) and only samples with ≥ 8 loci scored per individual were included. Full siblings collected from each study region were assigned to colonies using COLONY 2.0 [Wang, 2004]. In this assignment, the genotyping error rate was set to 0.001, based on error documented in the lab and in previous studies [Jha and Kremen, 2013] (population genetic details in appendix section 1.5).

Floral resource surveying. To estimate the distribution of floral resources within and across sampling sites, we conducted vegetation surveys along the transects in both time periods. Each sampling site represents a patch of floral resources (a total of 21 patches per time period), and within 50m of each sampling site we surveyed floral resources within 30 randomly placed 1m by 1m sampling quadrats. All locations on the transect that were halfway between adjacent sampling sites (a total of 18 inter-patches per time period) were also surveyed with 30 randomly placed 1m by 1m sampling quadrats. Floral survey data from patches and inter-patches were simultaneously analyzed to determine landscape-level floral cover. Specifically, floral cover was calculated based on inflorescence counts per plant species multiplied by the petal area per inflorescence (cm^2) per species, summed across all plant species in a quadrat. Thus, patch floral cover was calculated as the mean floral cover (cm^2) across quadrats within a single sampling site, while landscape floral

cover was calculated as the mean floral cover (cm^2) across patches and the area between the patches (as per [Jha and Kremen, 2013]). The mean floral cover within patches was highly correlated with the coefficient of variation of within-patch floral cover and with floral species richness (Pearson correlation of 0.79 and 0.77 respectively). Thus, there was a single measured axis of patch quality in this study: at the low extreme of this axis were poor quality patches with a low overall density of flowers, a sparse distribution of flowers, and few species of flowers. In our subsequent analyses, we only included floral cover as an indicator for patch quality as this exhibited the most variation between patches.

Statistical analysis of patch visitation and selectivity. To assess how foraging selectivity with regards to within-patch floral density and travel distance changed throughout the season, we employ Bayesian inference and directly model the occurrence of colony mates at transect sites. The colony locations are unknown and would be exceptionally difficult to locate directly, and so are treated as nuisance parameters that are estimated along with the parameters of interest. Our approach has similarities to that used by [Royle et al., 2009] for camera-trapping studies. In this framework, individual bees that are the sole representative of their colony are informative and thus are included in the analysis.

Let the vector $Y_{jkl} = [y_{1jkl}, \ldots, y_{7jkl}]$ be counts of captured foragers belonging to the jth colony, along a transect in the kth landscape in the lth

sampling round. Y_{jkl} is a multinomial sample of size n_{jkl}, with associated multinomial probabilities $p_{jkl} = [p_{1jkl}, \ldots, p_{ijkl}, \ldots, p_{7jkl}]$ that represent the probabilities of collection for the colony across patches on the transect. We assume that the distribution of bees among patches is deterministic and is driven by the distance d_{ij} to the bee's colony, and the floral cover x_{ikl} at the ith patch. In our model, the degree to which a bee prefers higher floral cover and the degree to which a bee prefers closer patches are represented by time- and landscape-specific parameters B_{kl} and Λ_{kl} respectively. The odds of collecting a bee from patch i rather than another patch v on the same transect are:

$$\frac{p_{ijkl}}{p_{vjkl}} = \exp\left\{\Lambda_{kl}\left(d_{ij} - d_{vj}\right) + B_{kl}\left(x_{ikl} - x_{vkl}\right) + \left(\epsilon_{ik} - \epsilon_{vk}\right)\right\}$$

And so the probability that the bee is collected on patch $\{i, k, l\}$ is:

$$\frac{\exp\left\{d_{ij}\Lambda_{kl} + x_{ikl}B_{kl} + \epsilon_{ik}\right\}}{\sum_{v=1}^{7}\exp\{d_{vj}\Lambda_{kl} + x_{vkl}B_{kl} + \epsilon_{vk}\}}$$

Where ϵ are Gaussian, patch-specific effects with standard deviation τ that capture the "attractiveness" of a patch that is not explained by distance from colony or floral cover.

Foraging preferences are allowed to change with the amount of forage available in the landscape. We model Λ_{kl} and B_{kl} as linear functions of the average forage cover $\bar{x}_{kl}$ of landscape k at time point l,

$$\Lambda_{kl} = \lambda_0 + \bar{x}_{kl}\lambda_1$$

$$B_{kl} = \beta_0 + \bar{x}_{kl}\beta_1$$

Note that $\bar{x}_{kl}$ is calculated using locations in the landscape that are additional to the patches on the transect. This simple model captures the foraging behaviors described in Figure 1.1. The composite parameter Λ controls how far bees are willing to travel from their colony, with reference to average landscape floral cover, and regardless of the floral cover of the destination: if λ_1 is negative, then bees will travel shorter distances in resource-rich landscapes. The composite parameter B controls the preference of bees for the floral cover of patches, with reference to average landscape floral cover: if β_1 is negative, then the preference for floral cover is reduced when average landscape floral cover is high. The colony locations are treated as unknowns and are estimated from the data simultaneously with the other parameters. There is a dependence in the sampling distributions of B, Λ, and the colony locations (Fig. 1.2). For example, consider a transect of seven patches of varying floral cover (Fig. 1.2, A-B points, size indicates floral cover). Three siblings are collected, one each from the three inner most patches (Fig. 1.2, A-B, blue points indicate a capture), and for ease of exposition the parameter B is fixed to a constant. If the probability of foragers' locations are not influenced by floral cover ($\Lambda = 0$), then the conditional distribution of the colony location is a ridge centered at the middle of the transect (Fig. 1.2, A). Alternatively, if bee location is strongly influenced by floral cover ($\Lambda \gg 0$), then the conditional distribution of the colony location 'flattens' and shifts (Fig. 1.2, B); bees found at low-cover locations carry more information about the colony location than do bees at high-cover locations. When the joint posterior of Λ and the colony location

are estimated for these toy data by Markov chain Monte Carlo (MCMC), it is evident that the marginal distributions for Λ and the colony location are a compromise between these extremes (Fig. 1.2).

Because our data are collected along a linear transect, they carry more information about the relative foraging distance than about absolute foraging distance. Therefore, we use prior data to inform our inference about absolute foraging distances. To capture a decrease in visitation with increasing distances from the colony, we assume an exponential prior distribution on foraging ranges, $p\left(d_{ij}\right) = 0.6^{-1} \exp\left\{-0.6^{-1} d_{ij}\right\}$, where d_{ij} is the distance to patch i from colony j. Based on direct measurements of the maximum flight distance in *Bombus* spp. with radio tracking [Hagen et al., 2011], we set the rate parameter of this prior distribution to 0.6^{-1}. This prior implies that 50% of the time, a foraging bee will be less than 0.4 km distant from her colony, and 95% of the time a foraging bee will be less than 2.7 km away from the colony. Because this is an informative prior, and the weight of the transmitters used by Hagen et al. [Hagen et al., 2011] impacted flight ability, we perform a sensitivity analysis (see appendix part 1.6) by systematically varying the rate parameter of the prior and reassessing our conclusions. The spatial location $z_j = \{z_1, z_2\}$ of the jth colony is assumed to arise from a two-dimensional homogeneous Poisson process. In other words, prior to any transect being established, all potential locations for colonies are considered equiprobable. We use vague priors for the remaining parameters: for $\lambda_0, \lambda_1, \beta_0, \beta_1$ we use Gaussian priors with mean 0 and variance 10, after scaling and centering floral cover at land-

scape and patch levels. For the standard deviation τ of site-specific random effects ϵ, we use half-Gaussian priors with variance 10 [Gelman, 2006]. Using the Bayesian platform JAGS [Plummer, 2003], we ran four Markov chains for 150,000 iterations and discarded the first 50,000 iterations. We thinned the remainder to every 10th sample, and assessed convergence visually and with the scale-reduction factor of [Gelman and Rubin, 1992].

Statistical analysis of foraging range. The model of patch visitation described previously provides estimates of foraging distance, defined as the distance from the collection location to the colony for each bee. To determine if seasonal variation in foraging selectivity leads to seasonal variation in foraging range, we calculate the correlation between the estimated foraging distances and the floral cover of the visited patch, separately for each resource period. To estimate the posterior distribution of the correlation coefficient while integrating over uncertainty in colony locations, we calculate Pearson's ρ across MCMC samples (appendix section 1.6).

The patch visitation model relies on assumptions about how patch utility changes with travel distance, patch floral cover, and landscape floral cover. The estimates of foraging distance calculated from this model depend on these assumptions. To provide a second line of evidence for a relationship between foraging distance and patch floral cover that is independent of the patch visitation model, we use the observed dispersion of siblings across the transects. The dispersion of siblings in space provides information about the distance

traveled by individual foragers. Specifically, for each sibling group we calculate a 'minimum foraging distance': the minimum of the set of distances from each sibling to their centroid. It is easy to see that this is a lower bound on the maximum foraging distance for the sibling group, as one of the siblings had to travel at least that far. We used a linear mixed effects model (lme4 package, [Bates et al., 2015]) to investigate how patch floral cover, landscape floral cover, and an interaction between patch and landscape floral cover (fixed factors) impact minimum foraging distance, while including random deviations across sampling events (random intercepts for sampling date nested within study region). Because bees were collected at discrete locations along a transect, there are a finite number of possible values for the distance between colony mates. Thus, it is possible that the spatial arrangement of patch cover within a site could induce a pattern where the largest distances on the transect occur between higher-cover patches, resulting in a spurious correlation between floral cover and foraging distance. Therefore we compare our fitted curves to those generated from a null model in which colony-mates occur uniformly at random across transect locations. We simulated data from this null model, repeated the model fitting process on each simulated dataset, and compared the distribution of these null simulations to our observed results (detailed description in appendix part 1.7). For all analyses, foraging distances were square root transformed and all continuous explanatory variables were centered. All minimum foraging distance analyses were conducted using the R language [R Development Core Team, 2011].

1.3 Results

We collected 110 sibling groups over the course of the study, but the majority of captured bees had no siblings (appendix section 1.5). Landscape-level floral cover declined substantially from the early season (mean = 252.54 $cm^2/m^2 \pm 21.18$) to the late season (mean = 38.86 $cm^2/m^2 \pm 9.64$, appendix section 1.5), and we found a significant difference in the selectivity of foraging bees with regards to patch floral cover between the two seasons. Our analysis of patch visitation revealed that foraging bees exhibited a strong preference for patches with high floral cover as the average floral density in the landscape declined (Table 1.1, Fig. 1.3). We estimated little preference for floral cover in the early season (posterior mean of preference parameter B averaged across sites: 0.14, 95% credibility interval -0.28 to 0.57), but found the converse in the late season (posterior mean of B averaged across sites: 2.16, 95% CI 1.42 to 2.94). Despite the large reduction in floral cover from the early to the late season, colony numbers and genetic diversity metrics did not decline ($P > 0.539$ for all tests, appendix part 1.5). Specifically, we documented a recapture-based estimate of 645.7 ($\pm$ 34.9) colonies per region for the first time period and 661.3 ($\pm$ 15.1) colonies per region in the second time period.

When landscape-level floral cover was low, bees traveled further from the colony to reach patches of high floral cover. The seasonal dichotomy in preference found in the patch visitation analysis translated into a positive correlation between destination patch floral cover and the estimated distance traveled to the patch in the late-season when landscape-level floral cover was

low (posterior mean of correlation: 0.39, 95% CI 0.19 to 0.54), and no correlation in the early-season when landscape-level floral cover was high (posterior mean of correlation: 0.02, 95% CI -0.10 to 0.16; appendix section 1.6). Additionally, we found that foraging siblings were more spatially dispersed on average when landscape-level floral cover was low, and that greater dispersion was associated with visitation to patches with high floral cover. Specifically, for the minimum foraging distance analysis, the coefficients revealed a positive effect of destination patch-level floral cover (coefficient = 8.388, $P = 0.015$), a negative effect of landscape-level floral cover (coefficient = -13.141, $P < 0.001$), and a negative effect of the interaction between these two factors (coefficient = -6.510, $P = 0.006$, Table 1.2, Fig. 1.4). These results were not an artifact of forager density, floral distribution, or sampling design; in repeated simulations from a null model where the spatial distribution of colony-mates was uniformly random, we found no inherent relationship between foraging distance, patch floral cover, and landscape-level floral cover (Fig. 1.4 null confidence bounds, appendix section 1.7). Estimated foraging distance varied substantially across landscapes and time periods. The observed minimum foraging distance for colonies varied from 25m – 1500m (mean = 357.4 ± 51.6 m, Fig. 1.4), and the estimated foraging distances for individuals from the patch visitation analysis varied from 118m – 3175m (mean = 453.7 ± 15.0 m).

1.4 Discussion

Seasonal variation in food resource availability is commonly experienced across animal groups, and patterns of resource selection can provide critical insight into the behavioral mechanisms that animals use to cope with environmental heterogeneity and food scarcity [Boyce and McDonald, 1999]. Nevertheless, understanding patterns of resource selection across large spatial scales is a challenging and complex: the accessibility of food resources to animals depends on physical, behavioral, and cognitive constraints on movement [Moorcroft, 2012]. Here, we document a seasonal increase in space use (foraging area) by bumble bees, driven by a shift in foraging strategy between resource-rich environments in the late spring and resource-poor environments in the summer. We found that as floral resources seasonally declined in abundance, *B. vosnesenskii* workers became more selective foragers with regards to patch floral density. In the late season when floral resources were relatively scarce, bees consequently traveled longer distances to reach relatively dense patches of flowers despite the energetic costs associated with long distance foraging. Within the context of the foraging behavior of wild bees, these findings provide a temporal compliment to molecular studies that have used whole-landscape sampling approaches to map colonies and measure foraging distance of bumble bee siblings [Redhead et al., 2016] and a spatial compliment to studies monitoring foraging duration [Westphal et al., 2006], all of which provide evidence for increased foraging effort in landscapes with sparse resources.

Optimal foraging theory generally predicts that foragers should adapt to heterogeneity in the distribution of food resources by concentrating their time on areas of relatively high densities of food [Arditi and Dacorogna, 1988]. Motivated by this prediction, the first aim of this study was to determine if the selectivity of foraging bees for patches varied with seasonal changes in the distribution of floral resources. We found that foraging bumble bees concentrated on patches with relatively higher floral resource densities during the resource-poor late season, but showed no such preference during the early season when floral resources were abundant (Fig. 1.1E, Fig. 1.4). We conjecture that this apparent difference in foraging strategy is due to diminishing returns for foragers with increasing patch floral cover. To a forager, the perceived utility of a patch may depend non-linearly upon the density of resources it contains. Animals that collect resources to provision a nest have only a finite carrying capacity, and bumble bees in particular are limited by crop and corbicula size (for nectar and pollen, respectively). When landscape-level resources are abundant, the energetic rewards that patches offer are likely effectively equivalent beyond a threshold of resource density determined by a bee's storage capacity. Second, risk-averse behavior can create a constraint on the amount of time spent foraging within a patch (e.g. due to risk of predation) by similarly imposing a threshold beyond which variation in resource density will likely have little influence on potential rewards [Kotler and Blaustein, 1995]. As a consequence, in environments where the average within-patch resource density likely exceeds this threshold, there will be little variation in utility

among patches and little advantage to selective behavior. Finally, 'selective behavior' must be defined with reference to variation in resources at a particular spatial scale [Utsumi et al., 2009]. In the context of this study, the simplest dichotomy in spatial scale is variation in resource density within- and between-patches. When resources are abundant across large spatial scales, such that patches are all of a relatively high resource density, then fewer patches need to be visited during a bout, and foraging efficiency may be better maximized by selective behavior within patches [Biernaskie et al., 2009, Laca et al., 2010].

In a heterogeneous and resource-poor landscape, dense clusters of resources should occur relatively infrequently. Under a foraging strategy that prioritizes visitation to areas of high resource density, a central place forager would need to travel further on average. Thus, the second aim of this study was to determine if the spatial area utilized by foragers increased as a consequence of selective foraging behavior. Our results suggest that patches of relatively high floral densities attracted foraging bumble bees from much greater distances than did small patches, but only when landscape-level resources were sparse. This trend was a consequence of an increasing preference for patches with relatively high floral cover, and resulted in a greater dispersion of siblings across space at the colony level. An increase in foraging range associated with food scarcity has been frequently observed in environments where resources are heterogeneously distributed (e.g. in passerine birds, [Siffczyk et al., 2003]; seals, [Breed et al., 2009]; deer, [Morellet et al., 2013]), but it is not the only possible behavioral response and it has critical consequences

for the survival and longevity of individuals. Long distance foraging is an energetically costly activity to maintain [Heinrich, 1975]. Periods of resource scarcity often coincide with difficult conditions (e.g. winter, drought) that can exacerbate the costs of traveling long distances by increasing environmental stress and susceptibility to disease [Nelson and Demas, 1996, Schmid-Hempel and Schmid-Hempel, 1990, Corbet et al., 1993]. Strategies for coping with food scarcity that do not necessarily imply increases in foraging range include switching to less preferred resources, stockpiling, nest relocation, increasing the time spent foraging, and reducing energetic needs (for example, by limiting reproductive behavior). However, for bumble bees, extended late-season foraging may be necessitated by increases in colony-level resource demands due to production of reproductive individuals (queens and males), which typically increase across the colony life cycle [Cartar and Dill, 1990, Prỳs-Jones and Corbet, 1991]. While an increase in long-distance foraging in the late-season has been indirectly observed in managed honey bees [Couvillon et al., 2014] and hypothesized for wild bees [Goulson et al., 2010] it has never been documented in the field. Our analyses suggest a significant shift in foraging distance related to seasonal declines in floral resources.

Seasonal fluctuations in food resources and increases in provisioning demands during the breeding season are common features of central-place foragers in general. Within the Hymenoptera, both solitary and social foragers often provision offspring into the later phases of their growing season, even though protein resources (e.g. pollen or prey) may be declining in the envi-

ronment [Richards, 2000]. Thus, even for solitary bees and wasps, it is possible that many females exhibit increased foraging distances as landscape-level resources decline and provisioning needs increase. In a study manipulating food source distance from solitary bees, Zurbuchen and colleagues [Zurbuchen et al., 2010a] show that while solitary species may be capable of long distance foraging, this extended foraging reduces brood cell provisioning, with negative impacts on total brood cell count. These results suggest that even if bees are capable of long-distance foraging, the increased time and energy spent in extended foraging may have negative implications for population growth. Thus, for both solitary and social species, we posit that late season flowering events may be critical for maintaining wild pollinator population densities. Future work should explore foraging shifts in landscapes where floral resources increase with pollinator/colony life span, in order to examine how experienced foragers navigate increasingly resource-rich environments.

In this study, we observed foraging siblings which were 50m to 3000m apart; this high level of variation in foraging distance indicates that bumble bees can vastly shift foraging patterns over space and time, and highlights why the single maximum foraging distance, the index primarily used to characterize pollinators [Greenleaf et al., 2007] and pollination models [Lonsdorf et al., 2009], is an exceedingly simplified measure of pollinator movement. We suggest that the variation in foraging distance exhibited in this study may be a common feature in other central place foraging pollinators, though likely at different spatial scales depending on body size [Greenleaf et al., 2007] and pollinator

ecology [Steffan-Dewenter et al., 2002]. Studies that have similarly genotyped and mapped wild bumble bee sibships have likewise documented substantial variation in foraging distances across different study regions [Carvell et al., 2012, Jha and Kremen, 2013, Redhead et al., 2016]. Regardless of the drivers that prompt the long-distance movement patterns documented in this study, our results suggest that a more challenging foraging environment is experienced by wild bumble bees in the late season, at least in regions where floral resources peak early and subsequently decline. Thus, this time period represents an important target for pollinator-supportive floral restoration efforts. Indeed, late season mass-flowering crops have been documented to positively impact wild bumble bee colony densities [Rao and Strange, 2012], whereas early season crops can improve early season colony growth but do not lead to increased numbers of reproductives later in the season [Williams et al., 2012].

In summary, while food is often the center piece of animal conservation [Raubenheimer and Simpson, 2012], and has been proposed as a critical target of global pollinator conservation efforts [Pollinator Health Task Force, 2015], these strategies often fail to incorporate a discussion of pollinator foraging dynamics and the relevant scales at which pollinators utilize floral resources. Pollinator foraging patterns are particularly important to understand given the increasing dependence of humans on animal-pollinated crops [Aizen et al., 2008] and growing negative pressures of urbanization, agricultural intensification, and climate change on wild pollinators (reviewed in [Goulson et al., 2015]). Specifically, land conversion that limits wild bee dispersal [Jha, 2015]

could also fragment floral resources and potentially exacerbate already challenging late-season foraging conditions. Interestingly, our study illustrates an ability for wild bumble bees to evaluate and distinguish among resource patches given distinct landscape-level resource contexts and thus they provide unique insight into the drivers of long-distance foraging. Specifically, our results provide support for the importance of 'bridging' plants in habitat restoration plantings that act to specifically target resource-poor time periods [Dixon, 2009], when pollinators may be most challenged by limited food resources. Given the potential impacts of global change on plant and pollinator interactions [Hegland et al., 2009], our findings emphasize the importance of landscape-level habitat conservation measures and suggest a phenologically-targeted approach to wild pollinator research and restoration efforts.

1.5 Appendix: Population genetic analyses

As documented in other studies within the region [Williams et al., 2012], floral cover during the early season (days 120-140 from the start of the year) was more than 10x the quantity in the late season (days 165 – 185). During early season, mean patch floral density was 64.92 cm^2/m^2 ($\pm$ 22.56) and ranged from 37.70- 128.97 cm^2/m^2, while in the late season, mean patch floral density was 6.03 cm^2/m^2 ($\pm$ 6.69) and ranged from 0.01-36.83 cm^2/m^2.

The probability of null alleles was calculated using the software Micro-Checker [van Oosterhout et al., 2006] and deviations from HWE and linkage disequilibrium (LD) were tested in GENEPOP v 4.0.10 [Raymond and Rous-

set, 1995] with 1000 dememorizations, 100 batches, and 1000 iterations per batch using the Markov chain approximation for the exact tests and likelihood-ratio tests, respectively. For foraging analyses, only colonies with greater than 1 representative were used. Specifically, of the 669 bees sampled, 51 had moderate genotyping success rate (<8 loci resolved) and thus were dropped to avoid assignment error, while the remaining were assigned to colonies (Table 1.3). For population genetic analyses, colony-mates (i.e., full siblings) were randomly removed, leaving just one representative per colony (as in [Jha and Kremen, 2013]; [Cameron et al., 2011]). Allelic richness (AR) and private allelic richness (PAR) per region were estimated using rarefaction, standardized to 50 gene copies per population, in HP-RARE [Kalinowski, 2005]. Heterozygosity per region was estimated using Nei's gene diversity, He [Nei and Kumar, 2000], and relatedness per region was calculated using the index of [Goodnight and Queller, 1999].

Nest densities were estimated from the distribution of resampled colonies per region using the software Capwire [Miller et al., 2005], which utilizes the number of times a colony is 'recaptured' to estimate the population size. To estimate total nesting density, we used the Two Innate Rate Model (TIRM) mark-recapture approach since this has been shown to align best with the expected truncated Poisson distribution of nest densities [Goulson et al., 2010]. Percent Unique Nests was calculated as the fraction of individuals representing unique colonies per region. Changes in AR, PAR, He, Nesting density, Percent Unique, and Relatedness per region as function of time period (fixed

effect) were examined using Linear Mixed Effects (LME) models with study region as a random effect.

MICRO-CHECKER results indicate that one locus (BT136) exhibited substantial evidence of null alleles (>50% of sampling sites with evidence of null alleles), therefore BT136 was excluded from the analysis. The remaining loci exhibited either low or no signs of null alleles (<30% of populations). Study regions exhibited deviations from HWE at 1-4 loci (mean = 29.0% loci, SD = 10.4%), likely due to small sample sizes. Significant LD was detected for multiple loci, but within <10% of the sampling sites and not consistent for any loci pair, therefore all markers were retained for the analyses, except for BT136 (excluded for null alleles). Across study regions, Heterozygosity (mean = 0.743 ± 0.013), Allelic Richness (9.085 ± 0.498), Private Allelic Richness (0.543 ± 0.198), Relatedness (-0.013 ± 0.001), estimated Nest densities (653.50 ± 42.590), and Percent Unique nests (0.859 ± 0.039) did not significantly decrease over time (LME with date as fixed effect and transect as a random effect, P>0.539 for all tests).

1.6 Appendix: Sensitivity analysis

To assess the sensitivity of our conclusions to the shape of the exponential prior on foraging distance, we varied the rate parameter of this prior distribution between $(0.25)^{-1}$ to 2^{-1}; and refit the foraging model under each value. This range of priors can be interpreted as prior mean foraging distances ranging from 0.25 km and 2. The spatial data lie on a transect and so carry

little information about average foraging distance. In other words, the prior on foraging distance is informative. As the prior mean of foraging distance increases, so will the posterior estimates of foraging distances. The purpose of the sensitivity analysis is to assess how the prior influences the conclusions of the main analysis: how the preference for the floral density of a patch and the proximity of the patch to the colony might change with the average floral quality of the landscape. We find that varying the prior mean foraging range does not alter the conclusions of our analysis: that preference for floral quality decreases with increasing landscape floral quality; and that aversion for distant patches does not decrease with increasing landscape floral quality (Figure 1.5).

This model of patch visitation provides estimates of the foraging distances of individual bees, and the degree of attraction of foragers for patches with varying quality of forage. Implicit in this model is the idea that preference drives visitation, and thus foragers will travel further to reach patches that they prefer. However, the shape of the relationship between forage quality and the distance travelled to reach the patch will depend on the spatial arrangement of forage quality and on the estimated colony locations. We measure the shape of this relationship from the MCMC output, by calculating a correlation between the estimated foraging distances and the forage quality of visited patches, over each MCMC iteration. This procedure provides samples from the posterior distribution of the correlation between the forage quality at a patch, and the distance travelled to reach that patch. To help visual-

ize the relationship between patch quality and foraging distance, we calculate the expected visitation rates for patches of different qualities, as function of distance from the colony. From the definition of multinomial and Poisson variables, if $Y_{jkl} = [y_{1jkl}, \ldots, y_{7jkl}]$ is a multinomial sample of bees across transects for colony j, with associated vector of probabilities in the form of $p_{jkl} = [\mu_{1jkl}(\sum_i^7 \mu_{ijkl})^{-1}, \ldots, \mu_{7jkl}(\sum_i^7 \mu_{ijkl})^{-1}]$, then the count y_{ijkl} associated with the ith patch is Poisson distributed with rate μ_{ijkl}. Using the notation defined in 1.2, we define a quantity proportional to the expected visitation rate of colony j on patch i: $\exp\{\ d_{ij}\Lambda_{kl} + x_{ikl}B_{kl} + \epsilon_{ik}\} \propto \mu_{ijkl} = \mathbb{E}[y_{ijkl}]$, that can be used to visualize the rate at which visitation decays with distance to the colony, for a patch of a given quality (as in Figure 1.4).

1.7 Appendix: Null model, minimum foraging distance

In this study, we collected foraging bees at discrete points along a transect. A consequence of this sampling scheme is that there are a finite number of observable values for the distance between foraging siblings. With our sampling design, a pair of foraging siblings on a transect could be observed only at the following distances apart (the number of possible configurations giving the observed distance are in parentheses): 3000 m (1), 2000 m (2), 1750 m (2), 1500 m (2), 1250 m (2), 1000 m (3), 750 m (2), 500 m (3), 250 m (4), 0 m (7). A major concern with using these distances as the response variable within a regression model is the presence of spurious relationships due to the spatial configuration of the predictor variables. For example, if the patches at the

edges of the transect have a higher-than-average floral density, we could observe a spurious relationship between floral density and the distance between foraging siblings.

To address this concern, we simulate data from a null model where bees are distributed uniformly at random among transect points, without regard for covariates. We simulate 1999 datasets to estimate the distribution of the regression coefficients under the null model, and then compare the regression coefficients estimated from the real data to this null distribution. A single simulation from the null model is computed as follows: (1) for each colony at each site, assign the bees of that colony to random transect locations with equal probability and calculate the average pairwise distance among bees; (2) fit the linear mixed-effects model described in section 1.2 to these simulated distances; (3) record the z-statistics of the regression coefficients. The trends that we observe in our analysis are unlikely to have occurred if this null model were true (Figure 1.6). For each regression coefficient, we calculate a Monte Carlo P-value as the proportion of the null simulations that lie between $\pm$ the absolute value of the z-statistic from the regression model fit to the observed data (Table 1.2). We conclude that our observed data are unlikely to have arisen from a situation where bees visit transect locations without regard for the floral quality at those locations.

	Posterior mean	95% CI	Pr(sign)
Patch floral cover	1.15	(0.73, 1.61)	<0.001
Patch by landscape interaction	-1.13	(-1.67, -0.63)	<0.001
Distance from colony	-4.10	(-4.78, -3.52)	<0.001
Distance by landscape interaction	-0.39	(-1.24, 0.49)	0.195

Table 1.1: Posterior estimates from a multinomial model of patch visitation. Pr(sign) is the posterior probability that a parameter has the opposite sign from its posterior mean. Posterior means and credibility intervals are on a logit scale.

	Estimate	Std. Error	*P*-value
Intercept	21.791	2.395	
Patch floral cover	8.388	2.759	0.015
Landscape floral cover	-13.141	3.410	<0.001
Patch by landscape interaction	-6.519	2.370	0.006

Table 1.2: Estimates from a linear mixed model of minimum foraging distance. *P*-values are calculated by Monte Carlo simulations from a null model (see appendix section 1.7).

		Sampled bees	Detected colonies	Total nesting density
Barry	Early season	127	119	108
	Late season	88	75	71
Pope	Early season	139	125	110
	Late season	93	87	80
Second	Early season	129	122	109
	Late season	93	90	84

Table 1.3: Number of sampled bees and colonies across regions. Non-singleton colonies are those with >1 assigned individual. Total nesting density was estimated using Capwire [Miller et al., 2005].

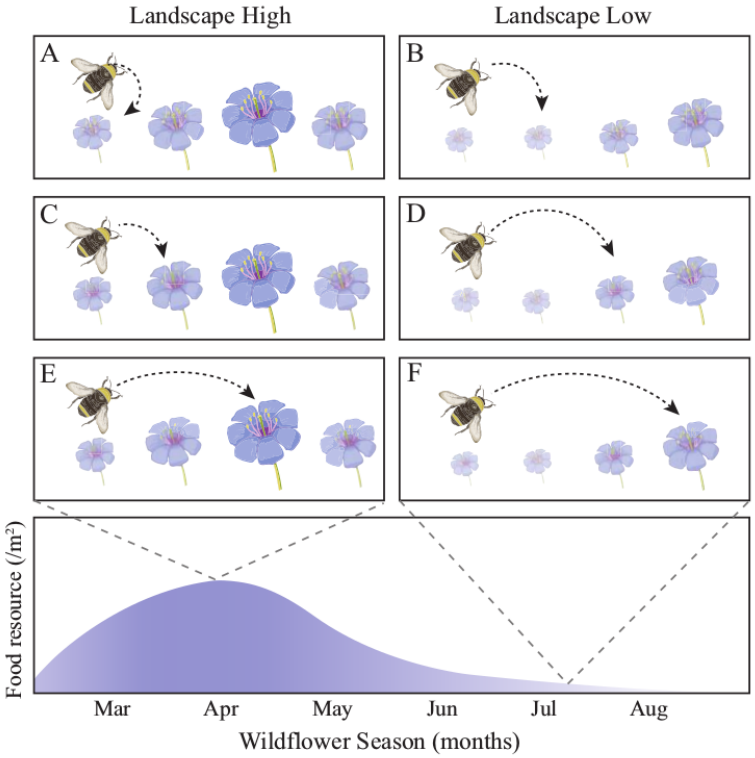

Figure 1.1: Foraging patterns of individual bumble bees where columns represent scenarios where landscape floral cover is high (early season) and low (late season), and destination patch floral cover is represented by flower size. Potential foraging patterns produced by varying selectivity with regards to distance from natal patch (nest) and patch floral cover: (A-B) a moderate preference for shorter travel distances but no preference for higher floral cover; (C-D) a moderate preference for both shorter travel distances and higher floral cover; (E-F) a low preference for shorter travel distance and a strong preference for higher floral cover.

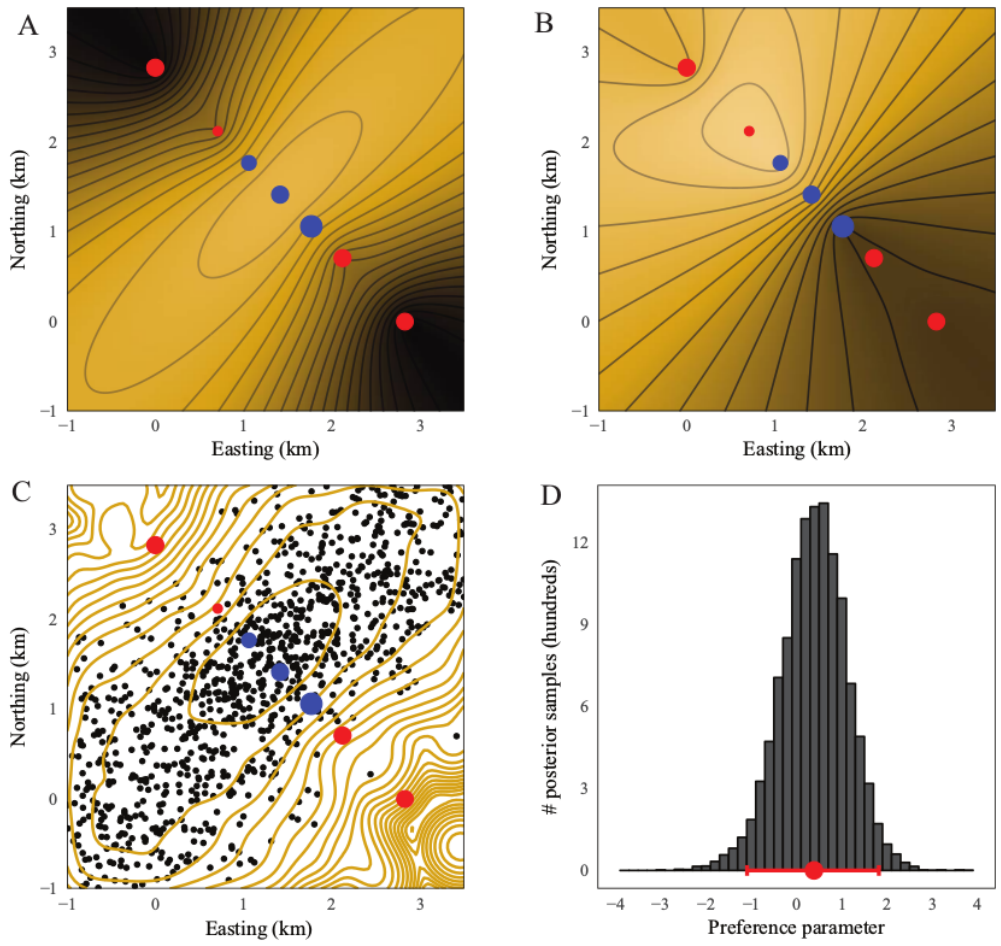

Figure 1.2: An illustration of the individual-level patch visitation model described in the text, with a simulated dataset of three siblings from the same colony. (A-B) Two log-likelihood surfaces for the colony location, where points represent a transect of collection sites: red had no bees collected, blue had a single bee collected. The size of points represents the floral cover at sites. Panel A shows the likelihood surface for a model where bees do not distinguish between sites with low and high floral cover, panel B shows the likelihood surface for a model where bees preferentially visit sites with high floral cover. (C-D) Samples from the posterior distribution of the colony location and the preference parameter for these data.

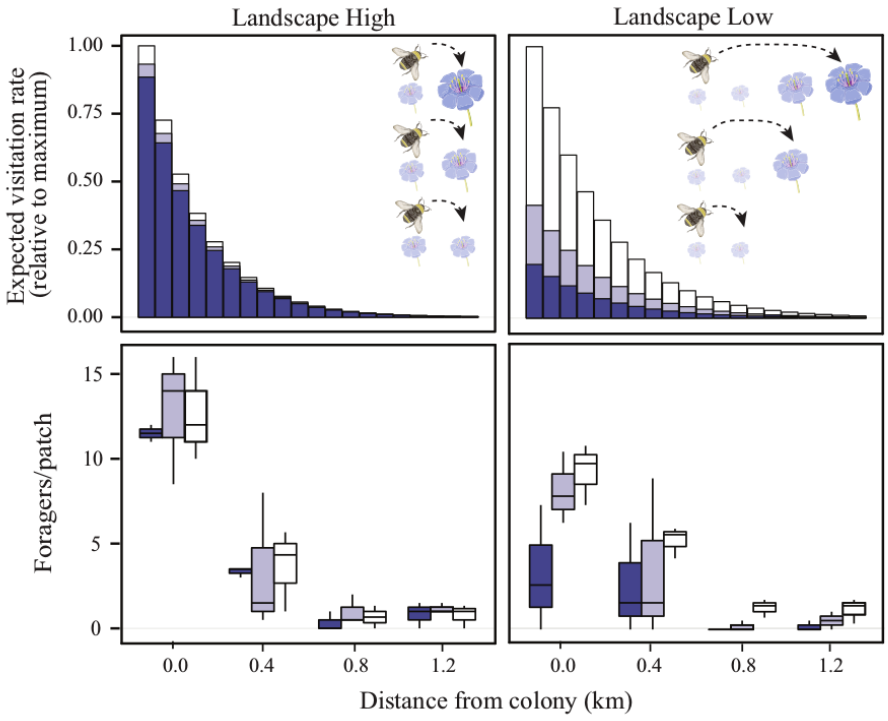

Figure 1.3: Model-derived individual-level patch visitation rate (top row) and observed patch visitation (bottom row) as a function of patch floral cover and the distance between patch and colony, for Landscapes with High (early season) and Low (late season) cover. The top row models the decline in relative visitation rate from the individual-level visitation analysis, illustrated for the transect corresponding to the median floral cover in each resource period. Expected visitation is shown at 60m intervals and decays at different rates depending on whether destination Patch floral cover is high (white, 0.66-1 quantiles), medium (light purple, 0.33-0.66 quantiles), or low (dark purple, 0-0.33 quantiles). The images (top to bottom) represent the three foraging responses to patch floral cover, respectively. The bottom row illustrates the observed number of foragers per number of Patches, within bins of estimated distance from the colony (maximum a posteriori estimate from the Bayesian analysis). Patch floral cover is binned into high, medium, and low quantiles as described above for each transect. Distance is binned at 400m intervals where the last distance bin includes all samples above 1.2km. Boxplots show the spread of values across transects (see also Table 1.1 and appendix 1.6).

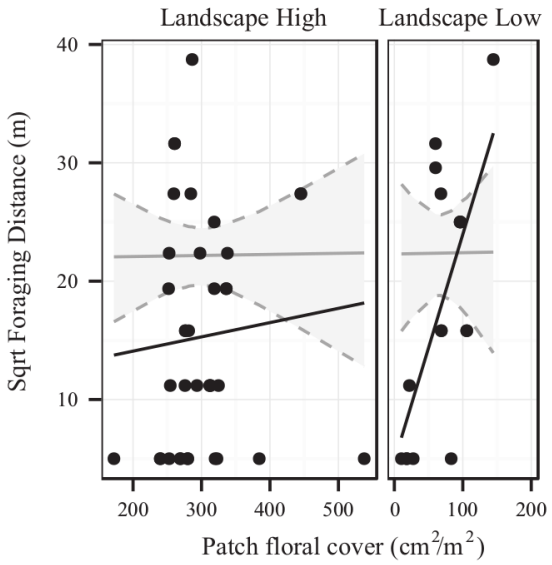

Figure 1.4: Colony-level minimum foraging distance as a function of destination patch floral cover (cm^2/m^2) where data has been binned to represent cases where landscape floral resources are high (early season) and low (late season). Each point represents mean foraging distance for a colony (some points overlap) and the solid black line is fitted to the observed data; the gray line represents simulations from a null model where foraging siblings were positioned randomly across the transect (shaded areas represent 95% confidence intervals). When landscape resources are high, the fitted slope does not differ significantly from the null expectation (no significant increase in foraging distance with patch floral cover); however, when landscape resources are low, the fitted slope is significantly greater than the null expectation (foraging distance increased with destination patch floral cover; see also Table 1.2).

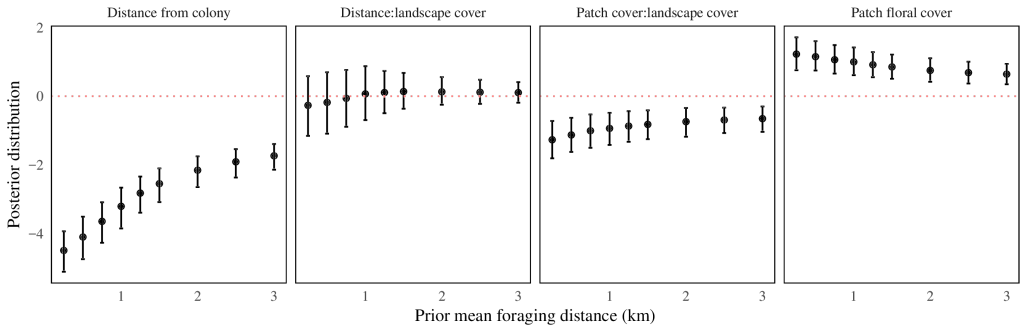

Figure 1.5: Posterior distributions of the parameters governing preference as a function of the prior on foraging distance: (left to right) preference for distance from colony (λ_0 in the main text); how preference for distance changes with landscape quality (λ_1); preference for floral quality (β_0); how preference for floral quality changes with landscape quality (β_1). Positive values indicate a preference, negative values indicate an aversion. Points are posterior means, bars are 95% credibility intervals.

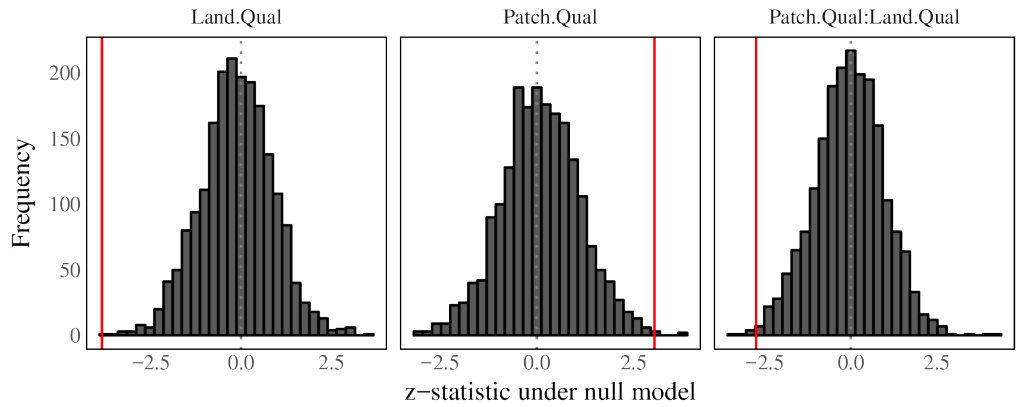

Figure 1.6: The approximate distributions of the z-statistics (estimate/std. error) of regression coefficients under a null model where siblings are placed uniformly at random across transect points. From left to right, the predictor variables are: patch floral density ('Patch.Qual'), landscape floral density ('Land.Qual'), and an interaction between these ('Patch.Qual:Land.Qual'). The red lines show the values of the z-statistics from the model fit to the observed data.

Chapter 2

Inferring the foraging ranges of social bees from sibling genotypes sampled across discrete locations

The research in this chapter represents a collaboration between the author and Dr. Shalene Jha, and as of the time of writing has been published as [Pope and Jha, 2017].

A knowledge of the distances regularly travelled by foraging bees is essential to understanding the movement of pollen across landscapes, and has implications for the conservation of both pollinators and plants. Unfortunately, the movements of bees are difficult to measure directly at ecologically relevant scales. A common strategy for quantifying the foraging ranges of social bees is to sample the genotypes of foragers across a landscape. Individual foragers can be assigned to colonies with polymorphic genetic markers, and the dispersion of siblings in space can be used to make inference about colony locations and foraging movements. Several previous studies have sampled sibling genotypes at discrete locations (for example, at regular points along a transect), rather than in continuous space. Restricting the collection of bees to discrete locations presents a number of considerations for sampling design and data analysis. In this study, we develop a spatially-explicit, model-based framework for the

simulation and estimation of foraging ranges. Using these tools, we simulated experiments to characterise the efficacy of different sampling strategies, and provide an example with actual data that demonstrates the advantages of our method over an approach based on regression.

2.1 Introduction

Social bees are among the most iconic groups of study in the field of foraging biology. Like other bees, they require pollen and nectar resources to feed themselves and produce reproductive offspring. However, unlike solitary species, social bees forage collectively and are believed to have much higher individual foraging demands due to the high and prolonged demands of brood care [Heinrich, 1975]. This high level of foraging activity is one potential reason why social bees, such as honey bees, bumble bees, and stingless bees, are managed alongside crops within many agricultural systems, and are also often highly effective crop pollinators [Bohart, 1972]. While landscape-level foraging is important for both natural and agricultural systems, past work on social bee foraging has largely focused on small spatial scales [Osborne et al., 1999] and little is known about the drivers of foraging across landscape scales.

The spatial scale at which colonies forage – the area within which foragers travel to find food, and disperse pollen among plants – is intimately related to the survival and growth of individual colonies [Williams et al., 2012, Osborne et al., 2008] and the plants they pollinate [Bond, 1994]. The spatial frequency distribution of foragers from a given colony (*foraging kernels*)

is key to predicting the movement of pollen between individual plants and the spatial distribution of floral resources required by bee populations [Goulson et al., 2010, Lonsdorf et al., 2009]. However, the foraging distances of small insects such as bees are extremely difficult to measure directly. Past studies examining foraging ability have largely used feeder or colony member displacement experiments to determine maximum foraging distances [Greenleaf et al., 2007]; while these studies allow for species-comparisons in feeder/displacement response, they do not measure foraging in response to the distribution of floral resources. More recent methods use radio or radar tracking [Osborne et al., 1999, Lihoreau et al., 2012], and these provide much more detailed information about finer scale foraging movements, response to local resources, and changes in foraging movements across a foraging bout. However, these studies are often costly and labour intensive, and do not scale to populations and landscapes. Technologies which can measure movements across a wide radius (such as harmonic radar) are often only suitable for open, unobstructed habitats and require colonies to be either located (a non-trivial task) or to be reared and placed at selected locations, limiting use for wild colonies.

For social bees, genetic tools provide a cost-effective means to estimate foraging range in wild populations, without prior identification of the colony locations [Darvill et al., 2004]. The essential idea is that sibling foragers can be associated with the same colony using polymorphic genetic markers, and the dispersion of siblings in space carries information about both foraging distance and the colony location. Since [Chapman et al., 2003] and [Darvill

et al., 2004] first proposed using the spatially-referenced genotypes of foraging bumble bee siblings to make inferences about foraging patterns, many studies have employed this technique to address questions about the spatial ecology of bumble bees. Initial efforts used sibling-genotype derived distances to compare the foraging ranges of different bumble bee species [Knight et al., 2005], whereas more recent applications have examined how foraging range is influenced by the floral community [Jha and Kremen, 2013], land use [Dreier et al., 2014], and plant phenology (Jha and Pope, *in review*). Foraging siblings that are captured in continuous space bring the most information about colony locations. However, sampling in continuous space involves humans searching for bees across the entire foraging kernel (often multiple km) with insect nets, and so requires a considerable effort to cover moderate spatial and temporal scales. A less laborious alternative is to catch bees and sample their DNA at discrete locations [Darvill et al., 2004, Jha and Kremen, 2013]. Discrete sampling can be performed in a systematic way across large spatial areas, either by active trapping (with insect nets), or with passive trapping (such as with blue vane traps). Passive traps can be left for several days, providing genetic material with relatively little monetary and logistic cost, although all passive traps which provide genetic material from bees are lethal. However, the accuracy and efficacy of these schemes has not been examined critically, and often the methods used to analyse these data falsely assume that data was collected in continuous space [Darvill et al., 2004, Knight et al., 2005, Jha and Kremen, 2013].

The literature on trapping methodology for the estimation of population densities and space use is vast and encompasses both design [Foster and Harmsen, 2012, Sun et al., 2014, Royle et al., 2013b] and analysis [Worton, 1987, Efford, 2004, Royle et al., 2013a]. In our opinion, this applied literature provides valuable insights into methodological approaches for inferring foraging movements from sibling genotypes. There are three main facets to trapping social bees that deserve close consideration, given their relevance to predicting nesting and foraging dynamics. First, the spatial distribution of forage and colony densities can range from clumped to homogeneous and should be considered in any generative model that aims to describe nesting and foraging behaviour. Specifically, we posit that relative visitation rate to a spatial location must consider forage quality, as this affects bee patch visitation [Robertson et al., 1999]. Past studies on social bee colonies have shown that foraging kernels are not always symmetric [Visscher and Seeley, 1982], and thus models should not automatically assume symmetry. Instead, we expect that when averaged over individuals, foraging patterns will reflect the distribution of forage in the landscape, relative to the colony location. The traps may non-randomly vary in attractiveness, as a function of the forage quality near the traps; and unobserved (but attractive) areas of the landscape may 'compete' with traps for bees.

Second, average foraging distance can be estimated at different levels of organisation, and it is important to distinguish among them. For example, past studies have estimated the foraging distance of individuals [Zurbuchen

et al., 2010b]; the average foraging distance of colonies [Jha and Kremen, 2013]; and the average foraging distance across landscapes and species [Knight et al., 2005]. The estimation of individual foraging distances can be rephrased as the estimation of colony locations, and is a necessary step in estimating the average foraging range at higher levels of organisation. In the past, the colony location has typically been estimated by the centroid of forager locations [Knight et al., 2005, Jha and Kremen, 2013]. When bees are sampled at discrete locations, the centroid will clearly be a function of the distance between traps and the trapping arrangement, and so is a biased estimate of the colony location. Whether or not bees are captured in discrete or continuous space, the reality is that the locations of colonies are unknown but can be estimated along with the foraging kernel. To accommodate these considerations, we advocate a model-based approach which explicitly incorporates the method of data collection and the spatial locations of collections.

Third, estimates of foraging will depend on the spatial distribution of traps [Sun et al., 2014], and the design of the trapping scheme should be carefully considered with reference to the size of the landscape and the question under investigation. For example, if the question revolves around the relative differences in average foraging range across landscapes, biased but consistent estimates may accurately answer the question. Studies which have used discrete trapping to sample bee genotypes have typically done so by collecting along a transect [Darvill et al., 2004, Knight et al., 2005, Goulson et al., 2010, Jha and Kremen, 2013]. Traps arranged in grids are commonly

used when estimating movement and density of mammals [Parmenter et al., 2003, Pearson and Ruggiero, 2003]. A compromise between a single transect and a grid is two perpendicular transects (a 'cross'), and another option is to place traps at random throughout the landscape. In general, the efficacy of a trapping scheme depends upon the extent and density of the grid, in relation to the spatial scale at which animals are moving [Sun et al., 2014] and the overlap between the animals' range and the traps [Bondrup-Nielsen, 1983]. By trap density, we mean the number of traps within a fixed area and given trap arrangement, such that increasing the density will decrease the space between traps.

In this study, we provide four main contributions: **(1.)** A simple simulation scheme that generates foraging kernels for various colonies, and incorporates the spatial location of the colony and the spatial arrangement of forage. From these foraging kernels, simulation of samples within a trapping array follows easily. **(2.)** A Poisson-process based approach to estimating foraging range from trapping data, that integrates over uncertainty in colony location and incorporates differential attractiveness of traps. **(3.)** A set of simulated experiments to assess the efficacy of different trapping schemes for estimating average foraging range at varying levels of sampling effort and organisation (i.e. colony, landscape). **(4.)** A comparison of our model to a previously used regression method, when applied to a dataset of bumble bee collections across a heterogeneous floral landscape. Our results illustrate how a combination of the genetic identification of sibships and passive trapping can be adapted to

specific goals, such as identifying colony locations, or testing hypotheses about differences in foraging distance across landscapes.

2.2 Methods and models

Simulation of data. To make simulation more tractable, we discretise continuous space into a raster by dividing the landscape into a grid of equal sized cells: let $\mathcal{J}$ be the set of all cells. Assume that some number of colonies nest in the landscape: let $\mathcal{C}$ be the set of all colonies. Let $\eta(j)$ be the rate at which colonies occur in cell $j \in \mathcal{J}$; then colonies are independently located according to an inhomogeneous Poisson process, with a given colony occurring in cell j with probability $\frac{\eta(j)}{\sum_{i \in J} \eta(i)}$.

We generate foraging kernels for colonies via a simple Poisson process model. Let $\lambda_i(j)$ be the rate of visitation for colony $i \in \mathcal{C}$ at cell $j \in \mathcal{J}$. Let $\{s, c\}$ be indices which denote the cell and colony for a random 'visitation' event in the Poisson process (an event where a bee of a given colony visits a given cell). For a given event, the probability that a bee from colony i visits site l is:

$$\Pr(s = l | c = i) = \frac{\lambda_i(l)}{\sum_{j \in \mathcal{J}} \lambda_i(j)} \tag{2.1}$$

Equation 2.1 gives the foraging kernel for colony i: the frequency of bees from that colony across the landscape. Using the foraging kernels of all colonies in the landscape, we can calculate the frequency with which different colonies will be represented in traps. Let κ be some subset of cells where traps are located. The probability that a given bee from colony i visits one of the cells

(traps) in κ is:

$$\Pr(s \in \kappa | c = i) = \sum_{k \in \kappa} \Pr(s = k | c = i) = \frac{\sum_{k \in \kappa} \lambda_i(k)}{\sum_{j \in \mathcal{J}} \lambda_i(j)}$$

The total number of foragers in the landscape is N, and the number of foragers in colony i is n_i. The probability that a bee selected at random from the population belongs to colony i is $\Pr(c = i) = \frac{n_i}{N}$. From the definition of conditional probability, the probability that a bee from a given site j belongs to colony i is:

$$\Pr(c = i | s = j) = \frac{\Pr(s = j | c = i) \Pr(c = i)}{\Pr(s = j)} \tag{2.2}$$

Where the denominator is the probability that a bee (from any colony) visits cell j, and is calculated as

$$\Pr(s = j) = \sum_{i \in \mathcal{C}} \Pr(s = j | c = i) \Pr(c = i)$$

Therefore, the probability that a bee (from any colony) visits any of a set of cells κ with traps is:

$$\Pr(s \in \kappa) = \sum_{i \in \mathcal{C}} \Pr(s \in k | c = i) \Pr(c = i)$$

Given that a bee visits any of a set of cells κ, the probability that a bee from any colony visits a *particular* trap $k \in \kappa$ is:

$$\Pr(s = k | s \in \kappa) = \frac{\Pr(s = k)}{\Pr(s \in \kappa)} \tag{2.3}$$

To simulate from the joint distribution $\Pr(s, c | s \in \kappa)$, draw $k \in \kappa$ from $\Pr(s = k | s \in \kappa)$ (Equation 2.3), draw a value of c from $\Pr(c = i | s = k)$

(Equation 2.2), and update N and n_i accordingly. Repeat this process until a stopping rule is reached, such as the acquisition of a certain number of samples per trap. Because a bee is removed from the population with each trapping event, the conditional probability in Equation 2.2 changes during the trapping process. Effectively, the more bees from a colony that are captured, the less likely is a subsequent capture from that colony.

Given this model, the expected foraging distance can be calculated at various levels of organisation. Define d_{ij} as the Euclidean distance between the centroids of the cell j and and the cell where colony i is located, i.e. as $d_{ij} \equiv \|x_j - \delta_i\|$ where x_j and δ_i are vectors, respectively containing the Cartesian coordinates of centroids for cell j and the cell containing colony i. The expected foraging distance for a colony can be calculated from the foraging kernel $\Pr(s|c = i)$ as $\mathbb{E}[d_{ij}] = \sum_{j \in \mathcal{J}} \|x_j - \delta_i\| \Pr(s = j|c = i)$. The expected foraging distance for a landscape can be calculated by averaging over colonies as $\mathbb{E}[d] = \sum_{i \in \mathcal{C}} \Pr(c = i)\mathbb{E}[d_{ij}] = \sum_{i \in \mathcal{C}} \frac{n_i}{N}\mathbb{E}[d_{ij}]$.

The distribution of colonies in space and the foraging kernel of a select colony are determined by the functions $\eta(j)$ and $\lambda(j)$. For succinctness, we define both as simple log-linear functions. Let the quality of nesting resources within cell j be v_j; then the rate with which colonies occupy the cell is $\eta(j) = \exp\{\phi v_j\}$. The parameter $\phi \in [0, \infty)$ controls the degree to which colonies are clustered in cells with high-quality nesting resources. Let f_j represent the quality of floral resources in cell j, and let d_{ij} be the geographic distance from the cell to colony i (as defined in the previous paragraph). The visitation

rate to a cell from the colony is $\lambda_i(j) = \exp\{-\beta d_{ij} + \theta f_j\}$. The parameters $\beta, \theta \in [0, \infty)$ control the degree to which bees are concentrated close to the colony and in cells with a high forage quality. The overall effect is to generate asymmetric foraging kernels which reflect to a greater or lesser extent the distribution of floral resources across the landscape (Figure 2.1A). We note that these foraging kernels are marginal with respect to individuals: we do not seek to replicate patterns of individual behaviour, but instead to represent the long-run frequency of foragers across the landscape, for the colony as a whole.

Given that the locations of both colonies and bees are modelled as a function of an underlying resource landscape, how is this resource landscape determined? We simulate the spatial distributions of nesting and floral resources as independent Gaussian random fields under a Brownian variogram [Schlather et al., 2015]. Each variogram model has a single parameter that controls the spatial clustering of resources: parameter values close to zero generate landscapes where resources of varying quality are more or less evenly scattered through space (white noise), while parameter values close to two generate landscapes where resource quality follows a gradient.

A model for discrete trapping. The simulation procedure described in the preceeding section uses a spatially explicit model of forage and nesting resources across the landscape. In contrast, when estimating foraging ranges from trapping data we assume that the investigator has no knowledge of colony sizes or the distribution of nesting and foraging resources, but can assess forage

quality at the exact location of the trap. In other words, the investigator has a limited understanding of the landscape and would like to estimate foraging ranges from collections at traps. To estimate colony locations and foraging distances, a simple model considers a set of traps κ in continuous two-dimensional space, with spatial coordinates $x_k = \{x_1^k, x_2^k\}$ and quality of forage f_k for trap $k \in \kappa$. The occurrence of bees from colony i in the traps follows a Poisson process with rate $\lambda_i(k)$. A simple form for $\lambda_i(k)$ allows the visitation rate to decay with the distance between trap and colony, to increase with forage quality, and also incorporates random trap-specific and colony-specific variation. For example,

$$\begin{gathered} \ln \lambda_i(k) = -\beta \|x_k - \delta_i\| + \theta f_k + \zeta_i + \epsilon_k, \\ \epsilon_k \sim \mathcal{N}(0, \sigma^2 \Sigma(\rho)),\ \zeta_i \sim \mathcal{N}(\mu, \tau^2) \end{gathered} \tag{2.4}$$

In this model, the set of unknown parameters which must be estimated is $\Theta = \{\delta_i, \beta, \theta, \zeta, \epsilon, \mu, \sigma^2, \rho, \tau^2\}$: where $\delta_i = \{\delta_1^i, \delta_2^i\}$ are the spatial coordinates of the colony, β controls the distance-decay of the rate with distance between colony and trap, θ controls the attractiveness of forage quality at traps, ζ_i is a colony-specific random intercept centered around a global intercept μ with standard deviation τ, and ϵ_k is a trap-specific random effect with standard deviation σ and spatial correlation matrix Σ with parameters ρ. Assume that some set of colonies $\mathcal{C}$ is observed during the course of the study: given a set $y = \{y_{ik} : k \in \kappa, i \in \mathcal{C}\}$ of trapped bees which have been associated with the ith colony through genetic markers, the likelihood can be written as

$$\mathcal{L}(\Theta|y) = \prod_{i \in \mathcal{C}} \left(\frac{\exp\{-\Lambda_i(\Theta)\}}{Y_i!} \prod_{k \in \kappa} \lambda_i(k; \Theta)^{y_{ik}} \right)$$

where $\Lambda_i(\Theta) = \sum_{k \in \kappa} \lambda_i(k; \Theta)$ and $Y_i = \sum_{k \in \kappa} y_{ik}$.

The intuition underlying the model is that traps which are located further away from a colony receive fewer bees from that colony, and traps which are located in resource-rich areas will receive more bees. Depending on the colony location, and on the relative attractiveness of traps, different frequencies of bees are expected to occur at traps. By finding values of parameters which maximise the similarity between expected and observed frequencies, we can estimate the geographic locations of colonies, the parameters underlying the foraging kernel, and the attractiveness of traps.

An important point is that the model described here treats colony locations as unknown quantities which must be estimated *simultaneously* with the parameters governing visitation rates. In practice, this is an important consideration as there is dependence in the joint distribution of colony locations and the parameters which determine visitation rates to traps. For example, consider a scenario where three traps have captured equal amounts of bees (Figure 2.1B). The traps have different levels of forage quality, indicated in Figure 2.1B by colour (darker shades indicate higher quality). The shape of the conditional probability distribution of the colony location depends on the attractiveness of forage quality to foraging bees (parameter θ in Equation 2.4), and how averse the bees are to travelling long distances from the colony (parameter β in Equation 2.4). In particular, if bees are attracted to high quality forage and not averse to travelling far, then the most probable location for the colony is proximal to the unattractive occupied trap. If bees are averse to trav-

elling far, then the most probable location for the colony is between the three occupied traps. An estimation scheme which assumes that the colony location is the centroid of observed foragers–or sequentially estimates the colony location/foraging distances then the parameters governing visitation rates–could easily be biased if traps differ in attractiveness. In contrast, the simultaneous estimation of colony locations and trap attractiveness will appropriately account for dependencies between these parameters.

We are intentionally vague about the definition of 'forage quality' in this model. In reality, forage quality can be decomposed into many constituent factors (i.e. floral display size and species richness), all of which can be included in the definition of the visitation rate $\lambda(k)$. Finally, note that the form of $\lambda_i(k)$ in Equation 2.4 can easily be extended to include behavioural effects such as trap avoidance, varying exposures (variation in trapping times across traps), *etcetera*. We refer the reader to the extensive literature of modelling of trapping processes [Royle et al., 2013b].

Estimation of average foraging range. We fit the model of discrete trapping detailed in section 2.2 by Markov chain Monte Carlo (see appendix 2.6 for implementation details). Assume that the Markov chains converge and we end up a total of T samples from the joint posterior distribution of the parameters Θ. We use the generic notation $\Theta^{(t)}$ to indicate the value of the parameters in sample $t \leq T$ of the Markov chain. An estimator of the location

of colony i is the expectation of δ_i w.r.t. the joint posterior distribution,

$$\hat{\delta}_i = T^{-1} \sum_{t=1}^{T} \delta_i^{(t)} \approx \mathbb{E}[\delta_i | \Theta_{-\delta_i}, y]$$

For a given Monte Carlo iteration, the expected foraging distance of the colony can be estimated as the weighted average of the distance between the colony location and trap locations, where the weights are the estimated probability of a trap being visited by a bee from that colony:

$$d_i^{(t)} = \sum_{k \in \kappa} \|\delta_i^{(t)} - x_k\| \frac{\lambda_i(k; \Theta^{(t)})}{\Lambda_i(\Theta^{(t)})}$$

And then the expectation of d_i w.r.t. the joint posterior is approximated as $\mathbb{E}[d_i] \approx T^{-1} \sum_{t=1}^{T} d_i^{(t)}$. Intuitively, $\lambda_i(k)$ is an model-based estimate of the visitation rate of colony i to location k: $\lambda_i(k)$ is estimated from the data, and is in turn used to estimate the average foraging distance. Clearly, this estimate will be sensitive to the form of the model; but will be accurate if the model is approximately correct. A more 'naive' estimate weights the distance between colony and trap by the proportion of bees found at that trap; i.e. by replacing the weights $\frac{\lambda_i(k;\Theta^{(t)})}{\Lambda_i(\Theta^{(t)})}$ with $\frac{y_{ik}}{Y_i}$.

The estimated average foraging distance for a landscape is calculated in a similar fashion, but sums visitation rates across colonies:

$$l^{(t)} = \sum_{i \in \mathcal{C}} \sum_{k \in \kappa} \|\delta_i^{(t)} - x_k\| \frac{\lambda_i(k; \Theta^{(t)})}{\sum_i \Lambda_i(\Theta^{(t)})}$$

and as before is a model-based estimator which can be averaged over Monte Carlo samples to get an approximate expectation. A naive estimator would

use the proportion of bees (out of the entire collection of bees) as a weight; i.e. would replace $\frac{\lambda_i(k;\Theta^{(t)})}{\sum_i \Lambda_i(\Theta^{(t)})}$ with $\frac{y_{ik}}{\sum_i Y_i}$.

To estimate the relative difference in foraging distance between two landscapes where the same trapping scheme was employed, we estimate the posterior probability that the first landscape has a greater expected foraging distance than the second landscape as:

$$\Pr(l_1 > l_2) \approx \frac{1}{T} \sum_{t=1}^{T} \mathbb{I}[l_1^{(t)} > l_2^{(t)}]$$

where $l^{(t)}$ is defined as above with a subscript that indicates the landscape, and $\mathbb{I}$ is the indicator function (which evaluates to 1 if the inner inequality is true, and 0 otherwise).

Simulated experiments. We run a number of simulated experiments where we randomly (uniformly) select values of the parameters controlling both the locations of colonies and foragers; and the configuration of traps in the landscape. The simulation process is: (1) simulate parameters for the foraging and nesting landscape; (2) simulate a nesting and foraging landscape; (3) simulate colony locations and parameters controlling forager behaviour; (4) randomly select a trapping setup from a set of predefined options; (5) simulate the trapping process; (6) fit the model and obtain estimates. We simulate nearly 7,500 simulated experiments and 1 million simulated colonies. The trapping schemes considered include grid, transect, cross, and random placement of traps. For each of these topologies, we vary the density of traps (the number of traps in a

fixed area). The spacing of traps is a function of both the spatial arrangement and the density, as described in the introduction. We use the same spatial resolution in all simulated experiments: a landscape raster which is 1000 by 1000 map units, within which is nested a 500 by 500 'study area' where traps are located.

2.3 Results

Colony locations. The accuracy with which a colony location is estimated using the methods described above depends primarily on the true location of the colony in reference to the trapping grid (Figure 2.2). Colonies which are proximal to traps will be located with greater accuracy.

A direct consequence is that the arrangement of traps influences how much improvement in the accuracy of colony location can be achieved by increasing the density of traps within a fixed area. This is a trivial consequence of the fact that in the limit of trap density, a grid becomes continuous on a rectangle, a transect becomes continuous on a line, and so on. In other words, traps arranged in a grid cover the trapping area to a nearly uniform degree and so an increase in the density of the grid improves accuracy nearly uniformly over the trapping area. In contrast, increasing density along the transect increases the accuracy nearly uniformly along the transect (but little benefits estimation for colonies lying outside the transect). The probability that a colony is detected also depends greatly on its spatial location. However, increasing the density of traps, regardless of the trap arrangement, will

increase the spatial scale at which colonies are detected (albeit at different rates, Supplementary Figure 1).

Average colony foraging distance. The average foraging distance of the colony can only be estimated up to limit determined by the size of the trapping area. The size of the trapping area in our simulations is 500 map units, and this asymptote occurs between 400 and 500 map units (Figure 2.3). Below this asymptote, the direction and magnitude of error is a function of the true average foraging distance: the shape of this relationship is influenced by the arrangement of traps, the density of traps, and the number of captured bees (Figure 2.3). For all trap arrangements, there is a positive bias in the estimated foraging range of the colony, when the number of captured bees per colony is low. In general, this bias is inconsistent across values of the true average foraging distance; but the inconsistency is most extreme for transects with a low density of traps.

Average landscape foraging distance. Like the estimated average foraging distances for colonies, estimates for the average foraging distance for landscapes are constrained by the size of the trapping grid. In general, an increase in the number of bees caught in the landscape improves the accuracy of estimation (Figure 2.4). When low numbers of bees were captured, estimates were positively biased. However, the arrangement of traps and density of traps influences whether this bias is consistent, and also how quickly accuracy increases with number of captured bees. By consistent bias, we mean

that although estimates may be biased upwards, the amount of bias does not vary across the true values of foraging range.

Relative foraging distance. All trapping arrangements and densities were able to distinguish between the average foraging ranges of landscapes, given that the relative magnitude of the difference was extreme enough. However, the arrangement and density of traps has a strong influence on the power to accurately detect the direction of the relative difference in the average foraging range (Figure 2.5). In general, the grid arrangement was slightly more accurate than other methods at high trap densities. However, all trapping schemes showed an increase in power with increasing trap density, and at the highest density all arrangements performed similarly.

2.4 Application to *Bombus* data

In this section, we illustrate how the model of discrete trapping developed in section 2.2 can be used to infer an influence of the environment on foraging movement, using data from [Jha and Kremen, 2013]. These data consist of *Bombus vosnenskii* foragers collected along eight 1-km transects in the California chaparral. Each transect consisted of five sites, and at each site the floral community was censused: the average density of floral resources, the variation in the density of floral resources, and the species richness of flowering plants were measured [Jha and Kremen, 2013] for details about data collection). Individual bees were genotyped at polymorphic microsatellite markers

and assigned to sibships using COLONY [Wang, 2004]. The goal of the analysis is to determine whether individual foragers will travel longer distances to reach certain types of floral communities. To facilitate comparison between different methods of analysis, we include only the 70 colonies with at least two siblings.

By modifying equation 2.4 to address the research question, we model the log capture rate of foragers at a site j that is d_{ij} km distant from colony i:

$$\ln \lambda_i(j) = d_{ij}(-\eta + \theta_1 r_j + \theta_2 f_j + \theta_3 v_j) + \zeta_i + \epsilon_{ij} \tag{2.5}$$

where for site j the covariates $\{r_j, f_j, v_j\}$ are the centered and scaled floral species richness, average floral density, and coefficient of variation of floral density. In this model, ζ_i is the log capture rate at the colony location (i.e., when $d_{ij} = 0$). As the distance from the colony increases, the log capture rate decreases linearly with slope $\Delta_d(\ln \lambda)$. If the floral assemblage is homogeneous, so that the centered covariates $r_j, f_j, v_j = 0$ for all j, then $\Delta_d(\ln \lambda) = \eta$. The coefficients θ allow $\Delta_d(\ln \lambda)$ to vary continuously for different types of floral assemblages. The errors ϵ_{ij} are Gaussian and are included to account for over-dispersion in the observed counts.

The biological interpretation of this model is that the number of foraging siblings decreases with the distance from the colony: the attractiveness of a site to foragers is effectively penalised by the travel distance. At the colony location, the capture rate is not influenced by the floral assemblage (because bees would be captured at the colony location regardless of the surrounding

vegetation). As the distance from the colony increases, the capture rate decreases at different rates for different types of floral assemblages (Figure 2.6A). Thus, floral assemblages that are attractive to foraging bees are visited despite being far from the colony. The motivation underlying this model is to express the decline in forager abundance with distance as a function of characteristics of the floral community.

For the sake of comparison, we also analyse the data using a method similar to that used in [Jha and Kremen, 2013]: a hierarchical regression model which regresses the average pairwise distance between siblings ($\bar{d}_i$) onto the floral covariates averaged across sibling locations ($\bar{r}_i, \bar{f}_i, \bar{v}_i$). Random intercepts are included for each transect, so that

$$\mathbb{E}[\bar{d}_i] = \alpha_{s_i} + \beta_r \bar{r}_i + \beta_f \bar{f}_i + \beta_v \bar{v}_i$$

where $\{\beta_r, \beta_f, \beta_v\}$ are regression coefficients that model the change in average pairwise distance per unit increase in the pooled floral covariates. We use Bayesian methods for inference, but both models could be fit by penalised likelihood.

The two approaches to analysis lead to very different conclusions. The regression model predicts that bees will travel greater distances to forage at species-rich sites; and gives no evidence that the average or coefficient of variation of floral density have an influence on foraging distance (Figure 2.6B; black points are posterior means, black lines are 95% credibility intervals). In contrast, our model of capture rates predicts that bees will travel greater

distances to sites with few flowering species, and a dense and homogeneous distribution of floral resources (Figure 2.6C). An example of this type of floral assemblage is one dominated by a mass-flowering, evenly distributed shrub species.

The contradiction between these two sets of results is striking. To compare the accuracy of the methods while making few assumptions about the true biological process, we simulated data from a null model where bees were placed randomly (uniformly) across transect sites, while retaining the floral covariates and the numbers of bees per colony from the original data. On a dataset simulated from this null model, an accurate method of analysis should conclude that distance travelled does not depend on floral covariates. The rate of spurious conclusions (Type-I errors) can be assessed by trials across many datasets simulated from the null model. In almost all of the trials, the capture rate model gave the correct conclusion for all floral covariates, and on average gave parameter estimates close to 0. These results are shown in Figure 2.6C: the grey numbers are the proportion of 95% credibility intervals that contained 0; and the grey density is the distribution of posterior means from 1000 null simulations. For all parameters, the true rejection rates were above the expected 0.95.

In contrast, the regression model gave parameter estimates that were biased away from 0, on average. The estimated regression coefficient for richness from the original data–despite being positive and apparently 'significant'–fell well within the distribution of posterior means from the null simulation, in-

dicating that the positive coefficient should not be taken as evidence for an effect of floral species richness on foraging distance. The true rejection rates for the regression model applied to the null simulations were well below the nominal 95% (Figure 2.6B).

Why does the regression model perform so poorly, and lead to apparently spurious conclusions? One possible reason is that bees are collected across a discrete sample space and there are a finite number of possible combinations between the response variable (average pairwise distance) and the covariates (average site characteristics). For example, a colony with two captured bees has only one possible spatial arrangement that gives the maximum possible pairwise distance of 1 km: the bees would have to be located at opposite ends of the transect. There are two arrangements that give the second largest possible pairwise distance of 0.75 km, and so on. If the sites near the ends of the transect have an above-average floral species richness, then large pairwise distances will always be associated with increasing species richness, regardless of how the foraging bees are actually behaving. In such a situation, an apparent effect of species richness from a regression would be an artefact of the spatial configuration of sampling locations with regard to the floral community. The model of capture rates developed in this section does not suffer from these artefacts, because the occurrence of bees is modelled directly across a discrete sample space.

2.5 Discussion

Bees are effective pollinators of many flowering plant species [Fenster et al., 2004], and so are an indispensable component of terrestrial ecosystems that also provide pollination services to many crop plants [Kremen et al., 2002]. Social bees are generalist pollinators, and can travel long distances within a single foraging bout [Hagen et al., 2011]. Bees depend upon floral resources for carbohydrates and protein, and many plants depend upon bees for transmission of gametes; and thus the spatial scale at which foraging bees regularly move is extremely relevant to our understanding of how the landscape impacts the fitness of both parties [Jha and Dick, 2010]. From an applied perspective, a knowledge of the foraging range of pollinators such as bees is of great importance for the planning of habitat restoration and crop pollination [Keitt, 2009, Lonsdorf et al., 2009]. The estimation of colony locations can also be used for estimating population densities, and evaluating nesting habitat for conservation planning.

Here, we have described a spatially explicit, model-based approach for simulating and estimating foraging range from siblings genotyped at discrete locations. Although most of the applications we describe are simple, such a model-based approach easily accommodates complex effects at both the landscape- and colony- level. For example, the foraging range of bees could be modelled as a function of the average forage quality of the landscape, such that foraging kernels expand or contract depending on the phenology of plants throughout the landscape [Pope and Jha, 2018]. Our approach accurately de-

picts the sampling process (repeated captures at discrete locations) rather than assuming that the trapping locations are located continuously across the landscape, and also treats the colony locations as a unknown parameter to be estimated along with the foraging kernel; rather than sequentially estimating the colony location and then the foraging kernel. In practice, this is important as the shape of the foraging kernel can cause traps to vary in attractiveness: failing to account for this while estimating colony locations can introduce substantial error.

Using simulated data, we have illustrated that different schemes vary in their efficacy for estimating foraging range at various levels of organisation (individuals, colonies). In general, traps arranged in grids provide the most accurate estimates of foraging range across scales. However, our simulations suggest that discrete sampling methods will provide low accuracy in the estimates of individual foraging ranges, or the average foraging distances of colonies; with anything less than unrealistic densities of traps and captured siblings. On the other hand, as long as sufficient numbers of bees and colonies are captured within a landscape, the average foraging range across the landscape can be estimated with reasonable accuracy, or at least with consistent bias for all trapping methods. Even small numbers of traps can be effective at detecting differences in foraging range across landscapes, and our simulations suggest diminishing returns with increasing trap density with regard to estimation of foraging ranges at different scales. However, increasing the density of traps may substantially increase the probability of detecting dis-

tant colonies. If the goal of estimation is a measure of colony density within a landscape, even a transect may provide reasonable spatial coverage with a sufficient density of traps.

Using a dataset of wild bumble bee genotypes from the Californian chaparral [Jha and Kremen, 2013], we gave an example of how a transect design with a low trap density can be used to infer foraging behaviour across a heterogeneous landscape. Our analysis of these data suggests that bumble bees travel further to forage on dense, less variable, less speciose floral communities. Areas dominated by an evenly distributed, mass-flowering species are relatively conspicuous, and may encourage return trips by foraging bees by consistently providing pollen and nectar resources. Previous work has suggested that in variable environments, foraging bumble bees act to increase consistency in rewards while reducing the time spent searching [Biernaskie et al., 2009]. The strongest effect in our analysis is a preference of bees for the sites with the least variability in floral density. Such sites would have a consistent spatial distribution of floral resources, and so would reduce the time spent by bees in intra-site movement. Most strikingly, our method of analysis gives very different results from a regression-based approach that found an increase in foraging distance to species-rich floral communities. By simulation, we show that the conclusion from the regression analysis could easily result from a null model where foragers are located uniformly at random across transect sites. In contrast, the model developed in this work consistently returns correct results. We speculate that the poor performance of the regression approach

under the null model is due to a chance association between high floral species richness and relatively distant transect locations. Collections of bumble bee genotypes from the wild often contain few bees per colony, and we conclude that the choice of the method used to analyse these sparse data can have a large influence on subsequent biological inference. Care must be taken to employ a model that makes realistic assumptions about the sampling process.

In this work, we are influenced by the vast applied literature on the design and analysis of trapping experiments stretching back to the 1940s [Worton, 1987, Royle et al., 2013b], especially recent work on spatially-explicit capture-recapture models [Royle et al., 2013a]. Our contribution is to develop a simulation framework for the particular case of trapping social bees, to develop inferential methods for data matching this framework, and to demonstrate that the general approach can be effective for answering certain questions and ineffective for others. The tools we present here will be useful to those planning to use these types of methods. In particular, the R and C++ programs used to simulate data are available online (`github.com/nspope/foraging`). These programs are implemented as classes and designed in an object-oriented fashion; the user can define novel methods that define the visitation rates of foragers, the spatial arrangement of traps, and the stopping rule. User-defined methods interface easily with the existing code, allowing a great deal of flexibility in terms of the simulated study design.

We do not expect the results we present above to be relevant to every study; however, we suggest that scientists use simulation to investigate the

efficacy of a study design before deploying it. Given that sampling genetic material across many colonies and landscapes involves a great deal of effort and also frequently results in substantial mortality of bees, it is essential to try to maximise the amount of information carried per bee. As an example, in our simulations we observe that a density of 16 traps provides equivalent results to trap densities twice as large. These results imply that savings in human effort and bee mortality can be achieved by optimising sampling design with regard to the research question, and our worked example with *B. vosnesenskii* illustrates that a small but efficient sampling scheme may be deployed effectively across multiple landscapes. Simulation tools, such as the ones we develop here, can provide rough estimates of the sampling effort that is optimal for these applications. Finally, we note that with any estimation method, it is important to characterise the error associated with specific assumptions. In the context of this work, we have presented a method which tries to generate estimates of foraging range by integrating over uncertainty in the location of the colony and the shape of the foraging kernel. A source of error which we have not explored here (but we believe to be extremely important) is the uncertainty associated with sibling assignment by probabilistic genetic methods. A second topic which we do not address in this study, but we feel is deserving of attention, is the use of extant land classification maps in study design and analysis. We will address these topics in a future study.

2.6 Appendix: Details of implementation

We fit the models described in Sections 2.2 and 2.4 by Markov chain Monte Carlo, using the Bayesian computational platform Stan [Carpenter et al., 2017]. Stan uses a variant of a technique known as Hamiltonian Monte Carlo to generate proposals that are relatively far apart in parameter space yet have a high acceptance probability, and so is quite efficient for fitting high-dimensional models with relatively short Markov chains. We use multiple Markov chains per model fit, and monitor mixing and convergence visually and with the scale-reduction factor of [Gelman and Rubin, 1992]. Initial runs suggested that models converge quickly, within a few hundred iterations. For our simulation experiments, we automatically flagged model fits that showed signs of not converging (using a threshold for the scale reduction factor), and also visually inspected a random sample of fitted models. The Stan code implementing our model is found at `github.com/nspope/foraging`. We use vague log-normal priors for parameters controlling the shape of the foraging kernel, half-normal priors for variance components, and uniform priors for colony locations (with support on the rectangular area of the landscape used for simulations).

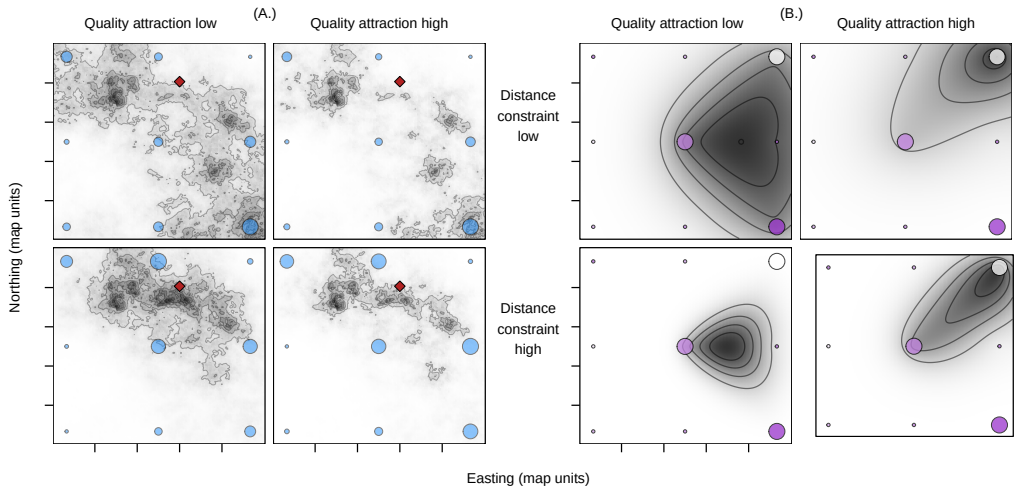

Figure 2.1: **(A)** The foraging kernel of bees (darker areas represent higher visitation) as a function of two parameters, which control the distance that bees travel (rows) and their affinity for quality forage (columns). The effect of increasing 'attractiveness' of forage quality is to focus bee activity on high-quality regions. The effect of the distance constraint is to focus bee activity on nearby regions. The diamond indicates the colony location. The points represent a trapping grid; the size of points reflects the relative probability that a bee will show up in that trap. This illustrates how the model can create asymmetric foraging kernels which depend both on the colony location and the configuration of the landscape. **(B)** The likelihood surface for the unknown location of a colony (darker areas represent a higher probability), where bees from the colony have been caught in equal number at three traps. The trapping grid is shown as coloured points: the size of the points reflects the number of bees captured at the trap, and the shade of the points represents the forage quality at the trap (low is light, high is dark). The colony is expected to lie close to the low-quality trap when affinity for forage quality is high. As the distance constraint increases, the expected colony location becomes equidistant to the three traps. The posterior distribution of the colony location is dependent on the parameters controlling the foraging kernel, and all must be estimated simultaneously.

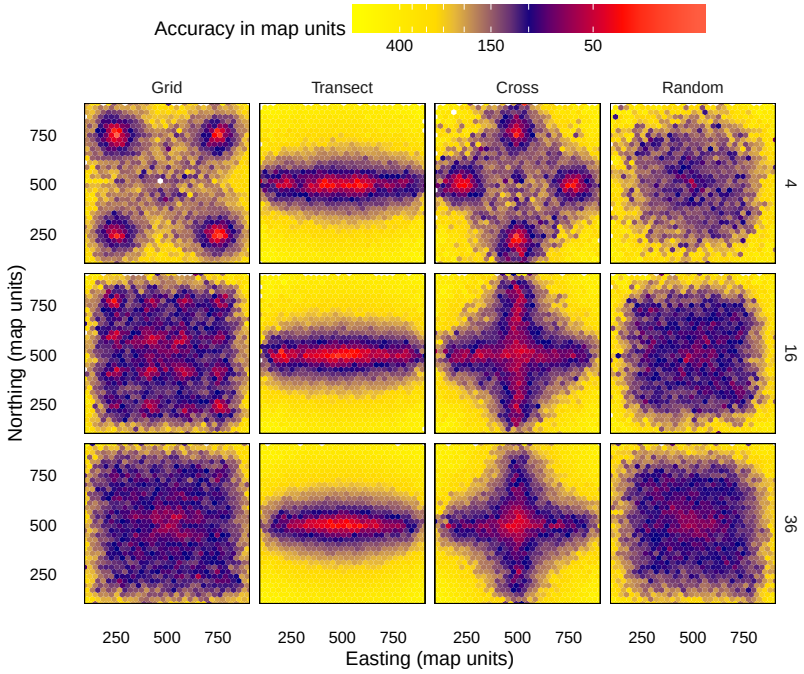

Figure 2.2: The accuracy with which a colony location is estimated, as a function of the spatial location of the colony. Colour at a given coordinate corresponds to the (average) accuracy with which a colony location at that coordinate was estimated. Shown for four trapping schemes (columns) across trap densities (rows; 4, 16, and 36 traps).

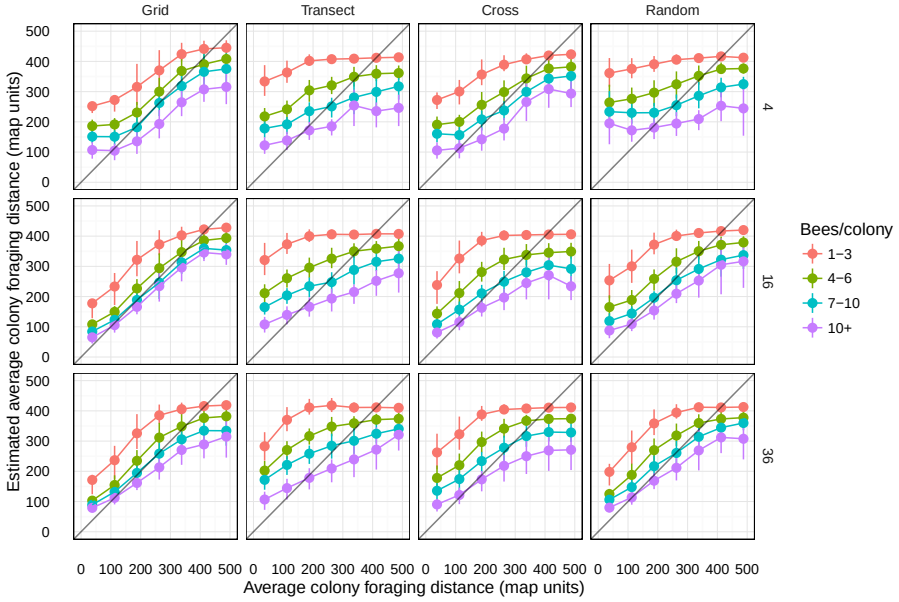

Figure 2.3: The true average foraging range for colonies, plotted against estimates of average foraging range (point: mean over all simulations; vertical lines: 50% quantiles). The black line shows a one-to-one relationship between estimated and true values. Shown for four trapping schemes (columns) across increasing trap densities (rows; 4, 16, 36 traps), at four different levels of sampling intensity (shade of lines/points).

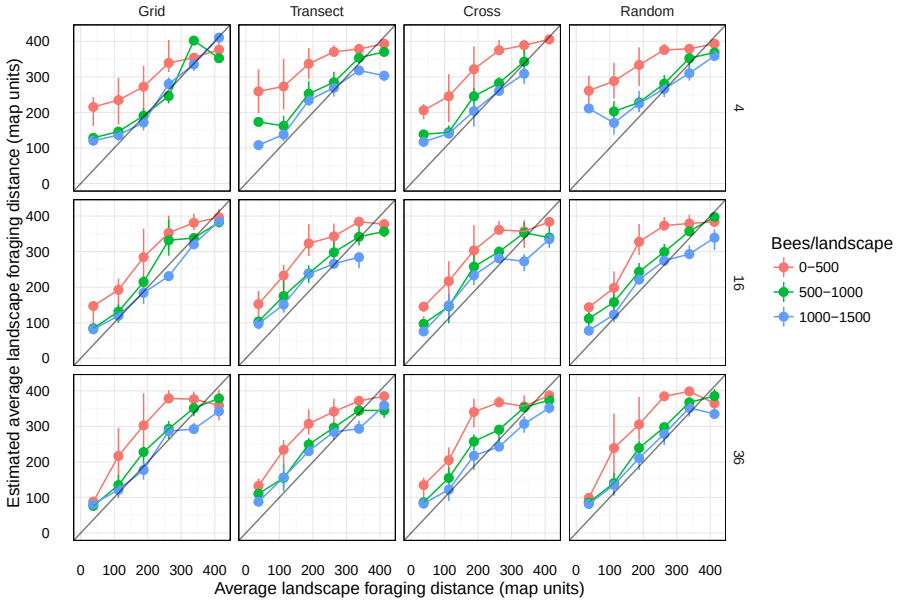

Figure 2.4: The true average foraging range of landscapes, plotted against estimates of average foraging range across simulated experiments. The points shown the average estimate over simulations, and the vertical lines give 50% quantiles. The black line shows a one-to-one relationship between estimated and true values. Shown for four trapping schemes (columns) across increasing trap densities (rows; 4, 16, 36 traps), at four different levels of sampling intensity (shade of lines/points).

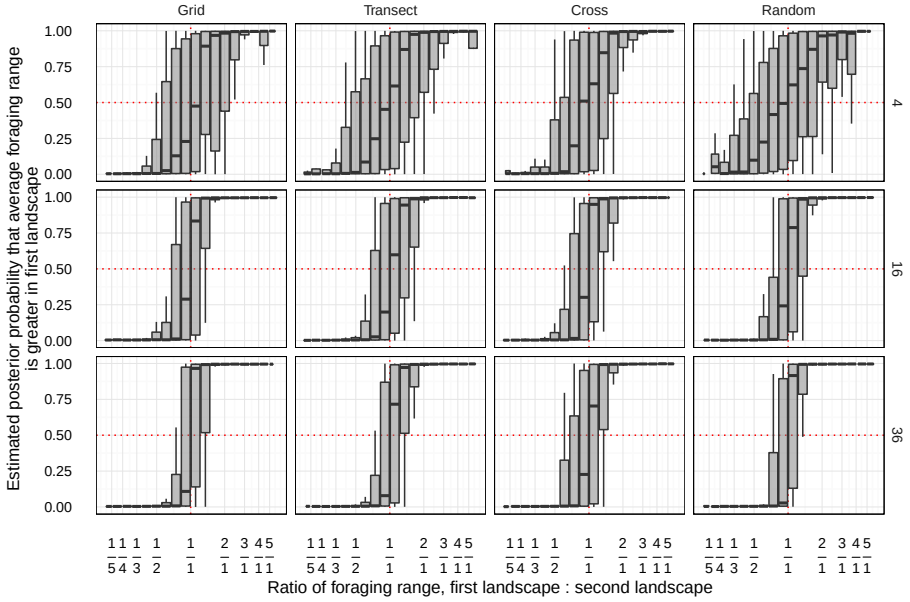

Figure 2.5: The estimated posterior probability that the first landscape (of a pair of landscapes) has a higher average foraging range; as a function of the true ratio of foraging ranges. The spacing on the x-axis is scaled as the log-ratio. Results from simulated experiments are binned into boxplots. Shown for four trapping schemes (columns) across increasing trap densities (rows; 4, 16, 36 traps).

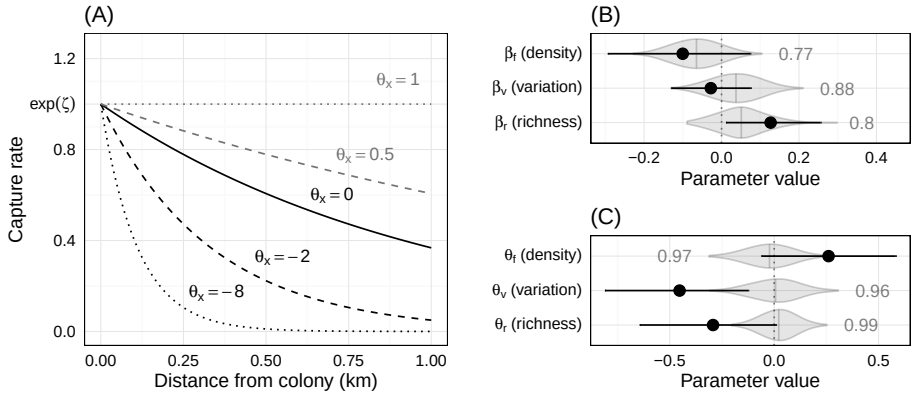

Figure 2.6: **(A)** An hypothetical illustration of how visitation can decline across distance at rates that depend on the floral community, following the model in equation 2.5. The parameter θ_x controls how a single floral covariate x influences the decline in visitation with distance from the colony. In this example, $x = 1$, $\exp\{\zeta\} = 1$, and $\eta = -1$. Negative values of θ_x imply that floral communities with $x > 0$ will be visited relatively less frequently at far distances. **(B-C)** Summary of results from the regression model (panel **B**) and the capture rate model (panel **C**) described in section 2.4. For key parameters, posterior means and 95% credibility intervals are shown as black points/lines. Positive values imply that foragers will travel further for increasing values of the covariate. The grey shaded regions show the density of posterior means across 1000 simulations from a null model where bees are distributed uniformly at random. The grey numbers give the proportion of 95% credibility intervals that contain 0 across these null simulations.

Chapter 3

Positive density-dependent reproduction regulated by local kinship and size in an understorey tropical tree

The research in this chapter represents a collaboration between the author, Dr. Antonio R. Castilla, and Dr. Shalene Jha, who jointly developed the research questions. The author led the modeling and statistical analysis, and co-wrote the study, which has been published as [Castilla et al., 2016b].

Global pollinator declines and continued habitat fragmentation highlight the critical need to understand reproduction and gene flow across plant populations. Plant size, conspecific density, and local kinship (i.e., neighbourhood genetic relatedness) have been proposed as important mechanisms influencing the reproductive success of flowering plants, but have rarely been simultaneously investigated. We conducted this study on a continuous population of the understory tree *Miconia affinis* in the Forest Dynamics Plot on Barro Colorado Island in central Panama. We used spatial, reproductive, and population genetic data to investigate the effects of tree size, conspecific neighbourhood density, and local kinship on maternal and paternal reproductive success. We used a Bayesian approach to simultaneously model the effects of our explanatory variables on the mean and variance of maternal viable seed

set and siring success. Our results reveal that large trees had lower proportions of viable seeds in their fruits but sired more seeds. We documented differential effects of neighbourhood density and local kinship on both maternal and paternal reproductive components. Trees in more dense neighbourhoods produced on average more viable seeds, although this positive density effect was influenced by variance-inflation with increasing local kinship. Neighbourhood density did not have significant effects on the siring success. This study is one of the first to reveal an interaction among tree size, conspecific density, and local kinship as critical factors differentially influencing maternal and paternal reproductive success. We show that both maternal and paternal reproductive success should be evaluated to determine the population-level and individual traits most essential for plant reproduction. Based on our findings, we suggest the inclusion of small trees and the conservation of dense patches with low kinship as potential strategies for strengthening the reproductive status of tropical trees.

3.1 Introduction

Forest fragmentation and habitat degradation represent major threats to terrestrial biodiversity [Sala et al., 2000, Laurance et al., 2014]. Deforestation and resulting declines in organism population density can fundamentally disrupt positive and negative density-dependent processes, potentially compromising survival and reproductive success for a variety of plant and animal taxa [Wright, 2002, Waters et al., 2013, Mugabo et al., 2014]. For instance,

negative density dependence due to shared enemies or intraspecific competition may lead to reduced spatial aggregation of conspecific individuals and coexistence of different species [Janzen, 1970, Connell, 1971]. Likewise, positive density dependence has been proposed as an important mechanism influencing reproduction and survivorship for a number of organisms, also known as 'Allee effects' [Allee et al., 1949, Stephens et al., 1999]. In such cases, conspecific individuals occurring at low densities may struggle to find mates, resulting in reproductive failure [Groom, 1998, Liebhold and Bascompte, 2003].

Plant reproductive processes may be particularly sensitive to changes in local density given that many plant species require animal pollination, and animals often exhibit frequency-dependent foraging behaviours [Ollerton et al., 2011, Kacelnik et al., 1986, Dreisig, 1995]. Plant density also drives conspecific flowering density, which can influence both maternal (e.g. seed viability) and paternal (e.g. siring success) components of plant reproductive success [Bosch and Waser, 1999, Ghazoul, 2005]. This is largely due to the fact that pollinators can change their foraging behaviour in response to flower density, foraging more in dense patches due to the reduction in inter-patch travel [Kacelnik et al., 1986, Dreisig, 1995]. Thus, plants growing at low densities may experience reproductive decline owing to difficulties in attracting pollinators from competing conspecifics occurring at higher densities [Kunin, 1997, Ghazoul, 2002, Waites, 2004]. In addition to conspecific density, individual traits like tree size may influence reproductive success, as floral displays in large trees may enhance pollinator attraction leading to increased seed set [Clark

and LaDeau, 2004] and siring success [Latouche-Hall et al., 2004, Tani et al., 2012]). While these past studies reveal a major role for both positive density dependence and individual size in plant reproduction, little is known about how plant reproductive processes are influenced by landscape-level patterns of genetic relatedness.

Specifically, recent studies have revealed that the net effect of positive density dependence on reproduction may be mediated by kinship within the conspecific neighbourhood [Jones and Comita, 2008, Hirao, 2010]. Kinship among plants frequently decreases with increasing spatial distance leading to fine-scale spatial genetic structuring within plant populations [Vekemans and Hardy, 2004]. Interestingly, despite the fact that most plants exhibit high levels of local kinship with potentially important consequences for both maternal and paternal components of reproductive success [Jones and Comita, 2008], we know comparatively little about the effects of this local kinship on plant reproductive success. For example, dense patches of conspecific trees can receive greater visitation from pollinators but may receive poorer quality pollen from neighbours with shared kinship [Byers, 1995, Souto et al., 2002, Elam et al., 2007]. Fruits resulting from matings between close relatives may exhibit higher levels of homozygosity or deleterious gene combinations that may result in embryos and endosperms with deficient maternal investment and thus, increased abortion rates [Korbecka et al., 2002, Hufford and Hamrick, 2003, O'Connell et al., 2006]. Furthermore, local kinship may critically impact plant reproductive success by modifying the *mean*, but also the

variance of maternal and paternal reproductive success. The variance exhibited in the proportion of viable seeds can be substantial among species with multiovulate ovaries [Gorchov, 1985, Jordano, 1991, Obeso and Herrera, 1994]. These differences in within-plant viable seed set may lead to among-plant differences in reproductive success through their influence on seed predation, the spatial characteristics of post-dispersal seed shadows, seed dispersal success, or some combination of these [Herrera, 1984, Herrera, 2009]. Available evidence suggests that both seed predators and frugivores may exhibit variance-averse behaviour in response to among-plant differences in the resource quality, with major implications for dispersal and population growth [Herrera, 2009]. Despite the ecological importance of within-plant reproductive variance, few studies have incorporated variance when investigating reproductive success in plants.

Interestingly, for hermaphroditic plants, reproductive success is a function of the proportional allocation to male vs. female functions with this sex allocation being expected to vary across ecological systems. Among conspecific individuals, sex allocation can vary due to genetic or environmental factors [Wright and Barrett, 1999, Mazer, 1992]. According to sex allocation theory, individuals may adjust sex allocation to their size (i.e., size-dependent sex allocation; [Klinkhamer and De Jong, 1997]). Specifically, in animal-pollinated plants, the male fitness-gain curve is expected to decelerate because increased pollen production leads to more competition for ovules by pollen grains of the same parent [Lloyd and Bawa, 1984]. Likewise, large flower numbers can result

in increased geitonogamy and, in turn, reduced pollen available for outcrossing, a process known as pollen discounting [Harder and Barrett, 1995, Jong, 2000]. These past studies suggest that larger plants may be expected to exhibit increased female function but decreased male function. Furthermore, the density of conspecific plants can also influence sex allocation patterns in hermaphroditic plants. For instance, Mazer [Mazer, 1992] found that increased local population density results in the production of male-biased flowers in *Raphanus sativus*. Thus, a comprehensive evaluation of size, density, and kinship impacts on hermaphroditic plant reproduction should include the analysis of both sexual functions. However, past research has largely focused on maternal fitness to characterize a plant's overall fitness, ignoring male reproductive success due to the practical limitations of measuring this component [Harper, 1977, Karron and Mitchell, 2012].

In this study, we use spatial, reproductive, and population genetic data to investigate both maternal and paternal reproduction and the interaction between conspecific density and local kinship in the understory tropical tree *Miconia affinis*. We used a Bayesian framework to simultaneously model the effects of tree size, neighbourhood density, and local kinship on the mean and variance of viable seed set (female reproductive success), and a fractional paternity model to investigate effects on siring success (paternal reproductive success). We conducted this study within the 50-ha Forest Dynamics Plot on Barro Colorado Island (BCI), Panama [Condit, 1998, Hubbell et al., 1999], focusing on *M. affinis,* given that this species exhibits potential for varia-

tion in local kinship, as documented in other regions [Jha and Dick, 2008]. Specifically, we investigated the following hypotheses: (A) *M. affinis* exhibits significant kinship at small spatial scales similar to other animal-dispersed tree species; (B) large trees and more dense conspecific neighbourhoods will exhibit greater and more consistent (i.e., less variable) proportions of viable seeds and will have greater and more consistent siring success than smaller trees and sparse neighbourhoods; (C) the positive effect of local density on maternal reproductive success will be negatively regulated by local kinship, resulting in lower and more variable proportions of viable seeds in trees within neighbourhoods of high kinship.

3.2 Materials and Methods

Study species and sampling. *Miconia affinis* D.C. (Melastomataceae) is a self-incompatible understory tree (3-6 m) that is broadly distributed in the neotropics, ranging from Mexico to Brazil [Jha and Dick, 2010]. It exhibits a typical "big bang" flowering pattern with individuals producing a large number of flowers over a short time frame (i.e., 2 days; [Augspurger, 1980]). The flowers are visited by a large diversity of social and solitary bees [Jha and Dick, 2010]. Inflorescences have 50-300 white flowers, each approximately 8cm in diameter, arranged in terminal panicles. Like many other melastomes, *M. affinis* has deep poricidal anthers which must be vibrated by a pollinator in order for pollen to be released (i.e., "buzz-pollination"). Fruit ripening takes 3-4 months (May-July), with globose berries (3 mm long; 6 mm wide) turning

from green to purple-black during the ripening. Fruits are dispersed by a variety of birds and bats [Jha and Dick, 2008, Luck and Daily, 2003]. Each fruit contains numerous minute seeds (30-50 seeds per fruit). Fertilized seeds are yellow, pyramidal, and 3-4x times larger than the dark, crescent-shaped, unfertilized ovules.

The study was conducted in the 50-ha Forest Dynamics Plot which was established in 1980 in the tropical moist forest of Barro Colorado Island (BCI) in Gatun Lake in central Panama. The plot consists of a standing number over 350,000 mapped stems 10 mm or above in diameter at breast height (DBH) of approximately 300 plant species (`ctfs.arnarb.harvard.edu/webatlas/datasets/bci`). Censuses have been conducted every five years since 1981.

Finally, to determine the density and spatial patterning of *M. affinis* with respect to other species in the 50-ha BCI plot, we calculated average density for 51 understory, 57 midstory, and 118 canopy tree species in the plot `www.ctfs.si.edu/site/Barro+Colorado+Island/abundance/`. We used data from the 2005 census (the most recent available), and for each species we included all trees greater than 10mm DBH. The density of M. affinis trees of $>$ 10mm DBH in the BCI plot was 7.78 trees/ha, which is lower than the average density found for understory tree species (23.12 $\pm$ 10.99 trees/ha). *M. affinis*' density in the plot was more similar to those reported for midstory and canopy tree species (10.42 $\pm$ 2.30 and 10.97 $\pm$ 2.73 trees/ha respectively). Furthermore, we evaluated the spatial patterning of M. affinis relative to other species by examining neighbourhoods of individual trees inside the plot follow-

ing the approach used in [Condit et al., 2000]. Specifically we used the mean conspecific density within 10 m of a tree relative to the species' overall density across the whole plot (Ω_{0-10}), as the estimate of species' spatial aggregation [Condit et al., 2000]. *M. affinis* trees exhibited a clumped spatial distribution ($\Omega_{0-10} = 7.9$), an estimate relatively close to the median for all the species in the plot.

In July 2010, we surveyed all *M. affinis* trees greater than 10 mm DBH (389 trees) to determine which trees were reproductive (exhibited infrutescences; hereafter "reproductive tree"), revealing 124 reproductive trees. Based on past studies of the species, only *M. affinis* trees greater than ~10 mm DBH produce flowers, though they may not flower regularly among years; in contrast trees greater than 15-20 mm typically flower annually. The geographic coordinates of each tree were recorded with a portable GPS GARMIN eTrex Vista (GARMIN, Southampton, UK). We checked that our geographic coordinates matched those reported in the Smithsonian Tropical Research Institute database. For each reproductive trees, we measured DBH, recorded the spatial location, and obtained leaf tissue samples. To measure seed viability (i.e., proportion of viable seeds per fruit) and to collect seed arrays for paternity analyses, 21-24 fruits were randomly sampled from each of 20 randomly chosen reproductive trees (N = 457 fruits). The mean number of total seeds and viable seeds per fruit were 44.06 ± 19.98 and 29.27 ± 17.12, respectively. For the paternity analysis, one seed was randomly selected from each fruit (N = 457 seeds). Multiple paternity is common in seeds from different fruits [Jha

and Dick, 2010], but it has not been still analyzed at the fruit level although is the focus of an ongoing study. The seeds were soaked for 48 hours in sterile water before DNA extraction. Total genomic DNA was extracted from both adult leaf tissue and seed tissue using the DNeasy Plant kit (Qiagen). All trees and seeds were screened at seven highly polymorphic microsatellite loci following the protocols described in [Jha and Dick, 2009] and [Le Roux and Wieczorek, 2008], and genotyped on an ABI 3730 Sequencer. Alleles were scored manually using GENEMARKER (Softgenetics).

3.2.1 Statistical analysis

Polymorphism of microsatellite markers and mating system. The probability of null alleles was calculated using the software Micro-Checker [Van Oosterhout et al., 2004]. Allelic richness was estimated using rarefaction in HP-RARE [Kalinowski, 2005]. Nei's gene diversity was calculated using GenAlEx 6.501 [Peakall and Smouse, 2012].

The multilocus outcrossing rate (t_{m}), single-locus outcrossing rate (t_{s}) and biparental inbreeding (t_{m} - t_{s}) were estimated using software based on the maximum likelihood method in MLTR v3.2 [Ritland, 2002]. Standard errors for each estimate were obtained using 10000 bootstrap replicates and mother family as the resampling unit. Furthermore, we calculated the inbreeding coefficient ($\mathrm{F_{is}}$) in adult trees and seeds using GENEPOP v4.0.10 [Raymond and Rousset, 1995].

Spatial genetic structure and tree size. We calculated the statistic F_{ij} using the software SPAGeDi [Loiselle et al., 1995, Hardy and Vekemans, 2002] as a measure of kinship between paired trees (i.e. higher pairwise F_{ij} represents greater kinship between two individuals). We used a randomization test to evaluate whether the study population of *M. affinis* has a greater degree of spatial genetic structure and size structure than would be expected at random, under a null model where the geographic coordinates of trees are fixed, but tree genotype and DBH are exchangeable within spatial strata. To detect spatial genetic structure at different scales, we used local polynomial fitting (LOESS) [Cleveland and Devlin, 1988] of pairwise kinship to pairwise spatial distance between all possible pairs of trees. To test if the average observed kinship predicted by LOESS at a given distance differed from the null model, we permuted row and column indices for the kinship matrix 999 times, and at each permutation we refitted the LOESS model using the permuted kinship and spatial distance matrix. We used the 95% percentiles of the permutation-derived LOESS predictions to generate a confidence envelope around the null expectation of $F_{ij} = 0$. In addition, we examined spatial autocorrelation in DBH by calculating spatial semivariance for DBH and fitting a LOESS curve to describe semivariance over spatial distance.

Model details We separately modelled seed viability (the proportion of viable seeds within fruits) and siring success (proportion of seeds attributable to a father). We used JAGS [Plummer, 2003] to fit the models via Markov

chain Monte Carlo (MCMC). For all models, we ran three Markov chains for 2 million iterations; chains were visually inspected to ascertain convergence then subsampled to ensure independent samples from the posterior. For our models of seed viability and siring success, our hypotheses are directional and thus, are one-way tests of the sign (positive or negative) of regression coefficients. For each regression coefficient, we summarized the posterior distribution by its expectation and 95% credibility interval.

Seed viability: maternal reproductive success. Because differences in within-plant reproductive variation are critical in reproductive ecology [Herrera, 2009], we used a Bayesian approach for a combined analysis of mean seed viability and within-plant variance in seed viability, by simultaneous regression of the logit-transformed mean and log-transformed variance. We fit a series of hierarchical, spatial regression models via MCMC to evaluate the effects of DBH, conspecific neighbourhood density and local kinship on seed viability. For each fruit, we defined seed viability as the proportion of viable seeds out of the total number of seeds (viable + aborted). We used seed viability as the estimate of maternal reproductive success because fruits of *M. affinis* can still mature when they contain a full complement of aborted seeds (unpubl. res.). Therefore, seed viability per fruit is the most reliable estimate of the maternal reproductive success for *M. affinis*. We considered three covariates in our seed viability model: mother DBH, mother neighbourhood density and mother local kinship (mean kinship of trees within 150 m from

the mother, the threshold distance for which trees exhibit increased kinship; see section 3.3). We also included an interaction between mother local kinship and mother neighbourhood density.

We denoted the proportion of viable seeds within the ith fruit as ϕ_i. Variability in ϕ across a tree can be expressed as a probability density with support on the interval [0,1] – denoted $f(\phi)$ where $0 < \phi < 1$. The value of $f(\phi)$ at any value $\phi = x$ is the frequency of fruits with a proportion x of viable seeds. Because $f(\phi)$ is a probability distribution on $[0, 1]$, the integral $\int_0^1 f(\phi)d\phi = 1$, and represents every fruit on the tree. The shape of $f(\phi)$ varies across trees. For the jth tree, let the distribution of seed viability in fruit be $f_j(\phi)$. A biologically meaningful way to summarise the distribution at a given tree is to evaluate the probability that a fruit selected at random from a tree has at least p proportion of viable seeds. This quantity can be found with the complement of the cumulative distribution function corresponding to $f_j(\phi)$, that is $1 - \int_0^p f(\phi)d\phi$, and equals the estimated fraction of fruits on a tree with at least a proportion p seeds that are viable.

We used a hierarchical, spatial regression to model the shape of $f(\phi)$ as a function of tree-level covariates. An expressive choice for $f(\phi)$ is the logit-normal distribution [Mead, 1965], which is parameterized by location θ (e.g. mean on logit scale) and dispersion ψ (e.g. std. deviation on logit scale). For the ith fruit on the jth tree, let logit $\phi_{ij} \sim \mathcal{N}(\theta_j, \psi_j)$, let the count of viable seeds equal y_{ij}, and the total number of seeds equal n_{ij}. At the level of individual fruits, we modelled the counts of viable seeds as a binomial

variable, $y_{ij} \sim \mathcal{B}i(n_{ij}, \phi_{ij})$, where ϕ_{ij} is the probability that a given seed will be viable. We allowed the distribution of ϕ_{ij} to vary across trees, according to tree-specific mean seed viability θ_j and within-tree variance in seed viability ψ_j. We fit a joint regression model that relates both θ_j and ψ_j to the matrix of tree-specific covariates, with spatially correlated, multivariate normal errors.

$$\begin{bmatrix} \theta_j \\ \ln \psi_j \end{bmatrix} \sim \mathcal{N}\left(\begin{bmatrix} x_j'\beta \\ x_j'\rho \end{bmatrix}, \begin{bmatrix} \tau^2 & \tau\omega\chi \\ \tau\omega\chi & \omega^2 \end{bmatrix} \right) \tag{3.1}$$

where x_j is the vector of covariates for the jth tree, β and ρ are vectors of regression coefficients, τ^2 and ω^2 are the variance and χ the correlation for the mean seed viability and within-tree variance in seed viability, respectively. We used a Gaussian correlation function to capture spatial autocorrelation among tree-specific mean seed viabilities and within-tree variances (e.g. so that the full covariance matrix is the Kronecker product of equation 3.1 and a parameterized spatial covariance matrix, appendix 3.5).

The observed proportion of viable seeds in a fruit could vary systematically as a function of the total seed production per fruit. In our seed viability models, we assume that the total number of seeds in a fruit is independent of the proportion of viable seeds in that fruit, and that the total number of seeds in a fruit is independent of the measured covariates. If the first assumption is violated, then any intrinsic or extrinsic factors which influenced the total number of seeds in a fruit would also influence seed viability. If the second assumption is violated, then any observed association between any covariate and the proportion of viable seeds may be an artifact of an association (with

the opposite sign) between that covariate and the total number of seeds. To test these assumptions, we fit two hierarchical models to estimate (1) the correlation between total seed production and the number of viable seeds, (2) the regression between mother covariates and total seed production (appendix 3.6).

Siring success: paternal reproductive success. We used the fractional paternity model of Hadfield [Hadfield et al., 2006] implemented in the R package MasterBayes to evaluate how siring success changes with spatial distance to the mother, tree DBH, and father's neighbourhood density. Siring success was defined as the probability of a seed sired by a specific father tree on a specific mother tree. In our siring success model, the spatial distance between mother and father trees was highly correlated with the mean nearest neighbour distance from the father tree (r = 0.82, 95% CI 0.75 to 0.87). To avoid collinearity between our explanatory variables, we used the coefficient of variation (CV) of mean nearest neighbour distances (hereafter "neighbourhood density") instead of the mean nearest neighbour distance. Although the neighbourhood density is highly negatively correlated with the mean nearest neighbour distances for any number of neighbours, it is less collinear with distance to mother trees (r = -0.47, 95% CI -0.32 to -0.60). For consistency with the siring success model, we also used this measure in place of mean nearest neighbour distance in the seed viability models. In addition, we ran the seed viability models using the mean nearest neighbour distance instead of

the neighbourhood density, and found consistent results with both analyses. We considered three covariates and an interaction in our siring success model: father DBH, father neighbourhood density, spatial distance to the mother and the interaction between father neighbourhood density and spatial distance to the mother.

We modelled the relative probability of paternity as a function of these covariates and the genotypes of parents and offspring. For a given seed i from mother j, the probability of paternity P_{ijk} for father k is proportional to:

$$P_{ijk} \propto \exp\left\{ z'_{jk}\eta + \sum_{l=1}^{L} \ln \Pr(G_{il}|G_{jl}, G_{kl}) \right\}$$

Where z'_{jk} is the vector of covariates listed above, η is a vector of regression coefficients, and $\Pr(G_{il}|G_{jl}, G_{kl})$ are the Mendelian inheritance probabilities (incorporating genotyping error) at the lth locus for offspring genotype G_{il}, paternal genotype G_{kl}, and maternal genotype G_{jl} when the mother is known [Marshall et al., 1998]. This model jointly estimates the regression coefficients and paternity probabilities of each father for each seed. We used the approximation of genotyping error described in [Hadfield et al., 2006]. Using the estimated fractional paternity probabilities, we calculated the averaged pollen dispersal distance in the study population and its standard deviation.

3.3 Results

Polymorphism of microsatellite markers and mating system. Micro-Checker indicated that none of the loci exhibited signs of having null alleles.

Average allelic richness based on rarefaction was 3.54 (± 0.56) and 3.54 (± 0.57) in adult trees and seeds respectively. Average Nei's gene diversity was 0.566 (± 0.102) and 0.560 (± 0.103) in adult trees and seeds respectively.

Adult trees and seeds did not differ in their average inbreeding coefficient (0.110 ± 0.051 and 0.139 ± 0.075 respectively). The multilocus outcrossing rate was near to 100 % ($t_{\mathrm{m}} = 0.970 \pm 0.011$). However, there was a significant difference between multilocus and single locus outcrossing rates ($t_{\mathrm{m}} - t_{\mathrm{s}} = 0.150 \pm 0.030$), which implies a relatively high proportion of biparental inbreeding in the *M. affinis*' population in the 50 ha Barro Colorado Island plot.

Spatial genetic structure and size. On average, we found that *M. affinis* trees separated by less than approximately 150 m exhibited significantly greater kinship than expected under the null model, while trees separated by approximately 200 m to 350 m exhibited significantly less kinship than expected under the null model (Fig. 3.1A). Based on these results, we set a spatial threshold of 150 m when calculating average local kinship in subsequent models. The mean spatial semivariance in tree DBH did not exceed the 95% quantiles of the null distribution at any distance (Fig. 3.1B).

Seed viability: maternal reproductive success. We did not find support for increased seed viability in larger trees (posterior probability = 0.049; Table 3.1). Instead, our results indicate a negative relationship between mean

seed viability and mother DBH (mean effect = -0.46; Table 3.1). We found strong evidence for an increase in the mean seed viability in dense neighbourhoods (Table 3.1, Fig. 3.2A). We did not find evidence for a decrease in the mean seed viability with increasing local kinship or for an interaction between neighbourhood density and local kinship (Table 3.1; Fig. 3.2A). We also found no support for a decrease in variance of seed viability with increasing mother DBH or increasing density in the neighbourhood (Table 3.1). However, we found strong evidence that the variance of seed viability increases with local kinship, and that the magnitude of this trend was influenced by the spatial isolation of the mother (Table 3.1; Fig. 3.2A). This interaction implied that the variance-inflating effect of local kinship was exaggerated in dense neighbourhoods (Fig. 3.2A right panel; Table 3.1).

The estimated probability that a random fruit will have a high proportion of viable seeds increased sharply with neighbourhood density in neighbourhoods with low kinship (Fig. 3.2B, left panel; Fig. 3.4). As local kinship increased, the rate of this positive density effect decreased (Fig. 3.2B, central panel; Fig. 3.4). Finally, in neighbourhoods with high kinship, the probability that a fruit drawn at random had a high or low proportion of viable seeds (i.e. high variance) increased with the neighbourhood density, leading to the variance-inflating effect of neighbourhood density in neighbourhoods with high kinship (Fig. 3.2B, right panel; Fig. 3.4). The estimated trends in mean seed viability do not appear to be artifacts of a relationship between the covariates and total seed production per fruit. Total seed production per

fruit did not change as a function of mother DBH (estimate: -0.03, 95% CI -0.17 to 0.10) or neighbourhood kinship (estimate: -0.12, 95%CI -0.30 to 0.06). We found no evidence for a general correlation between the total number of seeds per fruit and the proportion of aborted seeds in the same fruit (mean correlation partially pooled across trees: 0.05, 95% CI -0.20 to 0.12).

Siring success: paternal reproductive success. We estimate an average pollen dispersal distance of 231.4 m (95% CI 219.3 to 244.0) for the *M. affinis* population in the 50 ha Barro Colorado Island plot. We found that siring success increased with the DBH of the father, but we did not find that siring success decreased with the spatial isolation of the father (Table 3.1; Fig. 3.3). We found that the relative probability of paternity decreased with the spatial distance between a given mother and father, but the magnitude of this trend did not change with the degree of spatial isolation of the father (Table 3.1; Fig. 3.3).

3.4 Discussion

In this study, we reveal differential effects of tree size on the maternal and paternal reproductive success. Larger trees exhibit lower mean seed viability but greater siring success than smaller trees. Our results provide evidence for positive density dependence in mean seed viability, but also indicate that within-tree variance in seed viability increases with neighbourhood kinship. Specifically, we show that the rate of this variance inflation increases

with neighbourhood conspecific density. In contrast, neighbourhood density does not show significant effects on paternal reproductive success. These results have implications for plant reproductive biology, plant-pollinator and plant-seed-disperser interactions, and the conservation of flowering plant populations.

Maternal reproductive success. Results of the present study support a strong positive effect of neighbourhood density on mean seed viability. Increased female fecundity in dense conspecific neighbourhoods has been reported in other flowering plant species [Knight, 2003, Duffy and Stout, 2011, Waal et al., 2014]. In the specific context of this tropical tree species, positive density-dependent reproduction is expected to be especially relevant because most tropical plant species generally occur in low population densities and rely on animals for cross-pollination. Specifically, our findings of positive density dependence for seed viability are congruent with those of other tropical tree species [Jones and Comita, 2008, Caraballo-Ortiz et al., 2011]. One explanation for positive density-dependent reproduction is that more dense groups of trees have greater neighbourhood floral displays that can increase individual reproductive success by attracting positively density-dependent pollinators [Levin and Kerster, 1969, Schaal, 1978]. Pollinators often choose areas of high floral density in order to reduce foraging effort [Kacelnik et al., 1986, Harder, 1990, Dreisig, 1995]. In this regard, *Trigona* bees constitute a substantial component of *M. affinis* pollinator fauna [Jha and Dick, 2010]. and these

and other small-bodied species are often limited to a few hundred meters of foraging ability [Roubik and Aluja, 1983, Hubbell and Johnson, 1978, Slaa et al., 2003], potentially enhancing their preference for high-density *M. affinis* floral patches. However, positive density reproduction could be counteracted by negative density-dependent processes influencing other stages of the life cycle [Peters, 2003]. For example, the survival of seeds and seedling is often negatively related to the conspecific density in many tropical trees [Janzen, 1970, Comita et al., 2014]. Therefore, further studies should evaluate the role of density-dependent processes at different stages of the life cycle of *M. affinis* to understand the net contribution of positive-dependent reproduction on the individual fitness.

Our results also reveal that *M. affinis* trees separated by less than approximately 150 m exhibited significantly increased kinship. In a previous study, increased levels of local kinship were reported for *M. affinis* in forest habitats in Mexico [Jha and Dick, 2008]. Nevertheless, fine-scale spatial genetic structure can vary widely among plant populations [Born et al., 2008], and thus, we examined its existence in the BCI population before including local kinship as an explanatory variable in our seed viability model. Although few studies have examined the effect of local kinship on plant reproduction, the scarce available evidence points out a negative impact of increased local kinship on *mean* seed viability [Jones and Comita, 2008, Hirao, 2010]. In contrast, our results showed a significant interaction between the local kinship and conspecific density with high local kinship and conspecific density causing an

increase in within-tree *variance* in the seed viability rather than affecting the mean seed viabilities of the trees. Specifically, our results showed that trees in dense neighbourhoods with high kinship tended to have fruits with either high or low proportions of viable seeds. This marked bimodality in the seed viability of fruits could be related to a selective abortion of seeds in fruits with large biparental inbreeding load [Hufford and Hamrick, 2003, O'Connell et al., 2006, Zhao and Lu, 2009]. Our results indicated that biparental inbreeding was substantial in the BCI population, exceeding 10 % of the mating events. In addition, the mean dispersal distance for *M. affinis* in the 50-ha BCI plot was 231.4 m (95% CI: 219.3 to 244.0 m), indicating that most of the dispersal events occur among trees within the spatial scale of high kinship. This non-random or selective abortion resulting from competition among developing fruits, as described in the first scenario, is common in plants [Lee and Bazzaz, 1982]. Future studies using controlled crosses of trees with known kinship will help to clarify the role of the offspring's genetic composition and the abortion rate per fruit. Whatever the causal mechanism, within tree variability in viable seed set may lead to variation in seed predation and seed-shadow characteristics that could result in a number of downstream ecological changes, including differential fruit removal by seed dispersers and differential seedling recruitment [Herrera, 1984, Herrera, 2009].

Finally, plant size has been frequently proposed as a suitable predictor of the plant reproductive success, with large plants being considered conservation targets for the maintenance of reproductive processes in plant popula-

tions [Clark and LaDeau, 2004]. Interestingly, our results reveal a negative relationship between DBH and the proportion of viable seeds per fruit. In some ecological scenarios, total seed production may be positively related to DBH, such that the number of ovaries available for fertilization per fruit is a function of tree size. However, our results show that mean total seed production per fruit (i.e., viable + aborted seeds) did not vary as a function of mother DBH. Thus, we posit that a more likely explanation is that increased proportion of viable seeds per fruit in smaller trees is due to a decrease in geitonogamy through a reduction in the floral display, as seen in other studies [Klinkhamer and de Jong, 1993, Castilla et al., 2011]. *Miconia affinis* is a self-incompatible buzz-pollinated tree and thus, its reproductive success is highly sensitive to stigma clogging due to the receipt of self-pollen, which can be high in buzz-pollinated species [Duncan et al., 2004]. Regardless, it should be noted that we did not quantify the total fruit production per tree, thus large trees could potentially have higher total fruit production compensating for their reduced per-fruit seed viability. Therefore, we can conclude that increasing DBH negatively correlates with the quality of the female reproductive success, but further studies are required to determine impacts on overall maternal fecundity. Finally, we must highlight that despite the modest sampling size in the viability models (N = 20 mother trees, 457 fruits), the range of variation of DBH and conspecific density was similar for our data set and the entire reproductive population. Nevertheless, the largest trees in the population were underrepresented in our data set. Therefore, further analyses should

increase the number of mother trees as well as the representation of the largest individuals in the population.

Paternal reproductive success. According to sex allocation theory, larger plants are expected to exhibit increased female function at the expense of a decreased male function [Klinkhamer and De Jong, 1997], though increased siring success in larger trees has been reported in some species [Latouche-Hall et al., 2004, Tani et al., 2012]. Our combined analysis of both sexual functions reveals the existence of contrasting maternal and paternal reproductive success patterns, mediated by tree size. However, this pattern is in the opposite direction to theoretical expectations. While large trees sired more seeds in the population, they had lower proportions of viable seeds in their own fruits.

We posit that large trees may sire more seeds through higher pollinator visitation rates, however seed set may be reduced due to the high receipt of self-pollen by geitonogamy. This pattern also highlights the importance of evaluating both components of the reproductive success when determining the impact of individual size on population-level reproduction. In contrast to studies suggesting conservation prioritization of primarily the largest trees [Latouche-Hall et al., 2004, Tani et al., 2012], our results suggest the maintenance of diverse size structure could be a suitable strategy to promote reproductive processes and prevent the potential erosion of genetic diversity.

Conspecific density can also influence sex allocation patterns within hermaphroditic plants by increasing the male function in flowers of plants

growing in dense neighbourhoods [Mazer, 1992], though other studies report increased siring success in extremely spatially isolated tropical trees [Aldrich and Hamrick, 1998, Fuchs and Hamrick, 2011]. Our results do not support a relevant role of the neighbourhood density on the siring success of *M. affinis*. However, we found support for a major role of nearest-neighbour mating as evidenced by the negative relationship between the siring success of a particular tree and its distance to the mother tree. Nearest neighbour mating is a common phenomenon in tropical trees with high degrees of spatial clumping [Stacy et al., 1996], though there is great potential for deviations from this rule in cases of flowering asynchrony and pollinators with strong flight ability, among other factors [Dick et al., 2008]. Several features of our study species could explain the prevalence of the nearest neighbour mating. First, *M. affinis* trees exhibit a sharp clumped distribution within the 50-ha BCI plot. Second, *M. affinis* typically exhibits highly synchronous flowering in forest habitats such as the study population. Third, small-bodied social bees (e.g. *Trigona* sp.) constitute the main component of the species' pollinator fauna in forest habitats [Jha and Dick, 2010] and are common in the study area [Roubik and Wolda, 2001], and are known to exhibit shorter foraging distances than large-bodied bees [Greenleaf et al., 2007]. These small-bodied tropical social bees (mostly Meliponini tribe) also have a tendency to forage short distances from their nests [Hubbell and Johnson, 1978, Roubik and Aluja, 1983, Slaa et al., 2003], likely enhancing nearest-neighbour pollen movement.

In summary, continued deforestation of tropical regions and strong de-

pendence of tropical plant species on biotic pollination highlight the critical need to understand factors influencing reproductive processes for tropical trees. Our results reveal the importance of individual size, conspecific neighbourhood density, and local kinship as critical factors differentially influencing maternal and paternal components of plant reproductive success. Based on these findings, we suggest the conservation of dense patches with low kinship and the maintenance of diverse size structure as potential strategies for strengthening the reproductive output of tropical tree populations.

3.5 Appendix: Spatial autocorrelation

We used a Gaussian correlation function to capture spatial dependence in the location and dispersion regressions. Between tree j and any other tree k, the covariance among mean logit seed viability of fruit (θ), and among log dispersions ($\ln \psi$) was modelled as

$$cov(\theta_j, \theta_k) = \tau^2 \exp\{-d_{jk}^2/\delta^2\}$$

$$cov(\ln \psi_j, \ln \psi_k) = \omega^2 \exp\{-d_{jk}^2/\delta^2\}$$

$$cov(\theta_j, \ln \psi_k) = \chi\omega\tau \exp\{-d_{jk}^2/\delta^2\}$$

where d_{jk} is the distance in meters between two trees and δ controls the decay of spatial correlation over distance (δ is the distance at which the correlation equals approximately 0.35). We used vague priors for the hyperparameters; $\delta \sim \mathcal{U}(0, 500)$, $\chi \sim \mathcal{U}(-1, 1)$, $\beta, \rho \sim \mathcal{N}(0, 10^3)$, $\omega, \tau \sim i\mathcal{G}(10^{-2}, 10^{-2})$ ($i\mathcal{G}(.)$ is inverse Gamma, $\mathcal{U}(.)$ is uniform, $\mathcal{N}(.)$ is normal).

The spatial correlation of mean seed viability among trees was restricted

to a relatively small scale: the range parameter δ had a posterior expectation of 10.7 (0.95% CI: 0.5 to 29.2). The eigenvectors of the estimated spatial variance-covariance matrix indicated that a group of four closely clustered trees drives the spatial correlation: these trees are tightly clustered in space and have relatively high mean seed viabilities.

3.6 Appendix: Viability and total seed production

We fit a separate model to determine the degree of correlation between the total number of seeds and the proportion of viable seeds. We modeled the total number of seeds n_{ij} as a Poisson-distributed random variable with fruit-specific rate λ_{ij}, and the number of viable seeds y_{ij} as binomial with probability ϕ_{ij}. We modelled $\log \lambda_{ij}$ and logit ϕ_{ij} as multivariate normal with tree-specific means and tree-specific correlation c_j. We treated the inverse hyperbolic tangent of these correlations as i.i.d normal centered at a population-level correlation, with variance σ^2, so that $\tanh^{-1} c_j \sim \mathcal{N}(\tanh^{-1} c_{pop}, \sigma^2)$. This transformation allows partial pooling of tree-level correlations into a population level estimate. We gave c_{pop} a flat uniform prior over [-1,1], and σ^2 an inverse-Gamma prior with shape, rate equal 0.01.

To assess the relationship between total seed production and the covariates, we fit a separate hierarchical regression model where we treated total seed production for the ith fruit in the jth tree as a Poisson-lognormal random variable with rate λ and tree-specific dispersion σ_j. We modeled $\ln \lambda$ as a linear function of the covariates used for the seed viability model and regression

coefficients β, and allowed for spatial autocorrelation among trees as described for the seed viability model. We estimated separate dispersion parameters σ_j for each tree, assuming an inverse-Gamma prior with shape, rate equal to 0.01.

Mean seed viability across trees (logit scale)				
	$\mathbb{E}[.]$	0.95 CI	Hypothesis	Pr[Hypothesis] (odds)
intercept (β_0)	0.83	(0.31, 1.33)		
DBH* (β_{dbh})	-0.46	(-1.04, 0.09)	$\beta_{dbh} > 0$	0.049 (0.05)
neighbourhood density* (β_{nden})	0.50	(-0.01,1.03)	$\beta_{nden} > 0$	0.972 (34.7)
local kinship* (β_{nkin})	-0.16	(-0.99, 0.63)	$\beta_{nkin} < 0$	0.663 (2.0)
density* x kinship* ($\beta_{nden:nkin}$)	-0.12	(-0.90, 0.64)	$\beta_{nden:nkin} < 0$	0.628 (1.69)

Within-tree variance in seed viability (log scale)				
	$\mathbb{E}[.]$	0.95 CI	Hypothesis	Pr[Hypothesis] (odds)
intercept (ρ_0)	0.56	(0.25, 0.88)		
DBH* (ρ_{dbh})	-0.02	(-0.37, 0.31)	$\rho_{dbh} < 0$	0.547 (1.2)
neighbourhood density* (ρ_{nden})	-0.18	(-0.51,0.15)	$\rho_{nden} < 0$	0.871 (6.8)
local kinship* (ρ_{nkin})	0.83	(0.33, 1.36)	$\rho_{nkin} > 0$	0.998 (599)
density* $\times$ kinship* ($\rho_{nden:nkin}$)	0.66	(0.19, 1.16)	$\rho_{nden:nkin} > 0$	0.995 (199)

Relative siring success (logit scale)				
	$\mathbb{E}[.]$	0.95 CI	Hypothesis	Pr[Hypothesis] (odds)
DBH† (η_{dbh})	0.27	(-0.01, 0.56)	$\eta_{dbh} > 0$	0.969 (31.3)
neighbourhood density† (η_{nden})	-0.16	(-3.13,2.69)	$\eta_{nden} > 0$	0.550 (1.2)
mother-father distance (m) (η_{pdist})	-0.004	(-0.006, -0.003)	$\eta_{pdist} < 0$	> 0.999 (>999)
density† x distance ($\eta_{nden:pdist}$)	0	(-0.01, 0.01)	$\eta_{nden:pdist} < 0$	0.522 (1.09)

Table 3.1: Summary of posterior distributions of regression coefficients from the models detailed under the heading 'Seed viability and siring success'. All covariates are scaled, hence the 'mean effect' corresponds to the expected change in the linear predictor of the response (on the appropriate scale), with a change of 1 standard deviation in the covariate. *Of the mother, †of the father.

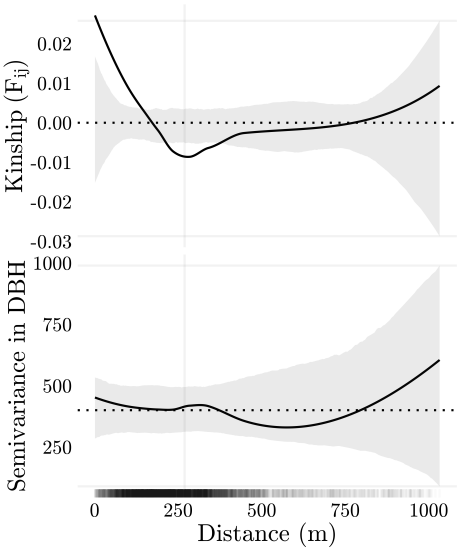

Figure 3.1: (A) Spatial genetic structure and (B) size structure in the population of reproductive trees. Black solid lines are LOESS fits to the observed data; grey shaded regions are 95% confidence bounds around the null expectation (black dotted line). Short vertical lines at the bottom of the figure are observed pairwise distances, where darkness indicates pairwise density, and the gray vertical line indicates the mean.

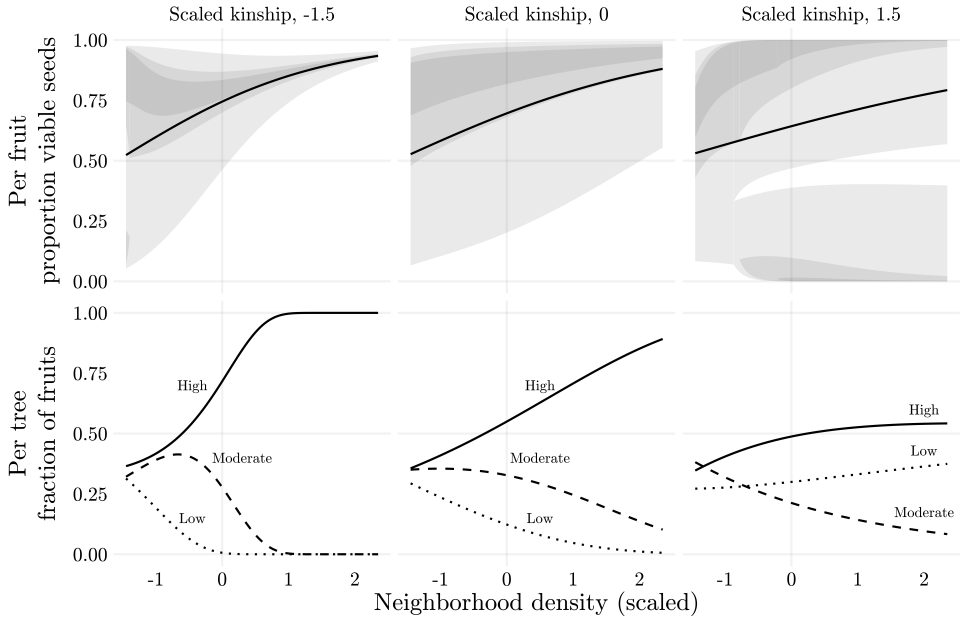

Figure 3.2: Predictions from the seed viability model. Neighbourhood density and local kinship are scaled, with negative values indicating lower values than the population average and positive values indicating higher values than the population average. (A) The distribution of the proportion of viable seeds across fruits on a tree. Each value of the x-axis has a unique logit-normal distribution where the black line indicates the mean, and the gray ribbons are the smallest intervals that contain 25%, 50% and 95% of the density (from the darkest to the lightest gray regions, respectively). (B) Fractions of fruits in three seed viability classes (low, moderate and high), on a tree at the corresponding value of the x-axis. The fraction of fruits in any given class is calculated as the integral of the corresponding distribution shown in the upper panels. Low includes fruit with < 0.33 proportion viable seeds; Moderate includes fruit with > 0.33 and < 0.67 proportion viable seeds; High includes fruit with > 0.67 proportion viable seeds.

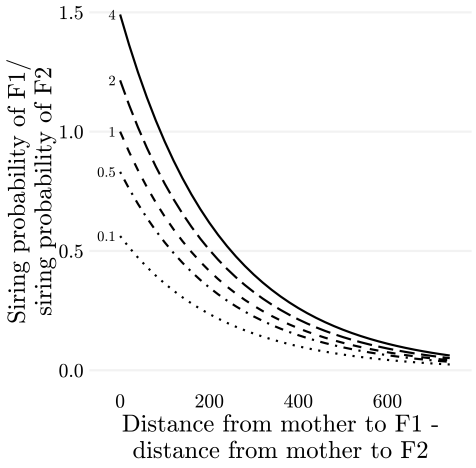

Figure 3.3: The estimated odds of paternity between two potential fathers (F1 and F2) for a given mother, as a function of the relative proximity of the fathers to the mother. When the odds equal 1, the fathers are equally likely to have paternity. The line dashing and numbers to the left of the lines indicate the ratio between the DBH of F1 to that of F2; for example, the solid line corresponds to a situation where F1 is four times larger than F2.

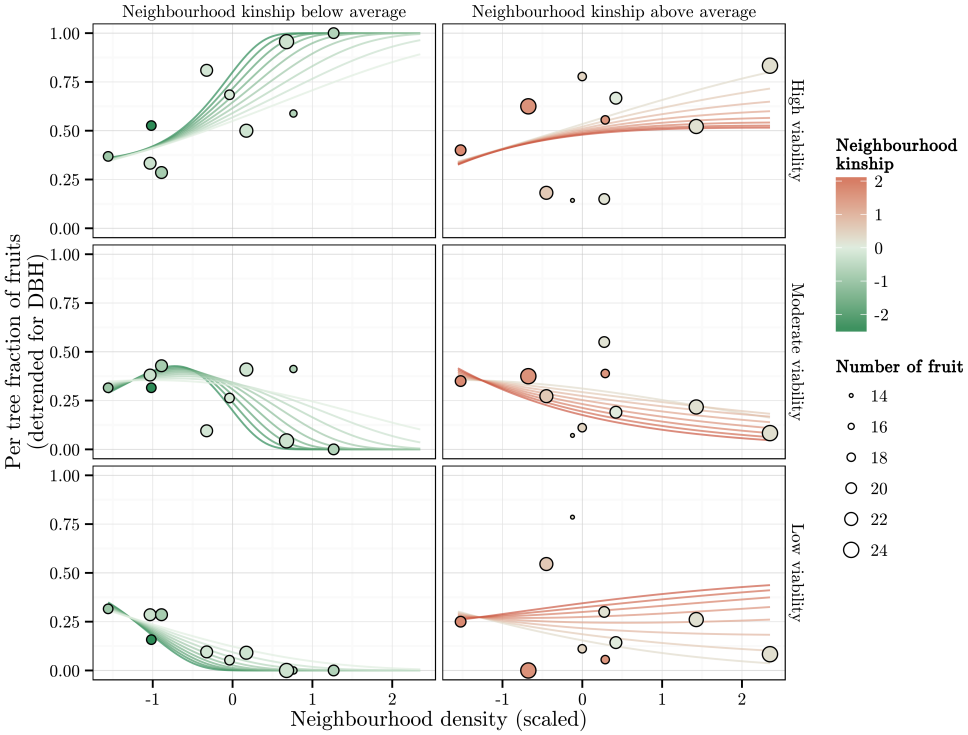

Figure 3.4: The fraction of fruit on the tree within three quality categories based on seed viability (vertical panels, including low viability with 0-33.3% viable seeds; medium viability with 33.3-66.6% viable seeds; high viability with 66.6-100% viable seeds), plotted against neighborhood density. The left series of panels shows trees that occurred in neighbourhoods with below-average kinship; the right series of panels shows trees that occurred in neighbourhoods with above-average kinship. The lines show the predictions from the seed viability model, for various neighbourhood kinship values. In both points and lines, the color indicates the average neighbourhood kinship.

Chapter 4

Adding landscape genetics and individual traits to the ecosystem function paradigm reveals the importance of species functional breadth

The research in this chapter represents a collaboration between the author, Dr. Antonio R. Castilla, Dr. Shalene Jha, and members of Dr. Jha's research group at the University of Texas. The author led the modeling and statistical analysis, and co-wrote the study, which as of the time of writing has been published as [Castilla et al., 2017].

Animal pollination mediates both reproduction and gene flow for the majority of plant species across the globe. Despite this fact, past functional studies have largely focused on seed production and often cite the largest-bodied pollinators as the most effective; although useful, this focus on seed set does not provide information regarding species-specific contributions to pollen-mediated gene flow. Here we quantify pollen dispersal for individual pollinator species across more than 690ha of tropical forest. Specifically, we examine visitation, seed production, and pollen dispersal ability for the entire pollinator community of a common tropical tree using a series of individual-based pollinator exclusion experiments followed by molecular-based fractional

paternity analyses. We investigate the effects of pollinator body size, plant size, local plant density, and local plant kinship on seed production and pollen dispersal distance. Our results show that while large-bodied pollinators set more seeds per visit, small-bodied bees visit flowers more frequently and were responsible for more than 49% of all long-distance pollen dispersal events (beyond 1 km). Thus, despite their size, small bodied bees play a critical role in facilitating long distance pollen-mediated gene flow. We also found that both plant size and local plant kinship negatively impact pollen dispersal and seed production. By incorporating genetic and trait-based data into the quantification of pollination services, we highlight the diversity in ecological function mediated by pollinators, the influential role that landscape attributes play in driving service provision, and the unexpected importance of small-bodied pollinators in the recruitment of plant population genetic diversity.

4.1 Introduction

As habitat alteration and climate change transform global ecosystems, there is growing concern about how subsequent changes in biodiversity will impact ecosystem functioning and the provision of ecosystem services [Hassan et al., 2005, Carpenter et al., 2009]. In this regard, the biodiversity-ecosystem function hypothesis posits that a reduction in biological diversity will lead to a concomitant reduction in ecosystem-level processes, potentially compromising service provision [Srivastava and Vellend, 2005, Balvanera et al., 2006, Mace et al., 2012]. For instance, if multiple species perform distinct roles with

respect to a particular ecological function, then overall function may be maximized by increasing biodiversity, as seen in the case of pollinator-mediated seed production [Hoehn et al., 2008, Frund et al., 2013], pest removal rates [Philpott, 2009], or plant contributions to C and N sequestration [Fornara and Tilman, 2008, Steinbeiss et al., 2008]. In contrast, some studies have challenged the relevant role of biodiversity and have alternatively suggested that a few keystone species can be sufficient for ecological function; this has been proposed for a number of indices quantifying mobile-agent based ecosystem function, such as seed production in pollination [Kleijn et al., 2015] and pest-removal in pest-control [Finke and Denno, 2004, Rodriguez and Hawkins, 2000].

However, ecological function can be characterized by multiple indices, and effectiveness at one index does not guarantee effectiveness at another [Villeger et al., 2008]. In the case of mobile-agent-based ecosystem services, ecological function is mediated by foraging organisms engaging in trophic interactions [Kremen et al., 2007, Kremen, 2005, Cardinale et al., 2012], and thus the quality of these functions depends on the traits of both the recipient and the mobile provider organism [Lavorel, 2013]; this potentially creates more opportunity for species-level differences across multiple indices of ecological function. For example in animal pollination, which is critical to 85% of all plant species [Ollerton et al., 2011], mobile provider organisms not only mediate seed production but also engage in pollen dispersal between plants, potentially enhancing genetic diversity within and across populations. While

both seed production and pollen dispersal are critical measures of pollination success, the latter is rarely measured or incorporated into indices of pollinator function [Ne'eman et al., 2010]. This measure is particularly relevant given that pollen dispersal can provide insight into the origin of offspring traits, the mechanisms driving variation in offspring fitness, and the future of pollen-mediated gene flow for a plant population. Despite the economic and ecological value of pollination services, little is known about the functional breadth of different pollinator species [Betts et al., 2015, Brosi and Briggs, 2013] and how these vary between functional indices, including pollen dispersal, across key pollinator and plant traits.

Pollinator body size has long been assumed to be a critical driver of pollination service, given that body size often correlates with the amount of pollen adhered to pollinator bodies [Tepedino et al., 1999], ability to buzz-pollinate flowers [De Luca et al., 2014, Solis-Montero et al., 2015], and capacity to trigger specialized pollination mechanisms [Stout, 2000]. Further, it is generally believed that larger-bodied animals have longer foraging ranges than smaller-bodied animals due to their higher energy demands [Cresswell et al., 2000, Reiss, 1988]; a number of multi-species comparisons suggest that body size may indeed correlate with pollinator foraging distance [Gathmann and Tscharntke, 2002, Greenleaf et al., 2007, Knight et al., 2005]. If true, then increased mobility in large-bodied pollinators may lead to enhanced levels of pollen-mediated gene flow, with larger pollinators contributing more to long-distance pollen dispersal and playing a more critical role in the maintenance

of genetic diversity within and across plant populations.

Additionally, while it has been hypothesized that plant population and individual attributes, such as degree of plant isolation, size of floral display, and level of local kinship may influence seed production and pollen dispersal [Duffy et al., 2013, Wagenius, 2006, Wagenius et al., 2010], these traits are rarely incorporated into species-specific assessments of pollination service, especially at large spatial scales. This is unfortunate given that lab-based foraging experiments suggest that pollinator species respond differently to spatial distributions of artificial flowers [Ohashi et al., 2007, Lihoreau et al., 2010] and transplant studies reveal that pollen dispersal can be mediated by the spatial distribution of individual plants [Ison et al., 2014]. Specifically, increased plant spatial isolation may limit pollination success through a reduction in the number of pollen donors [Ghazoul, 2005] and an increase in the transfer of self-pollen through geitonogamy, a process that may also be driven by large floral arrays [Makino et al., 2007]. Similarly, fine-scale spatial genetic structure (i.e. local kinship) is a common feature in plant populations and may impact estimates of pollination service [Jones and Comita, 2008, Castilla et al., 2016b, Hirao, 2010], possibly due to increased rates of inbreeding in high kinship neighborhoods, which could result in increased seed abortion rates [Korbecka et al., 2002, Hufford and Hamrick, 2003]. Thus, a comprehensive concept of pollination service should incorporate not only pollinator traits, but also plant population and individual traits, such as plant size, density of pollen donors, and local kinship.

In this study, we conduct a species-specific pollen dispersal analysis by means of fractional paternity, using 532 seeds and 1023 leaves gathered from individual pollinator visits to a common understory tree, *Miconia affinis*, across more than 690 ha in central Panama. We compare individual pollination events with respect to three indices of pollinator effectiveness: visitation, pollen dispersal distance, and seed viability. Specifically, we assess how these indices are impacted by plant and pollinator size, plant density, and local plant kinship. We show that while large-bodied pollinators are more effective at setting viable seeds on a per visit basis, small-bodied pollinators visit more frequently and engage in nearly half of all long-distance pollen dispersal events. Further, we show that plant population and individual attributes, specifically local kinship and plant size, can significantly negatively impact pollination function. By quantifying pollen-mediated gene flow across large spatial scales, and adding individual plant and pollinator traits into ecosystem service assessments, we highlight the breadth of ecological function mediated by a community of pollinators and we reveal the unexpected importance of small-bodied pollinators for long-distance pollen dispersal.

4.2 Materials and Methods

Study species and regions. *Miconia affinis* D.C. (Melastomataceae) is a self-incompatible understory tree (3-6 m) that is broadly distributed in the neotropics, ranging from Mexico to Brazil [Jha and Dick, 2010]. Inflorescences have 50-300 white flowers, and it exhibits a "big bang" flowering pattern with

all individuals in a population produce a large number of flowers over a short time frame (i.e., $\approx$ 1-2 days; [Jha and Dick, 2010]). The flowers have deep poricidal anthers which must be vibrated by a pollinator in order for pollen to be released (i.e., "buzz-pollination") and are visited by a diversity of bees [Jha and Dick, 2010]. Fruit ripening takes 3-4 months (May-July), and the black globose berries (3 mm long; 6 mm wide) are dispersed by a variety of birds and bats [Jha and Dick, 2008]. Each fruit contains numerous minute seeds (30-50 seeds per fruit), where fertilized seeds are yellow, pyramidal, and 3-4x times larger than the dark, crescent-shaped, unfertilized ovules.

The research was conducted in three study regions along Soberania National Park in Central Panama, Gamboa, Camino de Plantaciones, and Alfagia (GB, CP, and AG, hereafter; see [Castilla et al., 2016a] for a more detailed description of the study regions). Our sampling covered a total area of 698 ha, ~10 times the size of most molecular marker-based dispersal studies (often 50 ha, reviewed in [Dick et al., 2008]); geographic distances between the study regions ranged from 5.0 to 19.2 km (mean = 12.9 $\pm$ 4.2 km). In each study region, we surveyed all reproductive *M. affinis* trees and recorded their geographic coordinates using a portable GPS GARMIN eTrex Vista (GARMIN, Southampton, UK). Additionally, we surveyed 50m transects that were randomly distributed across the study system, where we simultaneously evaluated the reproductive status (reproductive if inflorescence present) and DBH of all trees within a 2.5 meters on either side (N= 36, 46, and 60 transects in GB, CP, and AG respectively). In two study regions (GB and CP), we also counted

the total number of inflorescences for each reproductive tree within each transect. For these two study regions, we analysed the relationship between DBH and the total number of inflorescences per tree using Pearson correlation.

Single pollinator visit experiment. During the dry season in 2013, we randomly chose 25 *M. affinis* reproductive trees (mother trees, hereafter) in each study region to conduct a 30-minute single pollinator visit experiment (N = 75 mother trees). For each mother tree, we recorded its DBH and calculated the mean distance to the ten nearest conspecific neighbours as an estimate of the spatial isolation of trees (spatial isolation). We bagged five closed inflorescences per mother tree in March and April, at the beginning of the dry season (N = 375 inflorescences). On the day of flowering, inflorescences were unbagged for up to 30 minutes, allowing for a single insect visit. After flower visitation, visitors were captured using entomological nets and the total number of flowers open per inflorescence were counted. Inflorescences were then re-bagged to allow for the development of fruits. We also re-bagged the non-visited inflorescences to confirm the absence of fruit formation without pollinator visitation. Floral visitors were identified to species at the Museo de Invertebrados G.B. Fairchild (Panama) and intertegular distance (ITD) was measured as the linear distance between a specimen's tegula (cap at base of wing) as a proxy for pollinator size. During July-August, we collected the ripe fruits from each visit and we quantified the number of viable and aborted seeds per fruit using a stereo microscope. We also estimated the percentage of forest

cover in a radius of 100 meters around each mother tree using the software QGIS and a 2008 land cover map `http://strimaps.si.edu/portal/home/`.

Fine-scale genetic structure and paternity assignment. We collected leaf material for all reproductive trees in each study region. Total genomic DNA was extracted from adult leaf tissue using the CTAB protocol [Doyle and Doyle, 1987]. For the paternity analyses, we used up to ten fruits for each infructescence resulting from a single pollinator visit. For those infructescences with more than ten fruits, we randomly chose ten fruits. We collected one viable seed per fruit and its total genomic DNA was extracted using the DNazol protocol. All trees and seeds were screened at eight highly polymorphic microsatellite loci following the protocols described in [Jha and Dick, 2009], and genotyped on an ABI 3730 Sequencer. Alleles were scored manually using GENEMARKER (Softgenetics).

Using the genotypes of the reproductive trees, we performed an analysis of the fine-scale spatial genetic structure, also known as local kinship [Castilla et al., 2016b]. We calculated the metric F_{ij} using the software SPAGeDi [Hardy and Vekemans, 2002] as a measure of kinship between paired trees (i.e. higher pairwise F_{ij} represents greater kinship between two individuals). For each focal mother tree, we estimated local kinship as the mean F_{ij} for all pairwise comparisons of reproductive trees within 400 meters. To calculate the probability of paternity across trees for each seed, we used fractional paternity assignment under a model of Mendelian inheritance in the presence of genotyping

error, which is detailed in the appendix (section 4.5), and was implemented via a Metropolis-in-Gibbs algorithm that is described in section 4.5 of the appendix. We estimated pollen dispersal distances as the expectation of distance between mother and father, taken with respect to paternity probabilities.

Analysis of visitation rates. To determine if bees with different body sizes differed in their visitation rates, we modelled visitation frequency (across pollinator species) as a function of ITD, using a multinomial model with pollinator species as a random effect. Across J pollinator species, the number of visits to mother i is given by the vector $\mathbf{Y}_i = \{y_{i,1}, \ldots, y_{i,J}\}$, where $\sum_j y_{i,j} = n_i$. To model visitation across mothers, we treated $\mathbf{Y}_i$ as a multinomial random variable with size n_i, and parameter vector $\mathbf{P}_i = \{p_{i,1}, \ldots, p_{i,J}\}$ which gives the frequencies of the species which pollinate mother i. For mother i, we modelled the log-odds that a given pollinator was of species j rather than a 'reference' species k as:

$$\ln \frac{p_{i,j}}{p_{i,k}} = \alpha_j + \beta(x_j - x_k)$$

Where α_j is a species-specific intercept (for identifiability, fixed to 0 for 'reference' species k); x_j is the intertegular distance for species j; and β is a parameter that controls the degree to which species of a larger size will be more likely to visit the tree. We modelled the random intercepts α_j as Gaussian with mean 0 and variance τ, and fit the model via Markov chain Monte Carlo (MCMC) using JAGS [Plummer, 2003].

Analysis of seed viability. We used generalized linear mixed models to evaluate the effects of DBH_{mother}, spatial isolation, local kinship, and ITD on seed viability. We did not include forest cover around mother tree as an additional explanatory variable in either our seed viability or pollen dispersal model due to its strong collinearity with spatial isolation (r = -0.40, P = 0.007). Further, we know from past work in the study region that spatial isolation can critically influence both seed viability and pollen dispersal, even when forest cover is relatively homogeneous [Jones and Comita, 2008]. For each fruit, we defined seed viability as the fraction of viable seeds out of the total number of seeds (viable + aborted). We used a binomial error distribution, where the number of trials was the total number of seeds per fruit and the number of successes was the number of viable seeds per fruit. We included ITD, DBH_{mother}, spatial isolation, and local kinship as predictors, after normalizing to a mean of zero and variance of 1. We included population, mother tree, and infructescence as random factors, with infructescence nested within mother tree and mother tree nested within population. To account for overdispersion, we included an observational-level effect where each data point receives a unique level of a random effect that models the extra variation present in the data [Bolker et al., 2009, Harrison, 2014].

Analysis of paternity probabilities. To determine how pollinator ITD may have influenced pollen dispersal distance while accounting for the spatial configuration of trees in our study regions, we explicitly modelled paternity

probabilities as a function of distance between trees. For the vth infructescence, we assumed that the rate of pollen transfer from a potential father k to a mother j decayed exponentially with distance at rate λ_v. Conditional on a successful pollination event for the ith seed, the probability that tree k was the father is proportional to $\exp\{\lambda_v d_{j,k}\}$ where the summation is across potential fathers and $d_{j,k}$ was the distance between trees j and k. For seed i, let $f_i, m_i, \mathbf{S}_i$ be the unknown father, the known mother, and the observed genotype respectively. Let $\mathbf{T}_j$ be the genotype of tree j. The joint probability of the dispersal event and the resulting seed genotype is

$$\Pr(f_i, \mathbf{S}_i|\lambda_v, \mathbf{T}_{f_i}, \mathbf{T}_{m_i}, \boldsymbol{\epsilon}) = \frac{\exp\{\lambda_v d_{j,k}\}}{\sum_{s\neq j}\exp\{\lambda_v d_{j,s}\}} \prod_l \Pr(\mathbf{S}_i^{(l)}|\mathbf{T}_{f_i}^{(l)}, \mathbf{T}_{m_i}^{(l)}, \boldsymbol{\epsilon})$$

where $\boldsymbol{\epsilon}$ are nuisance parameters for a model of genotyping error, and the product is of genotype probabilities over loci. We modelled the rates λ_v in the pth population as random and Gaussian with mean $\Lambda_p + \theta \cdot \mathrm{ITD}_v$ and variance σ_p^2. The parameter Λ_p represents the distance decay rate for a pollinator of "average" size, while θ modifies the rate depending on pollinator ITD. The likelihood is obtained by integrating across λ_v and possible paternal assignments:

$$\mathcal{L}(\Lambda_p, \sigma_p, \theta) = \int_{-\infty}^{\infty} \prod_{v=1}^{n_p} p(\lambda_v|\Lambda_p, \sigma_p, \theta) \times \prod_{i\in\Omega_v} \sum_{k\neq m_i} \Pr(f_i = k, \mathbf{S}_i|\lambda_v, \mathbf{T}_k, \mathbf{T}_{m_i}, \boldsymbol{\epsilon}) d\lambda_1 \ldots d\lambda_{n_p}$$

where Ω_v is the set of seeds for infructescence v, and there are n_p infructescences in population p. This likelihood captures the spatial context of the

mother by incorporating all distances to all potential fathers. We used adaptive Gauss-Hermite quadrature to calculate the integral.

The null model of primary interest occurs where $\theta = 0$, in which case spatial structure in mating varies randomly across infructescences but not systematically across pollinator species. To asses evidence for an effect of pollinator body size on spatial mating structure, we compared the two models ($\theta \neq 0$ and $\theta = 0$) by a likelihood ratio test where the distribution of the test statistic under the null was approximated via parametric bootstrapping. Briefly, for each visit, we simulated a new pedigree given the maximum likelihood estimates under the null model, and simulated new seed genotypes conditional on this pedigree. We fitted both models to the simulated data, and recorded the increase in likelihood associated with a non-zero θ.

There were two other particular cases of this model that were of interest. When $\lambda_v = 0$, there is no spatial mating structure (every tree has an equal chance of mating with every other tree). When $\sigma_v \to 0$, there is no random variation in distance decay rate among visits ($\lambda_v = \Lambda_p$), and this would indicate that the data are insufficient to distinguish differences in spatial mating structure on a per-visit basis. We assessed evidence against these submodels by calculating 95% confidence regions for Λ_p, σ_p via profile likelihood.

Analysis of expected dispersal distance. We fit a linear mixed-model to evaluate the effects of ITD, $\text{DBH}_{\text{mother}}$, spatial isolation, and local kinship on expected pollen dispersal distance. For each seed, we defined pollen dispersal

distance as the linear geographic distance between the mother and the father trees, and defined its expectation for each seed with regard to the probabilities of possible paternities. We included ITD, DBH_{mother}, spatial isolation, and local kinship as the fixed factors in our full model. All the explanatory variables were scaled to mean zero and variance 1. We included population, mother tree, and infructescence as random factors, with infructescence nested within mother tree and mother tree nested within population. There are a finite number of possible observable dispersal distances for each mother, which depend on their locations relative to other trees in the population. For the linear model of pollen dispersal distance, two possible consequences of spatial context are (1) non-independence of observations across mothers and (2) biased regression coefficients, making it challenging to determine the parameter values that would be expected under an appropriate null model. Thus, for a more robust analysis, we approximate the null distribution of regression coefficients in our fitted model by permuting data at the relevant level of replication. For example, by shuffling pollinator identity (and associated ITD) across infructescences, we approximated the sampling distribution of the regression coefficient for ITD under a model where pollinators were equivalent. Data was only permuted within populations. We note that if the number of dispersal events is much lower for the smallest pollinators and restricted to highly isolated mother trees, it could inflate mean pollen dispersal distance at the lower edge of the pollinator size distribution overriding a potential positive relationship between ITD and pollen dispersal distance. However, we

posit that this situation is unlikely in our analyses for two reasons. First, we had a reasonable number of dispersal events at both edges of the size distribution (174 and 79 dispersal events for the three largest and smallest pollinator species). Second, we did not find that long-distance dispersal events mediated by small pollinators occurred exclusively at spatially isolated mother trees.

4.3 Results

Flowers of *M. affinis* were visited by a total of twenty bee species during the single visit experiments, and unvisited flowers did not produce fruits. Fourteen bee species behaved as pollinators, with all visits leading to fruit production, and representing 96.5% of the total visited inflorescences. Pollinators varied markedly in body size as measured by intertegular distance (ITD, [Cane, 1987]), with ITD ranging from 0.91 to 7.72 mm. Eusocial species were responsible for 94.1% of the fruit production, thus we did not include sociality as an additional explanatory trait in our seed viability and pollen dispersal models. The visitation frequency of pollinators was negatively related to their ITD (β = -1.086; 95% CI = -2.164, -0.238), indicating that smaller-bodied pollinators were more frequent visitors. While large-bodied bees visited less frequently, they were more effective at setting viable seeds on a per visit basis than small-bodied bees (Fig. 4.1A). In our fitted model, pollinator body size accounted for most of the variation in mean seed viability between pollinator species. Based on the predicted mean seed viabilities, it is evident that no pollinator species deviated substantially from the positive relationship between

ITD and mean seed viability (Fig. 4.4A).

Despite documenting substantial variation in pollinator body size and a total of 532 pollen dispersal events, we found no significant relationship between the ITD of the pollinator and their mean pollen dispersal distance (Table 4.1). Most interestingly, a substantial number of dispersal events reached distances beyond 1 km, even for small-bodied pollinators with < 2 mm ITD (Fig. 4.2). In other words, while pollinators differed in size by more than eight orders of magnitude, they did not exhibit significant differences in their mean pollen dispersal distance based on body size. Using seed and tree genotypes, we directly modelled pollen flow between trees as a function of physical distance. Across infructescences, we estimated substantial variation in the rates at which paternity probability decays with distance, but we found no evidence that pollinator ITD is the cause of this variation ($p = 0.36$, likelihood ratio test; Fig. 4.5). Taken together, these analyses indicate that while the data are sufficient to detect variation in dispersal distances across single visits, there is no evidence that larger bees transport pollen longer distances (Fig. 4.4*B*).

Our results also revealed a negative relationship between mother DBH and pollen dispersal distance (Table 4.1 and Fig. 4.3*A*), where DBH correlates strongly with floral resource availability (r_p=0.85; $P < 0.0001$; Fig. 4.3*B*). In other words, pollinators, independent of their body size, exhibit shorter pollen dispersal distances when pursuing higher floral resource sites. In addition, we found a positive relationship between spatial isolation of the mother tree and pollen dispersal distances to the tree, indicating that more spatially isolated

trees tend to receive pollen from more distant trees. For the pollen dispersal model, repeated analyses removing pollinator species with less than 5 dispersal events indicated similar results.

Interestingly, we found a negative effect of local kinship on the proportion of viable seeds per fruit (Table 4.1), where fruits from mother trees in high kinship neighborhoods had fewer viable seeds than those from low kinship neighborhoods (Fig. 4.1*B*). This demonstrates that mother trees living near close relatives exhibit increased abortion rates, likely due to elevated levels of biparental inbreeding. Additionally, the interaction between ITD and local kinship was not significant in our seed viability model (Likelihood Ratio Test: $\chi^2 = 0.17$, P = 0.6801), indicating that increased seed abortion is occurring across all pollinator sizes, and is not predominantly mediated by small-bodied pollinators. Finally, neither $\mathrm{DBH}_{\mathrm{mother}}$ nor spatial isolation had significant effects on the proportion of viable seeds per fruit (Table 4.1).

4.4 Discussion

While pollen dispersal is arguably one of the most important components of pollination service, our study is the first to measure landscape-level pollen dispersal across an entire pollinator community. We reveal that visitation, seed production, and pollen dispersal indices are not mediated by the same individual and plant population traits. Specifically, our results contradict the conventional belief that large-bodied pollinators are more effective at long-distance pollen dispersal and instead highlight the importance of func-

tional breadth when considering the biodiversity and ecosystem function relationship. While we find that seed production is positively driven by pollinator body size, we reveal that the entire pollinator community can disperse pollen long distances ($>$ 1 km); this is in stark contrast to the classic assumption that large-bodied pollinators are the only vectors of long distance pollen-mediated gene flow. Further, given that small-bodied pollinators are more frequent visitors, they engage in a substantial proportion of long-distance dispersal events and thus play an important role in the maintenance of genetic connectivity within and across plant populations. Thus, by incorporating gene flow measures into our quantification of pollination service, we highlight the critical functional breadth exhibited by multiple pollinator species within a community.

While long-distance pollen dispersal events have frequently been documented for tropical trees [Latouche-Hall et al., 2004, Dick et al., 2003], they have primarily been ascribed to large-bodied animal species (but see [Nason et al., 1996]). Specifically, past research has asserted that because larger-bodied pollinators exhibit the greatest foraging distances [Greenleaf et al., 2007], they are also the most likely to mediate long-distance pollen dispersal [Breed, 2015]. In contrast, the contribution of small-bodied pollinators to pollen-mediated gene flow has long been assumed to be minimal, around 100-300 m (reviewed in [Dick et al., 2008]). We found that pollinator body size was positively related to seed production, likely because increased pollinator body size often translates into an improved ability to manipulate complex floral

structures, as seen in other buzz-pollinated plant [De Luca et al., 2014]. However, pollinator body size was not correlated with pollen dispersal distance; for example, some of the smallest-bodied species, *Tetragonisca angustula* (ITD = 1.28 mm) and *Trigona buyssoni* (ITD = 1.07 mm), regularly mediated pollen dispersal distances beyond than 2 kms. While surprising, these long-distance dispersal events are indeed possible, and have occasionally been documented for small-bodied tropical bees in the past [Jaffé et al., 2015, Duarte et al., 2014]. Though long-distance pollen dispersal events could be explained by secondary pollen transfer [Thomson and Eisenhart, 2003], this process is expected to be equally if not more likely for large-bodied pollinators due to their greater body surface area (57). Furthermore, the short flowering of *M. affinis* (24-36 hours) acts as a strong temporal limitation for secondary pollen transfer. Future studies should explore the role of secondary pollen transfer in pollen-mediated gene flow, and should examine the generality of our findings for plant species with different functional traits and under different ecological contexts.

Whatever the explanatory mechanism, our findings are particularly important given that small bees are often the most frequent floral visitors across plant taxa and study systems [Sahli and Conner, 2007, Vivarelli et al., 2011], and thus are likely mediating important long-distance pollen dispersal events in other systems, though they may not be conferring the highest seed production. Overall in our study, small-bodied pollinators (ITD $<$ 2mm) were the most common visitors and were also responsible for 49% of all pollen

dispersal events involving distances above 1 km. Thus as both frequent visitors and capable long-distance pollen dispersers, we show that small-bodied pollinators play a previously unacknowledged but critical role in maintaining pollen-mediated gene flow. Given that large-bodied bees are often less common visitors and tend to be more extinction-prone to human activities [Larsen et al., 2005], small-bodied bees could be particularly important for maintaining effective plant population sizes and genetic diversity in the face of global land use change. Thus, our results reveal that pollination service quantification that does not incorporate pollen dispersal may overlook important attributes of ecological function that are critical for the conservation of genetic diversity and long-term plant population viability.

The results of this study also demonstrate the importance of plant size in driving pollen dispersal function. We document a significant decrease in pollen dispersal distance for large mother trees, likely driven by changes in pollinator behavior in response to large floral displays. Specifically, our results suggest that when pollinators visit large flowering trees, they tend to arrive from nearby localities and continue their foraging more locally (exhibiting shorter pollen dispersal distances). Past studies provide complimentary evidence that plants with large floral displays offer a high rate of reward relative to travel and thus, pollinators use spatial memory to preferentially return and revisit these high-resource plants [Cartar, 2004]. Similarly, our results suggest that *M. affinis*' pollinators within high resource patches behave as 'area-restricted' searchers, moving stochastically but over short distances and

only engaging in long distance foraging after encountering low-reward patches (i.e. trees with reduced floral displays).

Finally, our results show that plant population and individual attributes mediate pollinator performance through significant impacts on seed production. Specifically, our analyses reveal a negative effect of local kinship on the proportion of viable seeds per fruit, likely driven by greater biparental inbreeding and thus higher abortion rates for plants living in higher kinship neighborhoods. While fine-scale spatial genetic structure is a common feature in plant populations [Vekemans and Hardy, 2004], few studies have addressed its impact on the reproductive success of individual plants. Our findings have important implications for pollination service provision in rare and threatened wild plant populations given that they typically exhibit neighborhoods with high levels of kinship among plants [Perez-Mendez et al., 2015]. Under this scenario, highly mobile pollinators may be critical for preventing the mating of closely related individuals and consequent reductions in seed production.

In this study, we quantify pollen movement and fine scale spatial genetic structure across extensive spatial scales to reveal an unexpected level of breadth in pollination function. Our results contrast the long-standing assumption that pollinator body size drives pollen dispersal and also provides unique support for the role of plant size and local kinship in mediating pollination service provision. Further, we show that pollinator traits can influence some indices of pollination service, but not others; thus, utilizing only a single index of pollinator effectiveness can critically underestimate the role of func-

tional diversity in overall service provision. Our findings are especially salient given current concerns about functional diversity loss driven by ongoing declines in global biodiversity [Ceballos et al., 2015] and a need to safeguard these multi-faceted ecological functions. Overall, results from this study highlight the value of incorporating vector-mediated gene flow, as well as individual and population traits, to effectively describe ecosystem service dynamics across large spatial scales.

4.5 Appendix: Fractional paternity estimation

In this appendix we detail the model and computational scheme used to assign paternities to individual seeds. First, we define notation for the partition of offspring among parents which will later be useful in defining conditional distributions. Throughout, we abuse notation and generically use $\varphi(.|.)$ to indicate a conditional probability density or mass function.

Assume that K offspring are genotyped from M mothers in a population of J trees. The ith offspring is assigned to a known mother m_i and an unknown father f_i. Trees are obligate outcrossers: $m_i \neq f_i$. Conditional on the identity of the mother, the paternal assignment is a random categorical variable; the prior probability that this variable equals father j is uniform across possible fathers, so that $\varphi(f_i = j|m_i = k) = \frac{1}{J-1}$. Let $\Omega(k) = \{i : m_i = k\}$ be the set of offspring with mother k, and $\Xi(j) = \{i : f_i = j\}$ be the set of offspring with father j. The set of offspring belonging to mother k and father j is $\Psi(j, k) = \Omega(k) \cap \Xi(j)$, and the set of offspring belonging to a tree j is

$\Lambda(j) = \Omega(j) \cup \Xi(j)$. There are a finite number of possible partitions of offspring among mothers and putative fathers; we assume a uniform (noninformative) prior across possible partitions.

Probability of observed genotypes. Observed genotypes are the true genotypes contaminated by measurement error. The probability of observed genotype $\mathcal{O} = \{o_1, o_2\}$ given true genotype $\mathcal{G} = \{g_1, g_2\}$ and error probabilities $\boldsymbol{\epsilon} = \{\epsilon_1, \epsilon_2\}$ is $\varphi(\mathcal{O}|\mathcal{G}, \epsilon)$. Assuming A alleles at the locus, let ϵ_1 be the probability of allelic dropout (a heterozygote erroneously appears as a homozygote), and ϵ_2 be the probability of a stochastic genotyping error (an allele erroneously appears as one of the $(A-1)$ other alleles). We use the model of genotyping error developed by [Wang, 2004], which follows from enumerating all possible ways to get from a given true genotype to a given observed genotype with the two error types described above:

$$\varphi(\mathcal{O}|\mathcal{G}, \boldsymbol{\epsilon}) = \begin{cases} (1-(A-1)\epsilon_2)^2 & \text{if } g_1 = g_2 = o_1 = o_2 \\ 2\epsilon_2(1-(A-1)\epsilon_2) & \text{if } g_1 = o_1, g_2 \neq o_2 \\ \epsilon_2^2(2-\delta(o_1, o_2)) & \text{if } g_1 \neq o_1, g_2 \neq o_2 \end{cases} \tag{4.1}$$

if the true genotype is homozygous ($g_1 = g_2$), and

$$\varphi(\mathcal{O}|\mathcal{G}, \boldsymbol{\epsilon}) = \begin{cases} (1-(A-1)\epsilon_2)^2 + \epsilon_2^2 - 2\epsilon_1(1-A\epsilon_2)^2 & \text{if } g_1 = o_1, g_2 = o_2 \\ \epsilon_2(1-(A-1)\epsilon_2) + \epsilon_1(1-A\epsilon_2)^2 & \text{if } g_i = o_1 = o_2 \\ \epsilon_2^2(2-\delta(o_1, o_2)) & \text{if } g_1 \neq o_1, g_2 \neq o_2 \\ \epsilon_2(1-A\epsilon_2) & \text{otherwise} \end{cases} \tag{4.2}$$

if the true genotype is heterozygous ($g_1 \neq g_2$). The indicator function $\delta(a, b)$ equals 1 if $a = b$, and 0 otherwise.

Conditional on **true** maternal and paternal genotypes $\mathcal{M} = \{q_1, q_2\}$ and $\mathcal{P} = \{p_1, p_2\}$, the likelihood of **observed** seed genotype $\mathcal{S} = \{s_1, s_2\}$ is obtained by integrating $\varphi(\mathcal{O}|\mathcal{G}, \boldsymbol{\epsilon})$ over possible genotypes given Mendelian inheritance probabilities:

$$\varphi(\mathcal{S}|\mathcal{M}, \mathcal{P}, \boldsymbol{\epsilon}) = \frac{1}{4} \sum_{i \leq 2} \sum_{j \leq 2} \Pr(\mathcal{O} = \{s_1, s_2\} | \mathcal{G} = \{p_i, q_j\}, \boldsymbol{\epsilon}) \tag{4.3}$$

Let $\mathbf{S}_i$ be the observed genotype for the ith seed, and let $\mathbf{T}_j$ and $\mathcal{T}_j$ be the observed and true genotypes (respectively) for the jth reproductive tree. We use the superscript (l) to denote the lth locus (out of L total loci). The joint probability of the observed genotypes can be factored as the probabilities of the observed tree genotypes given the true tree genotypes, and the observed offspring genotypes given the true tree genotypes and parental assignments:

$$\varphi(\mathbf{S}, \mathbf{T}|\boldsymbol{\epsilon}, \mathbf{f}) = \prod_{l=1}^{L} \prod_{j=1}^{J} \varphi(\mathcal{O} = \mathbf{T}_j^{(l)} | \mathcal{G} = \mathcal{T}_j^{(l)}, \boldsymbol{\epsilon}) \times \prod_{i=1}^{K} \varphi(\mathcal{S} = \mathbf{S}_i^{(l)} | \mathcal{M} = \mathcal{T}_{m_i}^{(l)}, \mathcal{P} = \mathcal{T}_{f_i}^{(l)}, \boldsymbol{\epsilon})$$

The product over loci follows from the assumption that loci are independent.

Probability of true tree genotypes. Let the A alleles at a locus have frequencies $\boldsymbol{\alpha} = \{\alpha_1, \ldots \alpha_A\}$ in the population. To capture deviations from Hardy-Weinberg equillibrium, we introduce an inbreeding coefficient $\zeta \in [0, 1]$ that allows homozygotes to be more frequent than would be expected in HWE. Assume that a fraction η of the population mates only with trees of an identical genotype (as would occur, for example, due to inbreeding within a stand

of siblings). Let a genotype $\mathcal{G} = j, k$ have frequency $\phi_{j,k}$ in the current generation. The frequency $\phi'_{j,k}$ in the next generation is a mixture of random and assortative mating:

$$\phi'_{j,k} = \begin{cases} 2\alpha_j\alpha_k(1-\eta) + \frac{1}{2}\phi_{j,k}\eta & \text{if } j \neq k \\ \alpha_j^2(1-\eta) + (\phi_{j,j} + \frac{1}{4}\sum_{i\neq j}\phi_{j,i})\eta & \text{if } j = k \end{cases}$$

The equilibrium genotype frequencies $\phi^*_{j,k} = \phi_{j,k} = \phi'_{j,k}$ are invariant, and some algebra gives:

$$\phi^*_{j,k} = \begin{cases} 2\alpha_j\alpha_k(1-\frac{\eta}{2-\eta}) & \text{if } j \neq k \\ \alpha_j^2 + \alpha_j\frac{\eta}{2-\eta}\sum_{i\neq j}\alpha_i & \text{if } j = k \end{cases}$$

Conventionally, we reparameterize as $\zeta = \frac{\eta}{2-\eta}$. Therefore, at equilibrium the probability of a randomly sampled genotype $\mathcal{G} = \{j, k\}$ is:

$$\varphi(\mathcal{G}|\boldsymbol{\alpha}, \zeta) = \begin{cases} 2(1-\zeta)\alpha_j\alpha_k & \text{if } j \neq k \\ \alpha_j^2 + \zeta\alpha_j(1-\alpha_j) & \text{if } j = k \end{cases}$$

As $\zeta \to 1$, homozygotes become more frequent; as $\zeta \to 0$, the expected frequencies of genotypes follow HWE. Uniform priors are used for $\boldsymbol{\alpha}$ and ζ.

Full probability model and conditional posteriors. With the definitions given in the preceeding section, and uniform priors on $\boldsymbol{\alpha}^{(l)}$, $\boldsymbol{\epsilon}$, ζ, the joint posterior is proportional to:

$$\varphi(\mathcal{T}, \boldsymbol{\alpha}, \zeta, \boldsymbol{\epsilon}, \mathbf{f}|\mathbf{S}, \mathbf{T}, \mathbf{m}) \propto \prod_{l=1}^{L}\Bigg(\prod_{j=1}^{J}\varphi(\mathbf{T}_j^{(l)}|\mathcal{T}_j^{(l)}, \boldsymbol{\epsilon})\varphi(\mathcal{T}_j^{(l)}|\boldsymbol{\alpha}^{(l)}, \zeta) \times \prod_{k=1}^{K}\prod_{i\in\Omega(k)}\varphi(\mathbf{S}_i^{(l)}|\mathcal{T}_k^{(l)}, \mathcal{T}_{f_i}^{(l)}, \boldsymbol{\epsilon})\Bigg)$$

Observed genotypes that are missing (for both seeds and trees) and are treated as unknown random variables, distributed as equations 4.1-4.2 (if seeds) or as equation 4.3 (if trees).

At locus l in tree j, the conditional posterior distribution of the true, unknown genotype $\mathcal{T}_j$ is a function of the observed parental genotypes and the observed genotypes of offspring:

$$\varphi(\mathcal{T}_j^{(l)}|\mathbf{f},\mathbf{S}^{(l)},\mathbf{T}^{(l)},\boldsymbol{\epsilon},\boldsymbol{\alpha}^{(l)},\zeta) \propto \varphi(\mathcal{T}_j^{(l)}|\boldsymbol{\alpha}^{(l)},\zeta)\varphi(\mathbf{T}_j^{(l)}|\mathcal{T}_j^{(l)},\boldsymbol{\epsilon})\times \prod_{i\in\Xi(j)} \varphi(\mathbf{S}_i^{(l)}|\mathcal{T}_{m_i}^{(l)},\mathcal{T}_j^{(l)},\boldsymbol{\epsilon}) \prod_{i\in\Omega(j)} \varphi(\mathbf{S}_i^{(l)}|\mathcal{T}_j^{(l)},\mathcal{T}_{f_i}^{(l)},\boldsymbol{\epsilon}^{(l)})$$

This is categorical over possible genotypes. The first product is over seeds putatively sired by tree j, and the second product is over seeds known to be dammed by tree j.

The conditional posterior of the paternal assignment f_i for seed i is a function of the observed genotypes of the seed, the true genotype of the known mother, and the true genotypes of putative fathers:

$$\varphi(f_i = j|\mathcal{T},\mathbf{S}_i,\boldsymbol{\epsilon},m_i) \propto \prod_{l=1}^{L} \varphi(\mathbf{S}_i^{(l)}|\mathcal{T}_{m_i}^{(l)},\mathcal{T}_j^{(l)},\boldsymbol{\epsilon})$$

This is categorical over putative fathers.

The conditional posteriors for $\boldsymbol{\alpha}$ and ζ are constrained to a unit simplex and unit interval respectively, and are functions of the true (tree) genotypes:

$$\varphi(\boldsymbol{\alpha}^{(l)}|\mathcal{T}^{(l)},\zeta) \propto \prod_{j=1}^{J} \varphi(\mathcal{T}_j^{(l)}|\boldsymbol{\alpha}^{(l)},\zeta)$$

$$\varphi(\boldsymbol{\zeta}|\boldsymbol{\alpha}, \mathcal{T}) \propto \prod_{j=1}^{J} \prod_{l=1}^{L} \varphi(\mathcal{T}_j^{(l)}|\boldsymbol{\alpha}^{(l)}, \zeta)$$

The conditional posterior for the error rates $\boldsymbol{\epsilon}$ is constrained to $[0, 0.5]$, and is a function of the true and observed genotypes, and paternal assignments,

$$\varphi(\boldsymbol{\epsilon}|\mathcal{T}, \mathbf{T}, \mathbf{S}, \mathbf{f}) = \prod_{l=1}^{L} \prod_{j=1}^{J} \varphi(\mathbf{T}_j^{(l)}|\mathcal{T}_j^{(l)}, \boldsymbol{\epsilon}) \prod_{k=1}^{K} \prod_{i \in \Omega(k)} \varphi(\mathbf{S}_i^{(l)}|\mathcal{T}_k^{(l)}, \mathcal{T}_{f_i}^{(l)}, \boldsymbol{\epsilon}).$$

Computation. Inference is straightforward with Markov chain Monte Carlo, except for sampling the allele frequencies $\boldsymbol{\alpha}$ in an efficient manner. We used the method described by [Director et al., 2017] to generate proposals for $\boldsymbol{\alpha}$ with a reasonably high acceptance probability. A single iteration of the MCMC algorithm is:

1. Update $\boldsymbol{\alpha}$. For $l \leq L$, $a \leq A^{(l)}$,

   (a) Propose new allele frequency $\tilde{\alpha}_a^{(l)} = \text{ilogit}(\text{logit}(\alpha_a^{(l)}) + h_a^{(l)} z_a^{(l)})$ where $h_a^{(l)}$ is a fixed tuning parameter and $z_a^{(l)}$ is a draw from the standard Gaussian.

   (b) Rescale the frequencies of the other alleles at the locus so that they lie on the unit simplex. For allele $b \neq a$, set $\tilde{\alpha}_b^{(l)} = (1 - \tilde{\alpha}_a^{(l)})(1 - \alpha_a^{(l)})^{-1} \alpha_b^{(l)}$ to get vector $\tilde{\boldsymbol{\alpha}}^{(l)}$

   (c) Set $\alpha_a^{(l)} = \tilde{\alpha}_a^{(l)}$ with probability

   $$1 \wedge \frac{\varphi(\tilde{\boldsymbol{\alpha}}^{(l)}|\mathcal{T}^{(l)}, \zeta) \tilde{\alpha}_a^{(l)} (1 - \tilde{\alpha}_a^{(l)})^{A^{(l)}-1}}{\varphi(\boldsymbol{\alpha}^{(l)}|\mathcal{T}^{(l)}, \zeta) \alpha_a^{(l)} (1 - \alpha_a^{(l)})^{A^{(l)}-1}}$$

2. Update ζ.

(a) Propose new inbreeding coefficient $\tilde{\zeta} = \text{ilogit}(\text{logit}(\zeta) + h_\zeta z_\zeta)$, where h_ζ is a tuning parameter and z_ζ is a draw from a standard Gaussian.

(b) Set $\zeta = \tilde{\zeta}$ with probability

$$1 \wedge \frac{\varphi(\tilde{\zeta}|\boldsymbol{\alpha}, \mathcal{T})}{\varphi(\zeta|\boldsymbol{\alpha}, \mathcal{T})}$$

3. Update $\mathcal{T}$. For $j \leq J$,

(a) For $l \leq L$, set $\mathcal{T}_j^{(l)} = \{a, b\}$ with probability

$$\frac{\varphi(\mathcal{T}_j^{(l)} = \{a, b\}|\mathbf{f}_j, \mathbf{S}^{(l)}, \mathbf{T}^{(l)}, \boldsymbol{\epsilon}, \boldsymbol{\alpha}^{(l)}, \zeta)}{\sum_{u=1}^{A^{(l)}} \sum_{v=u}^{A^{(l)}} \varphi(\mathcal{T}_j^{(l)} = \{u, v\}|\mathbf{f}_j, \mathbf{S}^{(l)}, \mathbf{T}^{(l)}, \boldsymbol{\epsilon}, \boldsymbol{\alpha}^{(l)}, \zeta)}$$

4. Update $\boldsymbol{\epsilon}$.

(a) For $i \in \{1, 2\}$, propose new error rates $\tilde{\epsilon}_i = 0.5 \exp\{\ln \frac{\epsilon_i}{0.5 - \epsilon_i} + h_\epsilon z_{\epsilon,i}\}(1 + \exp\{\ln \frac{\epsilon_i}{0.5 - \epsilon_i} + h_\epsilon z_{\epsilon,i}\})^{-1}$, where h_ϵ is a tuning parameter and $z_{\epsilon,i}$ is a draw from a standard Gaussian.

(b) Set $\boldsymbol{\epsilon} = \tilde{\boldsymbol{\epsilon}} = \{\tilde{\epsilon}_1, \tilde{\epsilon}_2\}$ with probability

$$1 \wedge \frac{\varphi(\tilde{\boldsymbol{\epsilon}}|\mathcal{T}, \mathbf{T}, \mathbf{S}, \mathbf{f})}{\varphi(\boldsymbol{\epsilon}|\mathcal{T}, \mathbf{T}, \mathbf{S}, \mathbf{f})}$$

5. Update $\mathbf{f}$. For $i \leq K$,

(a) Set $f_i = j$ with probability

$$\frac{\varphi(f_i = j|\mathcal{T}, \mathbf{S}_i, \boldsymbol{\epsilon}, m_i)}{\sum_{k \neq m_i} \varphi(f_i = k|\mathcal{T}, \mathbf{S}_i, \boldsymbol{\epsilon}, m_i)}$$

6. Update observed genotypes that are missing. For $l \leq L$,

(a) For $i \leq K$, if $\mathbf{S}_i^{(l)}$ is missing, set $\mathbf{S}_i^{(l)} = \{a, b\}$ with probability

$$\frac{\varphi(\mathbf{S}_i^{(l)} = \{a, b\} | \mathcal{T}_{f_i}^{(l)}, \mathcal{T}_{m_i}^{(l)}, \boldsymbol{\epsilon})}{\sum_{u=1}^{A^{(l)}} \sum_{v=u}^{A^{(l)}} \varphi(\mathbf{S}_i^{(l)} = \{u, v\} | \mathcal{T}_{f_i}^{(l)}, \mathcal{T}_{m_i}^{(l)}, \boldsymbol{\epsilon})}$$

(b) For $j \leq J$, if $\mathbf{T}_j^{(l)}$ is missing, set $\mathbf{T}_j^{(l)} = \{a, b\}$ with probability

$$\frac{\varphi(\mathbf{T}_j^{(l)} = \{a, b\} | \mathcal{T}_j^{(l)}, \boldsymbol{\epsilon})}{\sum_{u=1}^{A^{(l)}} \sum_{v=u}^{A^{(l)}} \varphi(\mathbf{T}_j^{(l)} = \{u, v\} | \mathcal{T}_j^{(l)}, \boldsymbol{\epsilon})}$$

Seed viability		
Fixed Effect	Estimate (95% CI)	P value
ITD	0.431 (0.175, 0.686)	<0.001
DBH_{mother}	0.040 (-0.243, 0.323)	0.781
SI	0.069 (-0.244, 0.383)	0.665
Kinship	-0.274 (-0.519, -0.028)	0.029

Pollen dispersal distance		
Fixed Effect	Estimate (95% CI)	P value
ITD	0.039 (-0.022, 0.100)	0.400 (0.310)
DBH_{mother}	-0.086 (-0.155, -0.018)	0.021 (0.041)
SI	0.069 (0.015, 0.124)	0.017 (0.018)
Kinship	-0.048 (-0.119, -0.023)	0.177 (0.183)

Table 4.1: Results of generalized linear mixed-effects models with binomial (seed viability) and Gaussian (pollen-dispersal distance) error distributions. SI, spatial isolation, is defined as the mean distance from the mother tree to its 10 nearest neighbor trees. Kinship refers to the local kinship between the mother tree and all trees in a radius of 400 meters. All explanatory variables were scaled in the analyses. For pollen-dispersal distance, P values in parentheses are approximated by repeatedly permuting covariates at the appropriate level of replication and refitting the model to each permutation.

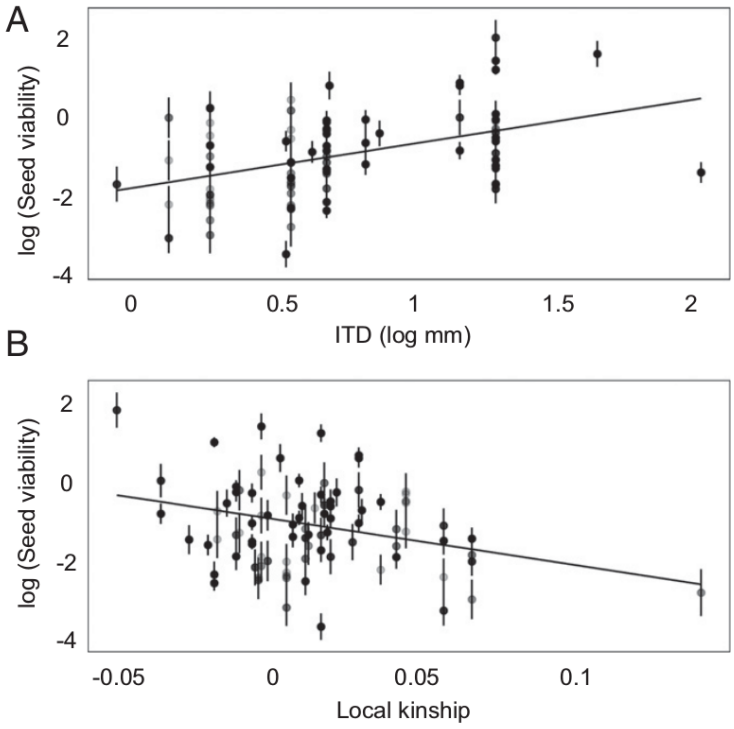

Figure 4.1: Effect of pollinator body size, as measured by ITD (intertegular distance) and local kinship on seed viability. Seed viability refers to the ratio between viable and aborted seeds. Dots represent the predicted means from the model at the inflorescence level on a logarithmic scale. Standard errors were calculated using 100 bootstrap replicates.

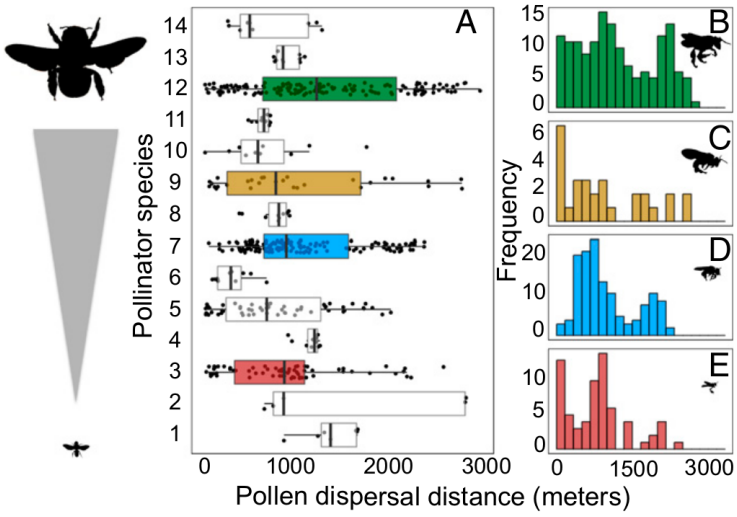

Figure 4.2: Pollen dispersal distances recorded for each *M. affinis* pollinator. (*A*) Boxplots indicate the median, upper, and lower quartile for each *M. affinis* pollinator. Increasing numbers in the y-axis correspond with the following pollinator species sorted in ascending order regarding their body size (ITD): (1) *Halictidae sp* 2, (2) *Trigona buyssoni*, (3) *Tetragonisca angustula*, (4) *Halictidae 1*, (5) *Trigona muzoensis*, (6) *Paratetrapedia lineata*, (7) *Trigona fuscipennis*, (8) *Trigona amalthea*, (9) *Trigona fulviventris*, (10) *Pseudaugochloropsis sp* 1, (11) *Melipona fuliginosa*, (12) *Melipona panamica*, (13) *Centris dichrootricha*, (14) *Xylocopa fimbriata*. (*B-E*) Frequency distribution of the pollen dispersal distances for a subsample of *M. affinis* pollinators representative of the body size gradient (B: *Melipona panamensis*; C: *Trigona fulviventris*; D: *Trigona fuscipennis*; E: *Tetragonisca angustula*).

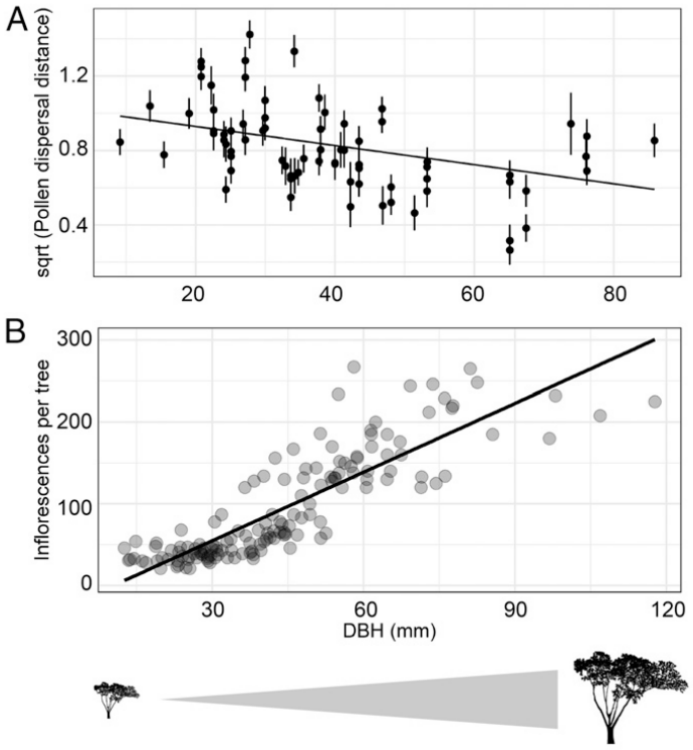

Figure 4.3: Effect of diameter at breast height of the mother tree (DBH_{mother}) on pollen dispersal distance. (A) Pollen dispersal distance was square-root transformed and DBH_{mother} is plotted at its original scale. Dots represent the predicted means from the model at the infructescence level. Standard errors were calculated using 1000 bootstrap replicates. (B) Relationship between DBH_{mother} and total number of inflorescences per tree.

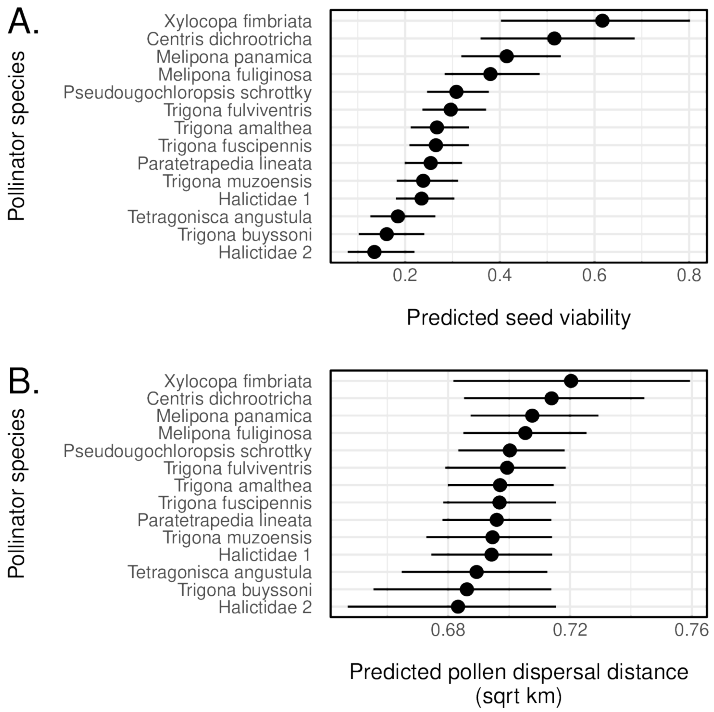

Figure 4.4: Species-level predicted estimates of seed viability and pollen-dispersal distances. For each pollinator species, points are predicted means with 95% confidence intervals calculated by parametric bootstrap from our seed viability (A) and pollen-dispersal distance (B) models. Seed viability refers to the proportion of viable seeds per fruit. Pollinator species are sorted in ascending order based on their body size.

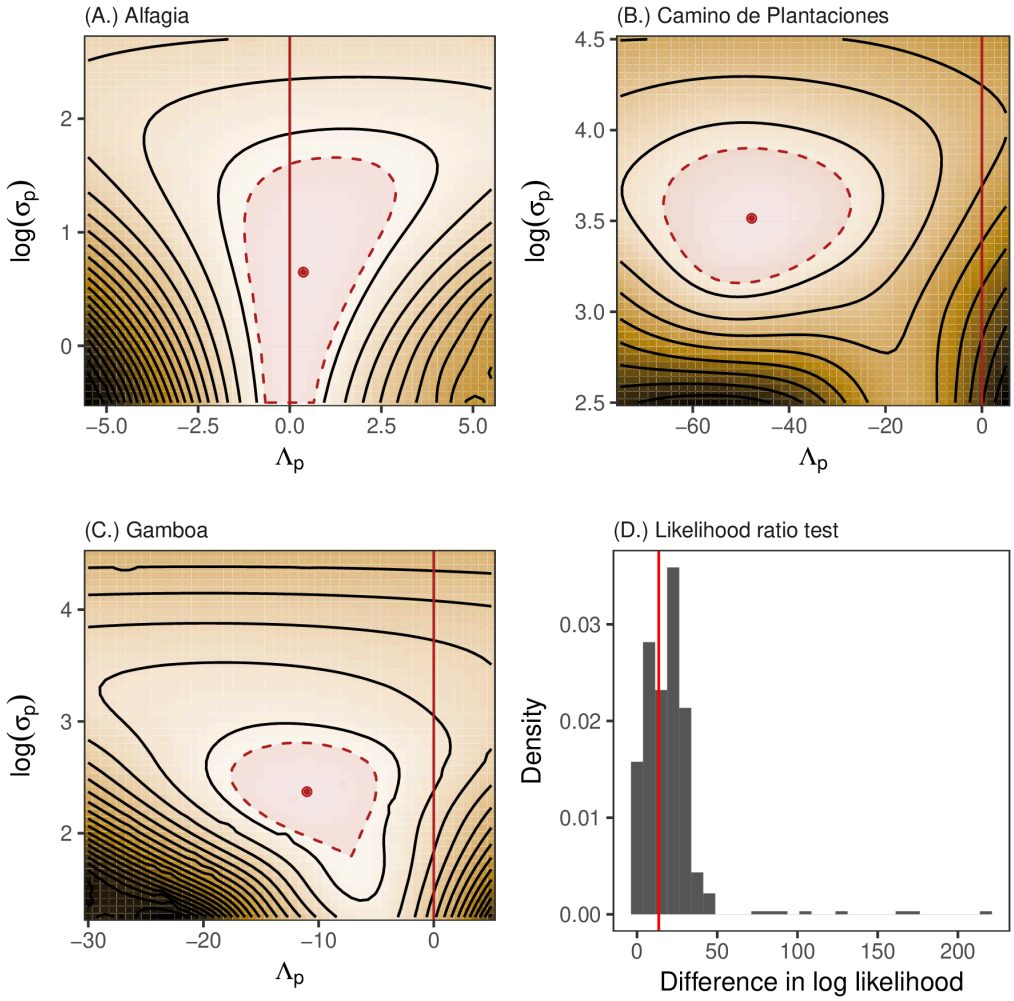
(A.) Alfagia
(B.) Camino de Plantaciones
(C.) Gamboa
(D.) Likelihood ratio test
log(σp)
Λp
Density
Difference in log likelihood

Figure 4.5

Figure 4.5: (A–C) Log likelihood surfaces for region-specific parameters of the multinomial model of pollen-dispersal distances described in section 4.2. For the ith visit from the pth region, λ_i is the rate at which pollen flow decays with distance. The $\log \lambda_i$ are modeled as Gaussian random effects and with region-specific mean Λ_p and standard deviation σ_p. In each figure, the maximum likelihood estimates of $[\Lambda_p, \sigma_p]$ are shown by a red point, and the 95% confidence region is the shaded red area. $\Lambda_p = 0$ corresponds to no spatial mating structure (every tree is equally likely to mate with every other tree) and is marked by a red dashed line. Black isoclines are separated by intervals of 5 on the log likelihood scale. For mother trees in Gamboa (C) and Camino de Plantaciones (B), we find evidence for spatial-restricted mating and for substantial variation across visits in the rate of distance decay of pollen flow. (D) Likelihood ratio test between a model in which the rate of distance decay in pollen flow is a function of pollinator body size (see section 4.2) against a null model in which there is no systematic variation in distance decay across pollinators. The histogram shows the approximate null distribution of the likelihood ratio statistic (twice the difference in log likelihood), generated with a parametric bootstrap. In each bootstrap replicate, data (including seed genotypes) were simulated from the null model (e.g., using parameters estimates shown in A through C), and both models were refit to the simulated data. The observed likelihood ratio test statistic ($\chi^2_{\text{obs}} = 13.5$, bootstrap P = 0.36) is shown by the red line. We find no evidence that the spatial extent of pollen flow is influenced by pollinator body size.

Chapter 5

A computationally efficient, covariance-based method for inferring landscape resistance to gene flow

The research described in this chapter represents a collaboration between the author, Dr. Rodolfo Jaffé, and Dr. Shalene Jha. As of the time of writing, this study has not been published elsewhere.

5.1 Introduction

One of the fundamental uses of molecular data in ecology and evolution is to infer dispersal from patterns of genetic similarity [Bohonak, 1999]. These sort of data provide only indirect observations about the movements of organisms, and often on a time scale that far exceeds contemporary processes, but can be applied in many situations where direct measurement is logistically infeasible or simply impossible [Sork et al., 1999, Zeller et al., 2012]. The indirect nature of this type of inference problem, and the formidable yet predictable noise that accompanies the collection of sequence data, require analytical frameworks and statistical methods that are tailored towards specific biological processes [Guillot et al., 2009, Balkenhol et al., 2009, Beaumont

et al., 2010].

For the particular problem of inferring an influence of environment on dispersal, a popular framework is to compare predictions from a given movement model with observed patterns of genetic similarity [McRae and Beier, 2007, Zeller et al., 2012]. A correspondence between these predictions and extant genetic structure is taken as evidence for the underlying hypothesis about movement [Cushman et al., 2006]. To date, the movement model most frequently used for this task is a simple random walk, motivated by analogy to Brownian motion or passage of electric current across circuits [McRae, 2006]. By approximating a heterogeneous landscape as discrete weighted graph and applying tools from the theory of graphs and stochastic processes, various metrics of spatial connectivity may be constructed [Urban and Keitt, 2001, McRae et al., 2008, Urban et al., 2009]. A ubiquitous example of such a derived connectivity metric is "resistance distance", that is the expected commute time between two nodes on a graph under the assumption of a memory-less random walk [Klein and Randić, 1993]. By parametrizing the movement model (and thus resistance distances) in terms of underlying, inhomogeneous environmental variables, quantitative predictions regarding complex hypotheses may be generated and tested [Spear et al., 2010].

This is a compelling approach, especially as the computational and statistical demands are far less than would be needed under an explicit population genetic model such as Wright-Fisher diffusion [Gutenkunst et al., 2009] or the spatial coalescent [Currat et al., 2004, Joseph et al., 2016]. However,

from a statistical perspective, the key challenge in this process is how to go about comparing a metric that is strictly spatial (such a commute time) with data that is strictly genetic (e.g. individual genotypes). The typical approach is to regress a metric of genetic divergence (like Fst or relatedness) onto a metric of spatial connectivity, while accounting in some fashion for the dependence between pairwise measurements [Shirk et al., 2010, Jaffé et al., 2016]. An obvious and useful extension is to treat the underlying movement model as a function of continuous parameters, and optimize these parameters with respect to the relationship between connectivity and divergence [Epps et al., 2007, Peterman et al., 2014]. However, it is not at all obvious that this should give correct or consistent inferences. For example, while in some cases the relationship between connectivity and genetic divergence will be monotonic or even linear, there is no compelling reason why deviations from monotonicity or linearity should be considered less likely *a priori* in the presence of complex demographic processes [Hutchison and Templeton, 1999]. While procedures like permutation tests and dyadic covariance structures [Clarke et al., 2002, Legendre and Fortin, 2010] may help to mitigate type I errors, with any distance regression the data collection process is not explicitly modelled and thus treatment of sampling error is ad hoc. Further, reducing genetic data to a summary statistic (such as Fst) will inevitably lose information, and if the statistic stabilizes fairly quickly with increasing numbers of loci, then the utility of high-throughput sequence data is limited. All of these issues revolve around a single core complaint: a regression between distance/dissimilarity

metrics is not a generative model. In other words, one cannot take a connectivity metric and a fitted relationship to Fst or relatedness and simulate genotypes across space.

Our goal in this study is to bridge this gap, by developing a generative model for single nucleotide polymorphisms (SNP) that embeds the structure of an underlying movement process (a random walk). Our approach is conceptually and technically related to resistance distance. We have four criteria: (1.) to explicitly model SNP frequencies through space, and accommodate genotyping and sequencing error; (2.) dependence among data that is directly related to a Markov process of movement on a landscape graph; (3.) computational speed, such that simpler models can be fit to data on the order of minutes, facilitating comparisons of a complex or diverse set of hypotheses; (4.) an interpretation of the likelihood as an approximation to a powerful and essential genomic summary statistic, the site frequency spectrum.

First, we motivate a likelihood for SNP counts via an approximation to the joint site frequency spectrum between demes. The tractability of the approximation allows us to link the frequencies of alleles across space to a covariance structure that is in itself computationally challenging, and reflects a Markov process of diffusion across an inhomogeneous landscape. We then derive an efficient approach to calculating the likelihood and a means to compute gradients with practically no additional cost, which greatly facilitates optimization of the likelihood. To validate our approach under realistic (e.g. not cherry-picked) conditions, we simulate data from a multi-population coa-

lescent defined on a lattice [Ray et al., 2010]. We compare the performance of our proposed method with a popular approach towards distance regression [Clarke et al., 2002, Peterman et al., 2014], across varying degrees of strength in an environment-gene flow interaction, to correctly determine the underlying model. Finally, we use real data from a system where we have a good *a priori* expectation as to underlying environmental factors structure dispersal – a tropical social bee [Jaffé et al., 2019] limited by altitude and the availability of forest habitat. This empirical example, where spatial genetic structure is strong and the direction of environmental effects on dispersal is clear, provides a good case study for relative performance of methods. Our method is implemented as a multi-threaded C++ program, wrapped into the R package *gaffer* (Green's Anisotropic Functions For Resistance Estimation) `www.github.com/nspope/inlassle`.

5.2 Methods

Approximation of the joint allele frequency spectrum. The allele frequency spectrum (AFS) for a set of N demes, $\Phi(x)$, $x \in [0,1]^N$, is the joint probability distribution on the unit hypercube for the frequencies of SNPs across demes. However, allele frequencies are only observed via finite samples of individual genotypes. Let $y = [y_1, \dots y_N]$ equal counts of the variant allele and $n = [n_1, \dots, n_N]$ equal the total number of genotyped haploids across demes. The probability of these data under the allele frequency spectrum is $\int_0^1 \cdots \int_0^1 \Phi(x) \prod_i p(y_i|x_i; n_i) dx$, where $p(y_i|x_i; n_i) = \binom{n_i}{y_i} x_i^{y_i}(1-x_i)^{n_i - y_i}$ are bi-

nomial sampling probabilities in for deme i. The values of $p(y; n)$ across all possible y form the site frequency spectrum (SFS) corresponding to a given AFS. The SFS carries information about population genetic processes (gene flow, genetic drift, etc.), that in turn carry information about the shared demographic history of the demes. Thus, the SFS has been of great utility for demographic inference from SNP data [Gutenkunst et al., 2009]. However, for collections of many demes, the computation of the SFS under a specific demographic model is intractable. However, a large collection of (spatially disparate) demes is exactly what is needed to make inferences about the influence of the landscape on gene flow.

Our strategy is to approximate the AFS by a tractable multivariate distribution, the multivariate logit-normal, that broadly captures the structure of the derived SFS and retains information about migration between demes (Figure 5.1). By parametrizing the logit-normal in such a way as to reflect migration across an inhomogeneous landscape, we are able to use the approximate SFS as a likelihood function that links observed SNP data to environmental influences on gene flow. Under the logit-normal approximation,

$$\begin{aligned}\Phi(x_i)\prod p(y_i|x_i;n_i) &\approx p(y,z;n,\mu,\Sigma)\\ &= |\Sigma|^{-1/2}\exp\{-\frac{1}{2}(z-\mu)'\Sigma^{-1}(z-\mu)\}\prod_i p(y_i|z_i;n_i),\\ p(y_i|z_i;n_i) &= \binom{n_i}{y_i}(1+\exp\{-z_i\})^{-y_i}(1-(1+\exp\{-z_i\})^{-1})^{n_i-y_i}\end{aligned}$$

The integral over the logit-normal that is necessary to calculate the SFS does not have a closed form, but because the density contains a multivariate

Gaussian kernel, the integral can be reasonably approximated by Laplace's method [Tierney and Kadane, 1986, Rue et al., 2009]. The Laplace approximation replaces the posterior distribution of z, $p(z|y; n, \mu, \Sigma)$, with a multivariate Gaussian $\tilde{p}(z|y; n, \mu, \Sigma)$ that has mean $\hat{z} = \arg\min_z - \log p(y, z; n, \mu, \Sigma)$, and covariance equal to the inverse of the Hessian $\mathcal{H}(\hat{z}) = (\Sigma^{-1} - D(\hat{z}))^{-1}$, where $D(z)$ is the diagonal matrix of second partial derivatives of $\log p(y|z; n)$ with respect to z. Evaluating Bayes' rule at the mode of $\tilde{p}(z|y; n, \mu, \Sigma)$,

$$\tilde{p}(\hat{z}|y; n, \mu, \Sigma) = (2\pi)^{N/2}|\mathcal{H}(\hat{z})|^{1/2} \approx p(y, \hat{z}; n, \mu, \Sigma)p(y; n, \mu, \Sigma)^{-1}$$

which gives an approximation to the likelihood,

$$\begin{aligned} p(y; n, \mu, \Sigma) &\approx Cp(y, \hat{z}; n, \mu, \Sigma)|\mathcal{H}(\hat{z})|^{-1/2} \\ &\propto |\Sigma|^{-1/2} \exp\{-0.5(\hat{z} - \mu)'\Sigma^{-1}(\hat{z} - \mu)\} \prod_i p(y_i|z_i; n_i) \end{aligned}$$

In practice, genotypes are not directly observed, but are inferred from sequence data. If sequencing depth is low, error in the inferred genotypes can bias downstream analysis, especially for rare variants [Korneliussen et al., 2014]. This issue may be bypassed by using genotype probabilities (given a model of sequencing error) instead of called genotypes. Consider a single locus l within deme i. Let $p(O_{i,k,l}|G_{i,k,l})$ be the probability of the observed sequence data $O_{i,k,l}$ given an unknown true genotype $G_{i,k,l}$ for individual k under a particular model of sequencing (e.g. from [Li, 2011]), calculated by a program like samtools [Li et al., 2009]. Then, the joint distribution of the variant count and the observed genotypes is $p(O_{i,l}, y_{i,l}|z_{i,l}) =$

$p(y_{i,l}|z_{i,l}) \sum p(G_{i,l}|y_{i,l}) \prod_k p(O_{i,k,l}|G_{i,k,l})$ where the sum is over all possible combinations of the unknown true genotypes $G_{i,l}$. Although seemingly complicated, this sum may be efficiently calculated using the dynamic programming algorithm from [Nielsen et al., 2012], and only needs to be calculated once. Summing over all possible variant counts y provides the joint distribution of the allele frequency spectrum and the sequence data, that is $p(O_l, z_l|\Sigma, \mu) = p(z_l|\Sigma, \mu) \prod_i \sum_{y_{i,l}=0}^{n_{i,l}} p(O_{i,l}, y_{i,l}|z_{i,l})$, which can be used in place of $p(y_l, z_l|\Sigma, \mu)$ in the Laplace approximation derivation above.

The utility of this approximation is to capture much of the information contained in the joint allele frequency spectrum about gene flow, while avoiding (to a large extent) the curse of dimensionality when calculating the likelihood. The logit-normal parameters Σ, μ can be chosen to reflect a spatially-explicit model of gene flow across many demes.

Diffusive model of gene flow. A spatial generalization of a multi-deme system is a lattice of k demes (a "landscape") where only direct neighbours exchange migrants. Under this scheme a haploid individual undergoes a random walk across demes, transitioning from a deme to its neighbour at a rate proportional to the (possibly asymmetric) migration rate. Assuming that the walker is "memory-less", the trajectory of the random walk satisfies the Markov assumption, and the spatial trajectory of a given individual is a realization of a continuous time Markov process on a finite state-space (the demes). This model of migration has an extensive history in population genetics and can

be viewed as a discrete approximation to the diffusion of alleles in continuous space [Kimura, 1964]. The rate matrix Q of this Markov process has off-diagonal entries $Q_{i,j} = -m_{i,j}$, where $m_{i,j}$ is the directional migration from deme i to j, and $m_{i,j} = 0$ if i, j are not neighbours. The diagonal entries are $Q_{i,i} = \sum_{j \neq i} Q_{i,j}$.

The goal is to construct a covariance model for log-transformed allele frequencies that captures the structure of the migration process at equilibrium. To do so, assume that at equilibrium the ratio of variant to wild-type alleles in a deme is equal to the weighted geometric average of the ratios of neighbouring demes, where the weights are transition probabilities of the Markov migration process. The geometric average of a ratio equals the ratio of geometric averages of numerator and denominator, and is the natural means to combine ratios of compositional data [Aitchison, 1994]. Let $a_{i,l}$ equal the ratio of variant to wild-type alleles in deme i at locus l at equilibrium, and let the vector $z_l = [\log a_{1,l}, \ldots, \log a_{k,l}]$. Then at equilibrium, if z_l is random and Gaussian, it solves the stochastic linear system $\Delta z_l = \xi$ where $\Delta = \text{Diag}\{Q\}^{-1}Q$ is the discrete Laplace operator and ξ is white noise. However, this condition cannot hold as Δ is singular: due to the fact that all of the rows of Q sum to zero, the kth value of z_l is completely determined by the other $k-1$ values. Therefore ξ can only be white noise on a $k-1$ dimensional subspace, and the law of the solutions z_l is defined on this subspace.

Let $UDV' = \Delta$ be a singular value decomposition, with u_k as the null space (the final column of U). The matrix $(I - u_k u_k')$ is a projection onto the

column space of Δ, and is symmetric and idempotent. Let $\xi = (I - u_k u_k')\tilde{\xi}$, where $\tilde{\xi}$ is $k-1$ dimensional white noise, and ξ is a (degenerate) Gaussian with covariance $(I - u_k u_k')$. Then,

$$UDV'z_l = (I - u_k u_k')\tilde{\xi} \implies UDV'VD^{+}U'\tilde{\xi} = (I - u_k u_k')\tilde{\xi}$$
$$\implies z_l = VD^{+}U'\tilde{\xi}$$

and so z_l is (degenerate) Gaussian with covariance $\Delta^{+}(\Delta^{+})'$ where Δ^{+} is the generalized inverse of Δ.

Intuition for the covariance comes from the importance of Δ^{+} (called the discrete Green function, [Chung and Yau, 2000]) in describing the dynamics of the Markov process. Using results from [Beveridge, 2016], $(\Delta^{+})_{ij}$ is the difference between the expected time needed for a trajectory that starts in deme i to reach deme j (the first hitting time), and the average hitting time for a trajectory from any starting point to reach deme j. An entry of $\Delta^{+}(\Delta^{+})'$ is the inner product between the Green functions for two demes, and is proportional to the covariance in their hitting times. Essentially, a pair of demes has greater covariance if both are accessible from similar parts of the landscape. This provides a covariance structure for z_l which reflects inhomogeneity in migration across the landscape, and can capture asymmetry in gene flow (e.g. anisotropy, Figure 5.2).

To relate migration to specific environmental conditions, let the migration between neighbouring demes equal log-linear functions of the pairwise average of environmental variables C with weights ζ, so that $m_{i,j} =$

$\exp \alpha + 0.5(c_i + c_j)'\zeta$. When the weights ζ equal zero, the covariance structure corresponds to isolation by distance. This construction is closely related to the resistance distance of the landscape landscape lattice [McRae and Beier, 2007]: the matrix of resistance distances between all demes is $R = -2Q^+ + 1\mathrm{diag}(Q^+)' + \mathrm{diag}(Q^+)1'$. The distinction is that by assuming that z_l is driven by white noise, the distribution of z_l is retrieved rather than a distance metric. Thus the model of migration described above gives rise to a flexible generative model for the covariance of a logit-normal approximation to the allele frequency spectrum.

This derivation does not take into account variation in average allele frequencies across loci due to genetic drift, which may also vary locally due to differences in effective population size across demes. To accommodate this, add a diagonal matrix of per-deme variances τ to $\Delta^+(\Delta^+)^{-1}$, and model the landscape-wide expectation of z_l as a Gaussian random variable β_l with mean β and variance γ. Integrating over β_l, the distribution of z_l for the observed subset of N demes is:

$$p(z_l; \beta, \gamma, \tau, \zeta) \propto |\Sigma|^{-1/2} \exp\{-0.5(z_l - \mu)'\Sigma^{-1}(z_l - \mu)\},$$
$$\Sigma = E'\Delta^+(\Delta^+)'E + \gamma 1'1 + \mathrm{diag}(\tau), \quad \mu = 1\beta$$

where E is a k-by-N design matrix with $E_{j,i} = 1$ if deme i is located at lattice point j and 0 else. The total covariance is the sum of a factor due to migration, a factor due to variation in average allele frequency across loci, and per-deme noise that may reflect spatial variation in genetic drift or other factors.

Computation of likelihood and gradient. Assembling these pieces, the Laplace approximation to the likelihood of the parameters given the sequence data is

$$\mathcal{L}(\beta, \gamma, \tau, \zeta; O, n) \approx \prod_l p(O_l|\hat{z}_l; n_l) p(\hat{z}_l|\beta, \gamma, \tau, \zeta) |\mathcal{H}(\hat{z}_l)|^{-0.5}$$

where $p(O_l|z_l; n_l)$, $p(z_l|\beta, \gamma, \tau, \zeta)$, and $\mathcal{H}$ are as defined above.

Calculating this likelihood involves computing certain rows of the generalized inverse of the Laplace operator Δ, via the singular linear system $Q'G = E$ (E is the design matrix mapping sampled locations to the landscape lattice, and $G = (\Delta^+)'E$ are the rows of the Green function needed to form the covariance matrix Σ). This is costly if the lattice is large. However, the sparsity and algebraic structure of Δ leads to an efficient scheme even when the number of demes is extensive [Pirotte et al., 2007]. As the lattice is fully connected, Δ has only a single zero eigenvalue and its nullspace is spanned by $v_k = 1/k$ (where k is the number of demes in the lattice). If Δ is symmetric then the left nullspace equals the nullspace; otherwise, the vector u_k that spans the left nullspace may be found efficiently using a Lanczos method [Pothen et al., 1990].

Let $\tilde{E} = (I - v_k v_k')E$ be the projection of the design matrix onto the row space of Δ. Drop an arbitrary (e.g. the kth) row and column from Δ and the corresponding row from $\tilde{E}$ to get $\Delta_{-k}, \tilde{E}_{-k}$. The reduced matrix Δ_{-k} is full rank; due to the singular nature of Δ the projected system of linear

equations is unchanged and the solution is:

$$G = (I - u_k u_k')[(\Delta'_{-k})^{-1}\tilde{E}_{-k}, 0]$$

To facilitate subsequent calculation of the gradient, first calculate $G^{(1)} = (\Delta'_{-k})^{-1}\tilde{E}_{-k}$ and then $G^{(2)} = \Delta_{-k}^{-1}(I - u_k u_k')_{-k}G^{(1)}$ and set $E'\Delta^{+}(\Delta^{+})'E = G'G$. The matrix Δ'_{-k} is large but extremely sparse, and so can be factorized by a sparse Cholesky decomposition that allows quick linear solves for an arbitrary number of right hand sides [Davis, 2005]. Computation of the sparse Cholesky factor is, by far, the most computationally demanding part of the likelihood when the landscape lattice is large.

The gradient may also be computed efficiently by backpropagation with quantities calculated for the likelihood. Let the third derivatives of the per-observation likelihood $p(O_{i,l}|z_{i,l})$ evaluated at $\hat{z}_l$, be contained in the vector $\dot{z}_l = [d^3p(O_{1,l}|\hat{z}_{1,l}), \ldots, d^3p(O_{N,l}|\hat{z}_{N,l})]$. Let $d_l = \mathcal{H}^{-1}(\mathrm{diag}\{\mathcal{H}^{-1}\} \circ \dot{z}_l)$ where $\circ$ is the elementwise product and the Hessian is evaluated at $\hat{z}_l$. Using the chain rule in reverse, the gradient of the negative log-likelihood with respect to the elements of μ and Σ is,

$$\begin{aligned}
\dot{\mu} &= -\sum_l \Sigma^{-1}(\hat{z}_l - \mu + \frac{1}{2}d_l) \\
\dot{\Sigma} &= \sum_l \frac{1}{2}(\Sigma^{-1} - d_l d_l' + \Sigma^{-1}(\frac{1}{4}d_l d_l' - \mathcal{H}(\hat{z}_l)^{-1})\Sigma^{-1})
\end{aligned}$$

and the gradient with regards to elements of Δ_{-k} is

$$\begin{aligned}
\dot{\Delta}_{-k} &= -2(\Delta_{-k}^{-1})'\tilde{E}_{-k}\dot{\Sigma}\tilde{E}'_{-k}\Delta_{-k}^{-1}(I - u_k u_k')_{-k}(\Delta_{-k}^{-1})' \\
&= -2G^{(1)}\dot{\Sigma}(G^{(2)})'
\end{aligned}$$

The gradient only needs to be calculated for the few non-zero elements of Δ_{-k}, which can be done on a per-element basis by forming the appropriate inner product out of rows of $G^{(1)}$ and $G^{(2)}$. Using gradient information within a quasi-Newton optimization scheme greatly accelerates optimization of the likelihood when transition rates are modelled as functions of multiple environmental variables.

Performance on simulated and actual data. We evaluated the performance of the likelihood derived in this paper (hereafter "covariance model") against maximum likelihood population effects (MLPE) [Clarke et al., 2002] (hereafter "distance regression"), a regression of Fst against resistance distance with a covariance structure designed to account for dependence among pairwise comparisons, that is frequently used in landscape genetics as an objective function for isolation by resistance models. To generate realistic simulations that were not an *a priori* match to our model, we used SPLATCHE2 [Ray et al., 2010] to simulate genotypes from 25 demes arranged in a grid across a 101 by 101 landscape lattice, where migration rates between demes varied with an underling spatial variable. SPLATCHE2 first simulates a forward-time demographic process (population expansion, colonization, migration) and then simulates genotypes from the multi-population coalescent process [Hudson, 2002]. We used a demographic scenario where a rapid expansion over 200 generations completely occupied the landscape, and subsequently demes exchanged migrants with neighbours for 500 generations.

In each simulation, we generated a spatial variable from a Matern random field [Schlather et al., 2015]. We mapped the variable onto migration rates via a logistic function, with weights chosen to reflect either a strong, weak, or absent influence of the spatial variable on gene flow (the final case corresponds to isolation by distance). For each objective function, we evaluated performance by fitting two models to each simulation (a model with the environmental variable and a null model reflecting isolation by distance), then calculating a likelihood ratio test statistic indicating support for the alternate model. To evaluate the relative efficiency of the methods across varying amounts of data, we simulated datasets with an effective number of SNPs varying from 50 to 1500. In these simulations, the effective number of SNPs is the number of unlinked, non-recombining blocks, and the total number of SNPs is approximately ten times greater. The software used to fit models with both MLPE and *gaffer* is available at `www.github.com/nspope/corMLPE` and `www.github.com/nspope/inlassle`.

Finally, to assess performance on actual data where we have a reasonable notion of the environmental conditions that influence dispersal, we applied both methods to genome-wide SNP data from 156 individuals of a tropical social bee, *Melipona subnitida*, collected across northeast Brazil (details regarding collections and sequencing found in [Jaffé et al., 2019]). *M. subnitida* is a commercially, culturally, and ecologically important species that like many stingless bees is primarily associated with tropical forests. In this study region, forestlands typically occur in coastal areas while the inland is

dominated by arid scrubland and mountains. Northeastern Brazil has undergone extensive deforestation over the past century, mainly related to logging, mining, and conversion of forestlands into agriculture. We modeled gene flow in this species as a function of lack of habitat (percent non-forested land, data from [Hansen et al., 2013]) and topographic dispersal barriers (altitude, data from [Fick and Hijmans, 2017]). In the study region, forest cover and altitude are causally related via climate, but show only a weak correlation (≈ 0.18 Pearson correlation). After removing SNPs that occurred in less than 80% of samples and at minor allele frequencies less than 0.05, we retained 3814 loci across 37 geographic locations (Fig. 5.5A). We used the Akaike information criterion (AIC) to compare models where dispersal was influenced by both environmental variables or by a single variable, against null models of isolation by distance and no spatial structure whatsoever (e.g. complete isolation of demes).

5.3 Results

Simulated data. For simulated data where the environment had a strong influence on migration (Figure 5.4, top panels), both the distance regression and the covariance model derived above were able to distinguish the true effect from the null model with relatively few SNPs. However, the distance regression effectively "saturated" in terms of evidence around at 300-500 unlinked SNPs (e.g. the likelihood ratio stopped increasing). We expect this results from the estimates of pairwise Fst stabilizing with a sufficient amount of data, at

which point the distance regression is unable to incorporate information from additional loci. In contrast, with the covariance model, the likelihood ratio grew consistently as more loci were added.

For the simulated scenarios wherein the environment weakly influenced migration (Figure 5.4, middle panels), the distance regression was consistently unable to recover an effect regardless of the number of loci used. In contrast, with few loci the covariance model found no evidence against the null, but with increasing numbers of loci was able to clearly support the alternate model. Finally, for the scenario of isolation by distance only (Figure 5.4, bottom panels), both likelihoods consistently found no evidence for an effect of landscape on migration, regardless of the number of loci used. However, the covariance model was generally noisier in terms of evidence, sometimes generating likelihood ratios that, while relatively low, suggested a (false) effect relative to the distance regression. This difference between methods in the scaling of the likelihood ratio under the null hypothesis may be due to the fact that SNPs are in linkage disequilibrium but are treated as unlinked in the covariance model (thus the likelihood is a composite likelihood, [Coffman et al., 2015]). As a whole, results from these simulations indicate that the covariance model is much more efficient at using information across large numbers of loci, and is more sensitive to signal in the data.

Dispersal in a tropical stingless bee. With 3187 high-frequency loci genotyped across 156 *M. subnitida* workers, both the distance regression and

the covariance model found that altitude was the primary factor influencing gene flow: models that included an altitudinal effect had substantially higher log likelihoods and lower AIC scores (Table 5.1). This is not an unexpected result given that several arid mountain ranges bisect the region (Fig. 5.3), reaching altitudes in excess of 1km above sea level. However, the covariance model detected a secondary, weaker influence of forest cover on gene flow (the best performing model in terms of AIC contained both forest cover and altitudinal effects). In contrast, the distance regression could not find an effect of forest cover that was distinguishable from altitude; while a model incorporating forest cover performed substantially better than simple isolation by distance, this apparent importance did not persist when altitude was considered in tandem (Table 5.1). Further, with the distance regression, the estimated effect of forest cover was opposite in direction from what biological intuition would predict (1.0 ± 0.15 in the univariate model, e.g. forest absence increases gene flow), and opposite from the direction estimated using the covariance model (-0.17 ± 0.03 in the univariate model).

The reason for this discrepancy – and possibly for the relatively poor performance of the distance regression across simulated datasets – is suggested by examining profile likelihood surfaces for the parameters corresponding to altitude and forest absence. The profile likelihood surface from the covariance model is approximately quadratic, and clearly distinguishes a single mode that is located far from the clines corresponding to isolation by distance or a isolation by a single variable alone (Figure 5.5A). In contrast, the likelihood

profile from the distance regression is complex and contains a saddle, where for a negative altitude parameters there are many plausible values for the forest absence parameter (Figure 5.5B). The presence of this poorly-behaved likelihood surface, despite the relatively simple model and large number of distinct geographic samples, suggests that the usefulness of distance regression as an objective function may scale poorly with model complexity, resulting in complex saddle points and local optima.

5.4 Discussion

In this age of affordable high-throughput sequencing, the utility of genomic SNP data for addressing questions in ecology, evolution, and conservation biology is hard to overstate [Allendorf et al., 2010, Savolainen et al., 2013]. An influential analytical framework, isolation by resistance, has spawned a cottage industry of inferring environmental effects on dispersal from genetic structure [Shirk et al., 2018]. However, critical assessment of the statistical application of this framework has been generally almost entirely concerned with distinctions among methods of correlating or regressing distance matrices [Zeller et al., 2016, Shirk et al., 2018], and not on shortcomings of these methods as a whole.

Motivated by the need for a tractable generative model for SNP frequencies in a spatially-explicit environment, we use a logit-normal approximation and basic results regarding Markov processes to derive a covariance structure that is flexible and parameterized by an underlying movement process. We de-

rive an efficient means to compute the likelihood and gradient, even when the graph approximating the landscape is very large. Computationally efficient gradient evaluations facilitate rapid optimization of the likelihood, especially when the covariance is highly parameterized.

With realistic simulated data, our proposed covariance model performed better as an objective function than did regression between resistance distance and Fst. Largely, this seems to reflect the relative ability of the two approaches to accumulate information with increasing numbers of loci. In simulations, a distance regression between genetic dissimilarity and resistance distance was unable to distinguish between alternative and null hypotheses when the underlying effect of environment on dispersal was weak; while the covariance model could, when given sufficient numbers of loci. Fst (and other summary statistics) do not retain the breadth of information contained within the allele frequency spectrum. The covariance in allele frequencies among demes is also a summary statistic, but it is a *more expressive* statistic, and the relative performance in our simulated and empirical example suggests that this has consequences for inference.

Our application of both methods to actual data also indicated issues with distance regression as an objective function. Even with a relatively simple two-parameter model, where the underlying environmental variables had weak linear correlation, the profile likelihood of the distance regression was ill-behaved, with a saddle around the maximum likelihood estimate. As a consequence, this method was either unable to clearly infer a secondary effect

of isolation by habitat availability, or worse, inferred an effect in the wrong direction. How generalizable these results are to other datasets and other landscapes is difficult to gauge, but they do not paint an encouraging picture. The advantage of distance regression as an objective function is that it is extremely quick to compute. However, with large landscapes the bulk of the computational cost is due to factoring a large sparse linear system to calculate resistance distance (or covariance), and so speed of the objective function becomes less of an issue. In addition, the fact that we treat SNPs as unlinked (following standard practice [Excoffier et al., 2013]) means that the likelihood of the covariance model can readily be parallelize. For example, on an 8-core laptop built in 2016, likelihood evaluations took 0.2 seconds with 5000 SNPs, which from a practical perspective is admissible (especially when combined with fast optimization via gradient information).

Finally, we stress that the method developed here is simple, which suggests that it can be further extended in various useful ways. We have already demonstrated how the likelihood can be modified to use genotype likelihoods instead of called genotypes, or to model anisotropic dispersal. More generally, we believe there is potential to make the essential statistic – the logit normal parameters that approximate the allele frequency spectrum – much more flexible and expressive. For example, alleles of different ages will reflect dispersal processes that occurred at different points in the past; thus, the allele frequency spectrum could be modelled as a mixture of logit normals, where mixture components represent environmental conditions from different tempo-

ral periods. Likewise, the allele frequency spectrum as a function of genomic location could be modelled as a hidden Markov model where states are mixture components. This could potentially leverage information about dispersal contained in patterns of linkage across the genome, in much the same way as the sequentially Markovian coalescent captures demographic information via modelling patterns of recombination [McVean and Cardin, 2005]. We hope that the model and software presented here can serve as a building block for statistical methods that are robust to misspecification and are tailored to key questions in ecology, evolution, and conservation biology.

A. Covariance model

	$\log \mathcal{L}$	df	ΔAIC	w_{AIC}	ζ_1 (forest absence)	ζ_2 (altitude)
No spatial structure	-375919.6	0	12310	0.0	.	.
Isolation by distance	-369977.6	1	426.8	0.0	.	.
Forest absence	-369957.7	2	388.8	0.0	-0.17 ± 0.03	.
Altitude	-369766.0	2	6.8	0.03	.	-0.28 ± 0.01
Forest absence, altitude	**-369761.6**	**3**	**0.0**	**0.97**	$\mathbf{-0.08 \pm 0.03}$	$\mathbf{-0.27 \pm 0.01}$

B. Distance regression

	$\log \mathcal{L}$	df	ΔAIC	w_{AIC}	ζ_1 (forest absence)	ζ_2 (altitude)
No spatial structure	1248.7	0	675.4	0.0	.	.
Isolation by distance	1523.3	1	128.2	0.0	.	.
Forest absence	1554.1	2	68.6	0.0	1.03 ± 0.15	.
Altitude	**1588.9**	**2**	**0.0**	**0.62**	**.**	$\mathbf{1.16 \pm 0.10}$
Forest absence, altitude	1589.4	3	1.0	0.38	0.2 ± 2.5	1.27 ± 1.01

Table 5.1: Model selection for the covariance model developed in this study, and for an alternate objective function (distance regression). The parameters are scaled such that negative values imply a decrease in gene flow with increasing values of the covariate.

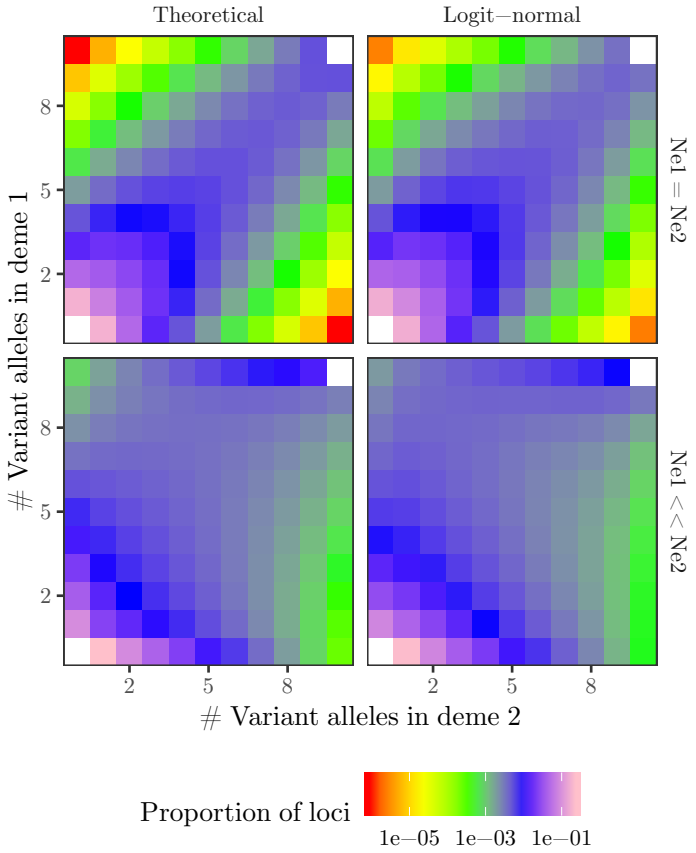

Figure 5.1: Theoretical and approximate (logit-normal) site frequency spectra (SFS) between two demes. The x- and y- axes correspond to the number of variant alleles (out of some total number of sampled haploid genotypes), and the color in each bin corresponds to the proportion of sites with that arrangement of variants, so that each panel is essentially a two-dimensional histogram. For example, the [2,1] bin shows the number of sites where a variant allele occurs in two haploids in deme one, and one haploid in deme two. Two demographic scenarios are shown: isolation with migration and equal population size, and with unequal population sizes. The theoretical spectra are numeric solutions to Wright-Fisher diffusion under a given demographic model, using the Python package moments [Jouganous et al., 2017]. The approximate SFS were generated by approximately integrating a logit-normal distribution via the Laplace approximation, and minimizing Kullback-Leibler divergence with reference to the theoretical SFS.

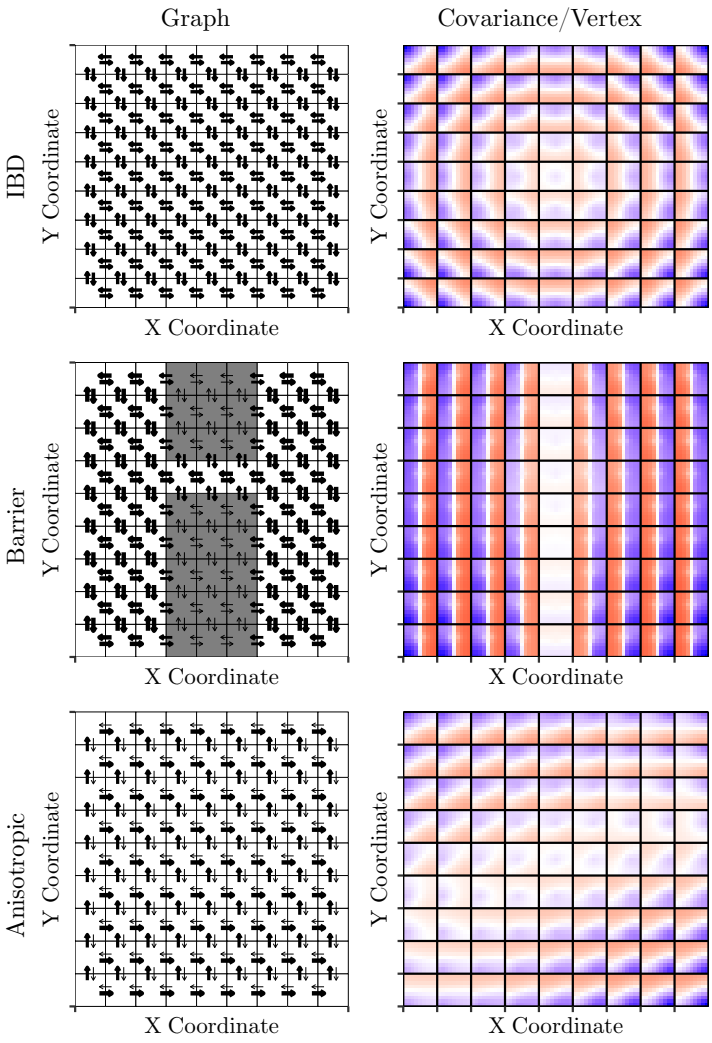

Figure 5.2: A lattice of demes ("landscape") and maps of the resulting covariance structure under (top) isolation by distance, (middle) isolation by a barrier, (bottom) anisotropic dispersal. The size of the directed edges in each graph is proportional to the migration rate among demes. The covariance is not displayed as a typical matrix, but is instead reordered so that each "sub-panel" corresponds to a deme in that position in the lattice, and the spatial arrangement of the covariance is preserved in each sub-panel (red → white → blue corresponds to negative → no → positive covariance). For example, in the upper-right figure, the lower-left sub-panel shows the covariance between the deme in the bottom-left corner and all other demes on the lattice.

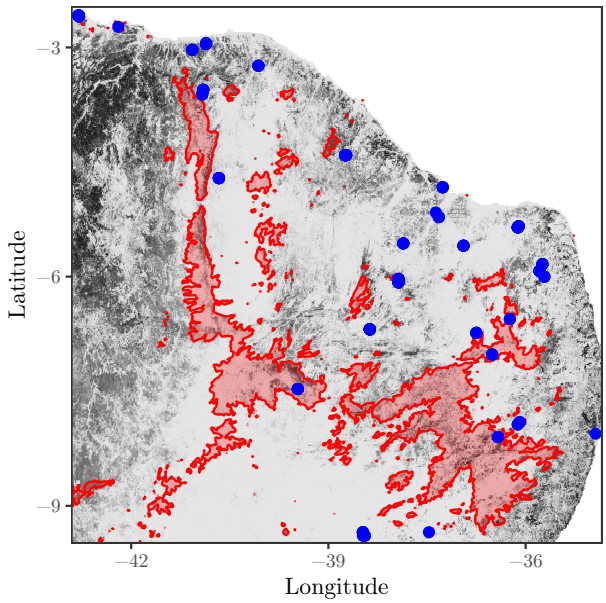

Figure 5.3: Forest cover in northeastern Brazil (increasing from light to dark), with high elevation areas shown as red shaded areas, and sampling locations of *M. subnitida* as blue points.

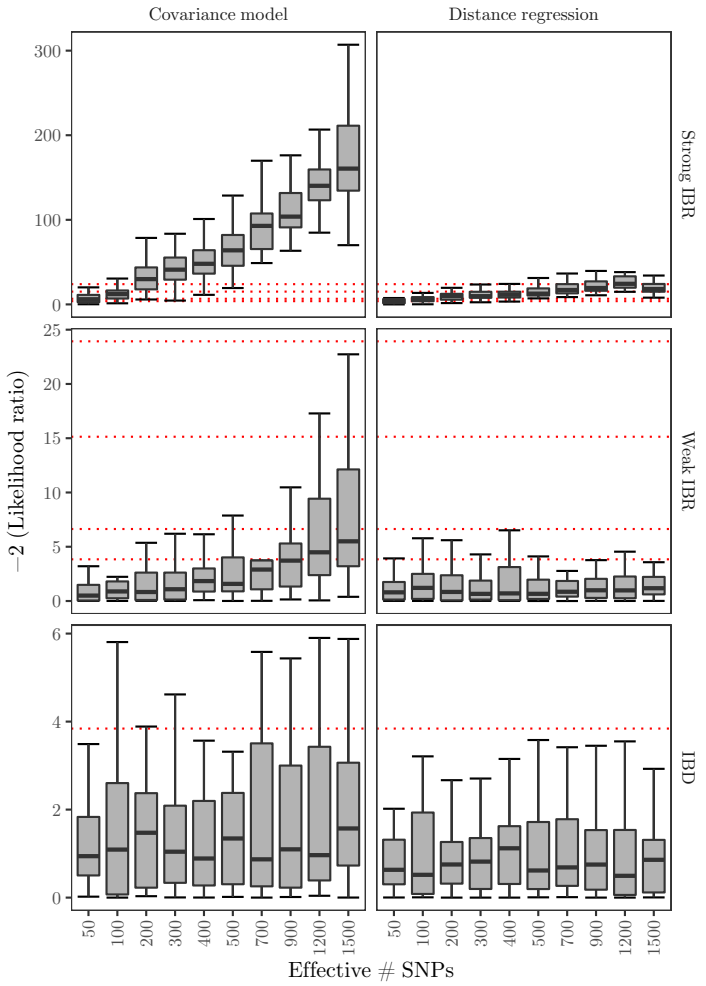

Figure 5.4: Evidence for the hypothesis of isolation by resistance (as measured by a likelihood ratio statistic) against effective number of SNPs, for the covariance model and distance regression methods described in the main text (columns), across simulated data where the landscape has a strong, weak, or absent effect on gene flow. The effective number of SNPs is the number of non-recombining, unlinked regions in the data; the actual number of SNPs is approximately five times greater. The red dotted lines are the $0.95, 0.99, 0.9999$, and 0.999999th upper quantiles from a $\chi^2(1)$ distribution (the asymptotic distribution of the likelihood ratio statistic under isolation by distance, assuming unlinked SNPs).

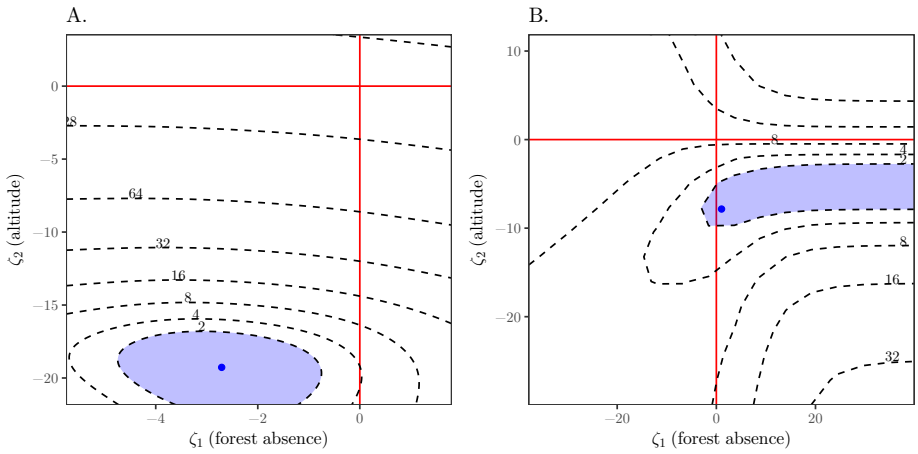

Figure 5.5: Profile likelihood surface for the parameters corresponding to altitude and forest absence, from the covariance model (A.) and the distance regression (B.). The parameterization is such that positive values indicate an increase in gene flow with increasing values of the covariate. The contour lines show likelihood isoclines decreasing with powers of two. The blue point and shaded region are the maximum likelihood estimate and a 95% confidence interval. The red lines correspond to null hypotheses of zero effects; where they intersect corresponds to the null model of isolation by distance. To show both plots on comparable scales, the axes are scaled by the standard error of the MLE, and the likelihood surface is normalized so that the maximum is 0.

Bibliography

[Aitchison, 1994] Aitchison, J. (1994). Principles of compositional data analysis. *Multivariate Analysis and its Applications*, 24:73–81.

[Aizen et al., 2008] Aizen, M. A., Garibaldi, L. A., Cunningham, S. A., and Klein, A. M. (2008). Long-term global trends in crop yield production reveal no current pollination shortage but increasing pollinator dependency. *Current Biology*, 18:1572–1575.

[Aldrich and Hamrick, 1998] Aldrich, P. and Hamrick, J. (1998). Reproductive dominance of pasture trees in a fragmented tropical forest mosaic. *Science*, 281:103–105.

[Allee et al., 1949] Allee, W., Emerson, A., Park, O., Park, T., and Schmidt, K. (1949). *Principles of animal ecology*. Saunders Co., Philadelphia.

[Allendorf et al., 2010] Allendorf, F. W., Hohenlohe, P. A., and Luikart, G. (2010). Genomics and the future of conservation genetics. *Nature Reviews Genetics*, 11:697.

[Arditi and Dacorogna, 1988] Arditi, R. and Dacorogna, B. (1988). Optimal foraging on arbitrary food distributions and the definition of habitat patches. *American Naturalist*, 131:837–846.

[Augspurger, 1980] Augspurger, C. (1980). Mass-flowering of a tropical shrub (*Hybanthus prunifolius*): influence on pollinator attraction and movement. *Evolution*, 34:475–488.

[Balkenhol et al., 2009] Balkenhol, N., Waits, L. P., and Dezzani, R. J. (2009). Statistical approaches in landscape genetics: an evaluation of methods for linking landscape and genetic data. *Ecography*, 32:818–830.

[Balvanera et al., 2006] Balvanera, P., Pfisterer, A. B., Buchmann, N., He, J.-S., Nakashizuka, T., Raffaelli, D., and Schmid, B. (2006). Quantifying the evidence for biodiversity effects on ecosystem functioning and services. *Ecology Letters*, 9:1146–1156.

[Bates et al., 2015] Bates, D., Maechler, M., Bolker, B., and Walker, S. C. (2015). Fitting linear mixed-effects models using lme4. *Journal of Statistical Software*, 67:1–48.

[Beaumont et al., 2010] Beaumont, M. A., Nielsen, R., Robert, C., Hey, J., Gaggiotti, O., Knowles, L., Estoup, A., Panchal, M., Corander, J., Hickerson, M., et al. (2010). In defence of model-based inference in phylogeography. *Molecular Ecology*, 19:436–446.

[Bergman et al., 2001] Bergman, C. M., Fryxell, J. M., Gates, C. C., and Fortin, D. (2001). Ungulate foraging strategies: energy maximizing or time minimizing? *Journal of Animal Ecology*, 70:289–300.

[Betts et al., 2015] Betts, M., Hadley, A., and Kress, W. (2015). Pollinator recognition by a keystone tropical plant. *Proceedings of the National Academy of Sciences*, 112:3433–3438.

[Beveridge, 2016] Beveridge, A. (2016). A hitting time formula for the discrete Green's function. *Combinatorics, Probability and Computing*, 25:362–379.

[Biernaskie et al., 2009] Biernaskie, J. M., Walker, S. C., and Gegear, R. J. (2009). Bumblebees learn to forage like Bayesians. *American Naturalist*, 174:413–423.

[Bohart, 1972] Bohart, G. (1972). Management of wild bees for the pollination of crops. *Annual Review of Entomology*, 17:287–312.

[Bohonak, 1999] Bohonak, A. J. (1999). Dispersal, gene flow, and population structure. *The Quarterly Review of Biology*, 74:21–45.

[Bolker et al., 2009] Bolker, B. M., Brooks, M. E., Clark, C. J., Geange, S. W., Poulsen, J. R., Stevens, M. H. H., and White, J.-S. S. (2009). Generalized linear mixed models: A practical guide for ecology and evolution. *Trends in Ecology and Evolution*, 24:127–135.

[Bond, 1994] Bond, W. (1994). Do mutualisms matter? assessing the impact of pollinator and disperser disruption on plant extinction. *Philosophical Transactions of the Royal Society B*, 344:83–90.

[Bondrup-Nielsen, 1983] Bondrup-Nielsen, S. (1983). Density estimation as a function of live-trapping grid and home range size. *Canadian Journal of Zoology*, 61:2361–2365.

[Born et al., 2008] Born, C., Hardy, O., and Chevallier, M. (2008). Small-scale spatial genetic structure in the central African rainforest tree species *Aucoumea klaineana*: a stepwise approach to infer the impact of limited gene dispersal, population history and habitat fragmentation. *Molecular Ecology*, 17:2041–2050.

[Bosch and Waser, 1999] Bosch, M. and Waser, N. (1999). Effects of local density on pollination and reproduction in *Delphinium nuttallianum* and *Aconitum columbianum* (Ranunculaceae). *American Journal of Botany*, 86:871–879.

[Boyce and McDonald, 1999] Boyce, M. S. and McDonald, L. L. (1999). Relating populations to habitats using resource selection functions. *Trends in Ecology and Evolution*, 14:268–272.

[Breed et al., 2009] Breed, G. A., Jonsen, I. D., Myers, R. A., Bowen, W. D., and Leonard, M. L. (2009). Sex-specific, seasonal foraging tactics of adult grey seals (*Halichoerus grypus*) revealed by state-space analysis. *Ecology*, 90:3209–3221.

[Breed, 2015] Breed, M. (2015). Mating patterns and pollinator mobility are critical traits in forest fragmentation genetics. *Heredity*, 115:108–114.

[Brosi and Briggs, 2013] Brosi, B. and Briggs, H. (2013). Single pollinator species losses reduce floral fidelity and plant reproductive function. *Proceedings of the National Academy of Sciences*, 110:13044–13048.

[Byers, 1995] Byers, D. (1995). Pollen quantity and quality as explanations for low seed set in small populations exemplified by *Eupatorium* (Asteraceae). *American Journal of Botany*, 82:1000–1006.

[Cameron et al., 2011] Cameron, S. A., Lozier, J. D., Strange, J. P., Koch, J. B., Cordes, N., Solter, L. F., and Griswold, T. L. (2011). Patterns of widespread decline in North American bumble bees. *Proceedings of the National Academy of Sciences*, 108:662–667.

[Cane, 1987] Cane, J. (1987). Estimation of bee size using intertegular span (Apoidea). *Journal of the Kanses Entomological Society*, 60:145–147.

[Caraballo-Ortiz et al., 2011] Caraballo-Ortiz, M., Santiago-Valentin, E., and Carlo, T. (2011). Flower number and distance to neighbours affect the fecundity of *Goetzea elegans* (Solanaceae). *Journal of Tropical Ecology*, 27:521–528.

[CaraDonna et al., 2014] CaraDonna, P. J., Iler, A. M., and Inouye, D. W. (2014). Shifts in flowering phenology reshape a subalpine plant community. *Proceedings of the National Academy of Sciences*, 110:4916–4921.

[Cardinale et al., 2012] Cardinale, B. J., Duffy, J. E., Gonzalez, A., Hooper, D. U., Perrings, C., Venail, P., Narwani, A., Mace, G. M., Tilman, D.,

Wardle, D. A., et al. (2012). Biodiversity loss and its impact on humanity. *Nature*, 486:59–67.

[Carpenter et al., 2017] Carpenter, B., Gelman, A., Hoffman, M., Lee, D., Goodrich, B., Betancourt, M., Brubaker, M. A., Guo, J., Li, P., and Riddell, A. (2017). Stan: a probabilistic programming language. *Journal of Statistical Software*, 76.

[Carpenter et al., 2009] Carpenter, S. R., Mooney, H. A., Agard, J., Capistrano, D., DeFries, R. S., Díaz, S., Dietz, T., Duraiappah, A. K., Oteng-Yeboah, A., Pereira, H. M., et al. (2009). Science for managing ecosystem services: Beyond the millennium ecosystem assessment. *Proceedings of the National Academy of Sciences*, 106:1305–1312.

[Cartar, 2004] Cartar, R. (2004). Resource tracking by bumble bees: Responses to plant-level differences in quality. *Ecology*, 85:2764–2771.

[Cartar and Dill, 1990] Cartar, R. V. and Dill, L. M. (1990). Colony energy-requirements affect the foraging currency of bumble bees. *Behavioral Ecology and Sociobiology*, 27:377–383.

[Carvell et al., 2012] Carvell, C., Jordan, W., Bourke, A. F. G., Pickles, R., Redhead, J., and Heard, M. (2012). Molecular spatial analyses reveal links between colony-specific foraging distance and landscape-level resource availability in two bumblebee species. *Oikos*, 121:734–742.

[Castilla et al., 2011] Castilla, A., Alonso, C., and Herrera, C. (2011). Exploring local borders of distribution in the shrub *Daphne laureola*: individual and populations traits. *Acta Oecologica*, 37:269–276.

[Castilla et al., 2016a] Castilla, A., Pope, N., Jaffe, R., and Jha, S. (2016a). Elevation, not deforestation, promotes genetic differentiation in a pioneer tropical tree. *PLoS One*, 11:e0156694.

[Castilla et al., 2016b] Castilla, A., Pope, N., and Jha, S. (2016b). Positive density-dependent reproduction regulated by local kinship and size in an understorey tropical tree. *Annals of Botany*, 117:319–329.

[Castilla et al., 2017] Castilla, A. R., Pope, N. S., O'Connell, M., Rodriguez, M. F., Treviño, L., Santos, A., and Jha, S. (2017). Adding landscape genetics and individual traits to the ecosystem function paradigm reveals the importance of species functional breadth. *Proceedings of the National Academy of Sciences*, 114:12761–12766.

[Ceballos et al., 2015] Ceballos, G., Ehrlich, P. R., Barnosky, A. D., García, A., Pringle, R. M., and Palmer, T. M. (2015). Accelerated modern human-induced species losses: Entering the sixth mass extinction. *Science Advances*, 1:e1400253.

[Chapman et al., 2003] Chapman, R., Wang, J., and Bourke, A. (2003). Genetic analysis of spatial foraging patterns and resource sharing in bumble bee pollinators. *Molecular Ecology*, 12:2801–2808.

[Chung and Yau, 2000] Chung, F. and Yau, S. (2000). Discrete Green's functions. *Journal of Combinatorial Theory*, 91:191–214.

[Clark and LaDeau, 2004] Clark, J. and LaDeau, S. (2004). Fecundity of trees and the colonization-competition hypothesis. *Ecological Monographs*, 74:415–422.

[Clarke et al., 2002] Clarke, R. T., Rothery, P., and Raybould, A. F. (2002). Confidence limits for regression relationships between distance matrices: estimating gene flow with distance. *Journal of Agricultural, Biological, and Environmental Statistics*, 7:361.

[Cleveland and Devlin, 1988] Cleveland, W. and Devlin, S. (1988). Locally weighted regression: an approach to regression analysis by local fitting. *Journal of the American Statistical Association*, 83:596–610.

[Coffman et al., 2015] Coffman, A. J., Hsieh, P. H., Gravel, S., and Gutenkunst, R. N. (2015). Computationally efficient composite likelihood statistics for demographic inference. *Molecular Biology and Evolution*, 33:591–593.

[Comita et al., 2014] Comita, L., Queenborough, S., and Murphy, S. (2014). Testing predictions of the Janzen-Connell hypothesis: a meta-analysis of experimental evidence for distance- and density-dependent seed and seedling survival. *Journal of Ecology*, 102:845–856.

[Condit, 1998] Condit, R. (1998). *Tropical forest census plots*. Springer Science & Business Media, Berlin.

[Condit et al., 2000] Condit, R., Ashton, P., and Baker, P. (2000). Spatial patterns in the distribution of tropical tree species. *Science*, 288:1414–1418.

[Connell, 1971] Connell, J. H. (1971). On the role of natural enemies in preventing competitive exclusion in some marine animals and in rain forest trees. *Dynamics of Populations*, 298:312.

[Corbet et al., 1993] Corbet, S. A., Fussell, M., Ake, R., Fraser, A., Gunson, C., Savage, A., and Smith, K. (1993). Temperature and the pollinating activity of social bees. *Ecological Entomology*, 18:17–30.

[Couvillon et al., 2014] Couvillon, M. J., Schürch, R., and Ratnieks, F. L. (2014). Waggle dance distances as integrative indicators of seasonal foraging challenges. *PLoS One*, 9:e93495.

[Cresswell et al., 2000] Cresswell, J., Osborne, J., and Goulson, D. (2000). An economic model of the limits to foraging range in central place foragers with numerical solutions for bumblebees. *Ecological Entomology*, 25:249–255.

[Crone and Williams, 2016] Crone, E. E. and Williams, N. M. (2016). Bumble bee colony dynamics: quantifying the importance of land use and floral resources for colony growth and queen production. *Ecology Letters*, 19:460–468.

[Currat et al., 2004] Currat, M., Ray, N., and Excoffier, L. (2004). SPLATCHE: a program to simulate genetic diversity taking into account environmental

heterogeneity. *Molecular Ecology Notes*, 4:139–142.

[Cushman et al., 2006] Cushman, S. A., McKelvey, K. S., Hayden, J., and Schwartz, M. K. (2006). Gene flow in complex landscapes: testing multiple hypotheses with causal modeling. *American Naturalist*, 168:486–499.

[Darvill et al., 2004] Darvill, B., Knight, M. E., and Goulson, D. (2004). Use of genetic markers to quantify bumblebee foraging range and nest density. *Oikos*, 107:471–478.

[Davis, 2005] Davis, T. A. (2005). Algorithm 849: A concise sparse Cholesky factorization package. *ACM Transactions on Mathematical Software*, 31:587–591.

[Dawson and Chittka, 2012] Dawson, E. H. and Chittka, L. (2012). Conspecific and heterospecific information use in bumblebees. *PLoS One*, 7:e31444.

[De Luca et al., 2014] De Luca, P., Cox, D., and Vallejo-Marin, M. (2014). Comparison of pollination and defensive buzzes in bumblebees indicates species-specific and context-dependent vibrations. *Naturwissenschaften*, 101:331–338.

[Dick et al., 2003] Dick, C., Etchelecu, G., and Austerlitz, F. (2003). Pollen dispersal of tropical trees (*Dinizia excelsa*: Fabaceae) by native insects and African honeybees in pristine and fragmented Amazonian rainforest. *Molecular Ecology*, 12:753–764.

[Dick et al., 2008] Dick, C., Hardy, O., Jones, F., and Petit, R. (2008). Spatial scales of pollen and seed-mediated gene flow in tropical rain forest trees. *Tropical Plant Biology*, 1:20–33.

[Director et al., 2017] Director, H. M., Gattiker, J., Lawrence, E., and Vander Wiel, S. (2017). Efficient sampling on the simplex with a self-adjusting logit transform proposal. *Journal of Statistical Computation and Simulation*, 87:3521–3536.

[Dixon, 2009] Dixon, K. W. (2009). Pollination and restoration. *Science*, 325:571–573.

[Doyle and Doyle, 1987] Doyle, J. and Doyle, J. (1987). A rapid DNA isolation procedure for small quantities of fresh leaf tissue. *Phytochemical Bulletin*, 19:11–15.

[Dreier et al., 2014] Dreier, S., Redhead, J. W., Warren, I. A., Bourke, A. F. G., Heard, M. S., Jordan, W. C., Sumner, S., Wang, J., and Carvell, C. (2014). Fine-scale spatial genetic structure of common and declining bumble bees across an agricultural landscape. *Molecular Ecology*, 23:3384–3395.

[Dreisig, 1995] Dreisig, H. (1995). Ideal free distributions of nectar foraging bumblebees. *Oikos*, 72:161–172.

[Duarte et al., 2014] Duarte, O., Gaiotto, F., and Costa, M. (2014). Genetic differentiation in the stingless bee, *Scaptotrigona xanthotricha* Moure, 1950

(Apidae, Meliponini): A species with wide geographic distribution in the Atlantic rainforest. *Journal of Heredity*, 105:477–484.

[Duffy et al., 2013] Duffy, K., Patrick, K., and Johnson, S. (2013). Does the likelihood of an Allee effect on plant fecundity depend on the type of pollinator? *Journal of Ecology*, 101:953–962.

[Duffy and Stout, 2011] Duffy, K. and Stout, J. (2011). Effects of conspecific and heterospecific floral density on the pollination of two related rewarding orchids. *Plant Ecology*, 212:1397–1406.

[Duncan et al., 2004] Duncan, D., Cunningham, S., and Nicotra, A. (2004). High self-pollen transfer and low fruit set in buzz-pollinated *Dianella revoluta* (Phormiaceae). *Australian Journal of Botany*, 52:185–193.

[Efford, 2004] Efford, M. (2004). Density estimation in live-trapping studies. *Oikos*, 106:598–610.

[Elam et al., 2007] Elam, D., Ridley, C., Goodell, K., and Ellstrand, N. (2007). Population size and relatedness affect fitness of a self-incompatible invasive plant. *Proceedings of the National Academy of Sciences*, 104:249–252.

[Elzinga et al., 2007] Elzinga, J. A., Atlan, A., Biere, A., Gigord, L., Weis, A. E., and Bernasconi, G. (2007). Time after time: flowering phenology and biotic interactions. *Trends in Ecology and Evolution*, 22:432–439.

[Epps et al., 2007] Epps, C. W., Wehausen, J. D., Bleich, V. C., Torres, S. G., and Brashares, J. S. (2007). Optimizing dispersal and corridor models using landscape genetics. *Journal of Applied Ecology*, 44:714–724.

[Estoup et al., 1995] Estoup, A., Scholl, A., Pouvreau, A., and Solignac, M. (1995). Monoandry and polyandry in bumble bees (Hymenoptera; Bombinae) as evidenced by highly variable microsatellites. *Molecular Ecology*, 4:89–93.

[Excoffier et al., 2013] Excoffier, L., Dupanloup, I., Huerta-Sánchez, E., Sousa, V. C., and Foll, M. (2013). Robust demographic inference from genomic and SNP data. *PLoS Genetics*, 9:e1003905.

[Fenster et al., 2004] Fenster, C. B., Armbruster, W. S., Wilson, P., Dudash, M. R., and Thomson, J. D. (2004). Pollination syndromes and floral specialization. *Annual Review of Ecology, Evolution, and Systematics*, 35:375–403.

[Fick and Hijmans, 2017] Fick, S. E. and Hijmans, R. J. (2017). WorldClim 2: New 1-km spatial resolution climate surfaces for global land areas. *International Journal of Climatology*, 37:4302–4315.

[Finke and Denno, 2004] Finke, D. and Denno, R. (2004). Predator diversity dampens trophic cascades. *Nature*, 429:407–410.

[Fornara and Tilman, 2008] Fornara, D. and Tilman, D. (2008). Plant functional composition influences rates of soil carbon and nitrogen accumulation. *Journal of Ecology*, 96:314–322.

[Forrest and Miller-Rushing, 2010] Forrest, J. and Miller-Rushing, A. J. (2010). Toward a synthetic understanding of the role of phenology in ecology and evolution. *Philosophical Transactions of the Royal Society B*, 365:3101–3112.

[Foster and Harmsen, 2012] Foster, R. J. and Harmsen, B. J. (2012). A critique of density estimation from camera-trap data. *Journal of Wildlife Management*, 76:224–236.

[Frund et al., 2013] Frund, J., Dormann, C., Holzschuh, A., and Tscharntke, T. (2013). Bee diversity effects on pollination depend on functional complementarity and niche shifts. *Ecology*, 94:2042–2054.

[Fuchs and Hamrick, 2011] Fuchs, E. and Hamrick, J. (2011). Mating system and pollen flow between remnant populations of the endangered tropical tree, *Guaiacum sanctum* (Zygophyllaceae). *Conservation Genetics*, 12:175–185.

[Gallai et al., 2009] Gallai, N., Salles, J.-M., Settele, J., and Vaissière, B. E. (2009). Economic valuation of the vulnerability of world agriculture confronted with pollinator decline. *Ecological Economics*, 68:810–821.

[Garibaldi et al., 2013] Garibaldi, L. A., Steffan-Dewenter, I., Winfree, R., Aizen, M. A., Bommarco, R., Cunningham, S. A., and Kremen, C. (2013). Wild pollinators enhance fruit set of crops regardless of honey bee abundance. *Science*, 339:1608–1611.

[Gathmann and Tscharntke, 2002] Gathmann, A. and Tscharntke, T. (2002). Foraging ranges of solitary bees. *Journal of Animal Ecology*, 71:757–764.

[Gelman, 2006] Gelman, A. (2006). Prior distributions for variance parameters in hierarchical models. *Bayesian Analysis*, 1:515–534.

[Gelman and Rubin, 1992] Gelman, A. and Rubin, D. B. (1992). Inference from iterative simulation using multiple sequences. *Statistical science*, 7:457–472.

[Ghazoul, 2002] Ghazoul, J. (2002). Flowers at the front line of invasion? *Ecological Entomology*, 27:638–640.

[Ghazoul, 2005] Ghazoul, J. (2005). Pollen and seed dispersal among dispersed plants. *Biological Reviews*, 80:413–443.

[Goodnight and Queller, 1999] Goodnight, K. F. and Queller, D. C. (1999). Computer software for performing likelihood tests of pedigree relationship using genetic markers. *Molecular Ecology*, 8:1231.

[Gorchov, 1985] Gorchov, D. (1985). Fruit ripening asynchrony is related to variable seed number in *Amelanchier* and *Vaccinium*. *American Journal of Botany*, 72:1939–1943.

[Goulson, 1999] Goulson, D. (1999). Foraging strategies of insects for gathering nectar and pollen, and implications for plant ecology and evolution. *Perspectives in Plant Ecology, Evolution and Systematics*, 2:185–209.

[Goulson et al., 2010] Goulson, D., Lepais, O., O'Connor, S., Osborne, J. L., Sanderson, R. A., Cussans, J., Goffe, L., and Darvill, B. (2010). Effects of land use at a landscape scale on bumblebee nest density survival. *Journal of Applied Ecology*, 47:1207–1215.

[Goulson et al., 2015] Goulson, D., Nicholls, E., Botias, C., and Rotheray, E. L. (2015). Bee declines driven by combined stress from parasites, pesticides, and lack of flowers. *Science*, 347:1435–1441.

[Greenleaf et al., 2007] Greenleaf, S. S., Williams, N. M., Winfree, R., and Kremen, C. (2007). Bee foraging ranges their relationship to body size. *Oecologia*, 153:589–596.

[Groom, 1998] Groom, M. (1998). Allee effects limit population viability of an annual plant. *American Naturalist*, 151:487–496.

[Guillot et al., 2009] Guillot, G., Leblois, R., Coulon, A., and Frantz, A. C. (2009). Statistical methods in spatial genetics. *Molecular Ecology*, 18:4734–4756.

[Gutenkunst et al., 2009] Gutenkunst, R. N., Hernandez, R. D., Williamson, S. H., and Bustamante, C. D. (2009). Inferring the joint demographic history of multiple populations from multidimensional SNP frequency data. *PLoS Genetics*, 5:e1000695.

[Hadfield et al., 2006] Hadfield, J., Richardson, D., and Burke, T. (2006). Towards unbiased parentage assignment: Combining genetic, behavioural and

spatial data in a Bayesian framework. *Molecular Ecology*, 15:3715–3730.

[Hagen et al., 2011] Hagen, M., Wikelski, M., and Kissling, W. D. (2011). Space use of bumblebees (*Bombus* spp.) revealed by radio-tracking. *PLoS One*, 6:e19997.

[Hansen et al., 2013] Hansen, M. C., Potapov, P. V., Moore, R., Hancher, M., Turubanova, S., Tyukavina, A., Thau, D., Stehman, S., Goetz, S., Loveland, T. R., et al. (2013). High-resolution global maps of 21st-century forest cover change. *Science*, 342:850–853.

[Harder, 1990] Harder, L. (1990). Behavioral responses by bumble bees to variation in pollen availability. *Oecologia*, 85:41–47.

[Harder and Barrett, 1995] Harder, L. and Barrett, S. (1995). Mating cost of large floral displays in hermaphrodite plants. *Nature*, 373:512–515.

[Hardy and Vekemans, 2002] Hardy, O. and Vekemans, X. (2002). SPAGeDi: a versatile computer program to analyse spatial genetic structure at the individual or population levels. *Molecular Ecology Notes*, 2:618–620.

[Harper, 1977] Harper, J. (1977). *Population biology of plants*. Academic Press, Cambridge.

[Harrison, 2014] Harrison, X. (2014). Using observation-level random effects to model overdispersion in count data in ecology and evolution. *PeerJ*, 2:e616.

[Hassan et al., 2005] Hassan, R., Scholes, R., and Ash, N. (2005). Millennium ecosystem assessment—ecosystems and human well-being: Current state and trends.

[Hegland et al., 2009] Hegland, S. J., Nielsen, A., Lazaro, A., Bjerknes, A. L., and Totland, O. (2009). How does climate warming affect plant-pollinator interactions? *Ecology Letters*, 12:184–195.

[Heinrich, 1975] Heinrich, B. (1975). Energetics of pollination. *Annual Review of Ecology and Systematics*, 6:139–170.

[Herrera, 1984] Herrera, C. (1984). Selective pressures on fruit seediness: differential predation of fly larvae on the fruits of *Berberis hispanica*. *Oikos*, 42:166–170.

[Herrera, 2009] Herrera, C. M. (2009). *Multiplicity in unity: plant subindividual variation and interactions with animals*. University of Chicago Press.

[Hirao, 2010] Hirao, A. (2010). Kinship between parents reduces offspring fitness in a natural population of *Rhododendron brachycarpum*. *Annals of Botany*, 105:637–646.

[Hoehn et al., 2008] Hoehn, P., Tscharntke, T., Tylianakis, J., and Steffan-Dewenter, I. (2008). Functional group diversity of bee pollinators increases crop yield. *Proceedings of the Royal Society B*, 275:2283–2291.

[Hubbell et al., 1999] Hubbell, S., Foster, R., and O'Brien, S. (1999). Light gap disturbances, recruitment limitation, and tree diversity in a neotropical forest. *Science*, 283:554–557.

[Hubbell and Johnson, 1978] Hubbell, S. and Johnson, L. (1978). Comparative foraging behavior of six stingless bee species exploiting a standardized resource. *Ecology*, 59:1123–1136.

[Hudson, 2002] Hudson, R. R. (2002). Generating samples under a Wright–Fisher neutral model of genetic variation. *Bioinformatics*, 18:337–338.

[Hufford and Hamrick, 2003] Hufford, K. and Hamrick, J. (2003). Viability selection at three early life stages of the tropical tree, *Platypodium elegans* (Fabaceae, Papilionoideae). *Evolution*, 57:518–526.

[Hutchison and Templeton, 1999] Hutchison, D. W. and Templeton, A. R. (1999). Correlation of pairwise genetic and geographic distance measures: inferring the relative influences of gene flow and drift on the distribution of genetic variability. *Evolution*, 53:1898–1914.

[Ison et al., 2014] Ison, J., Wagenius, S., Reitz, D., and Ashley, M. (2014). Mating between *Echinacea angustifolia* (Asteraceae) individuals increases with their flowering synchrony and spatial proximity. *American Journal of Botany*, 101:180–189.

[Jaffé et al., 2015] Jaffé, R., Castilla, A., Pope, N., Imperatriz-Fonseca, V. L., Metzger, J. P., Arias, M. C., and Jha, S. (2015). Landscape genetics of a

tropical rescue pollinator. *Conservation Genetics*, 17:267–278.

[Jaffé et al., 2016] Jaffé, R., Pope, N., Acosta, A. L., Alves, D. A., Arias, M. C., De la Rúa, P., Francisco, F. O., Giannini, T. C., González-Chaves, A., Imperatriz-Fonseca, V. L., and Tavares, M. (2016). Beekeeping practices and geographic distance, not land use, drive gene flow across tropical bees. *Molecular Ecology*, 25:5345–5358.

[Jaffé et al., 2019] Jaffé, R., Veiga, J., Pope, N., Lanes, E., Carvalho, C., Alves, R., Andrade, S., Arias, M., Bonatti, V., Carvalho, A., Castro, M., Contrera, F., Francoy, T., Freitas, B., Giannini, T., Hrncir, M., Martins, C., Oliveira, G., Saraiva, A., Souza, B., and Imperatriz-Fonseca, V. (2019). Landscape genomics to the rescue of a tropical bee threatened by habitat loss and climate change. *Evolutionary Applications*, in press.

[Janzen, 1970] Janzen, D. (1970). Herbivores and the number of tree species in tropical forest. *American Naturalist*, 104:501–528.

[Jha, 2015] Jha, S. (2015). Contemporary human-altered landscapes and oceanic barriers reduce bumble bee gene flow. *Molecular Ecology*, 24:993–1006.

[Jha and Dick, 2008] Jha, S. and Dick, C. (2008). Shade coffee farms promote genetic diversity of native trees. *Current Biology*, 18:1126–1128.

[Jha and Dick, 2009] Jha, S. and Dick, C. (2009). Isolation and characterization of nine microsatellite loci for the tropical understory tree *Miconia affinis*

Wurdack (Melastomataceae). *Molecular Ecology Resources*, 9:344–345.

[Jha and Dick, 2010] Jha, S. and Dick, C. W. (2010). Native bees mediate long-distance pollen dispersal in a shade coffee landscape mosaic. *Proceedings of the National Academy of Sciences*, 107:13760–13764.

[Jha and Kremen, 2013] Jha, S. and Kremen, C. (2013). Bumble bee foraging in response to landscape heterogeneity. *Proceedings of the National Academy of Sciences*, 110:555–558.

[Jones and Comita, 2008] Jones, F. and Comita, L. (2008). Neighbourhood density and genetic relatedness interact to determine fruit set and abortion rates in a continuous tropical tree population. *Proceedings of the Royal Society B*, 275:2759–2767.

[Jong, 2000] Jong, T. (2000). From pollen dynamics to adaptive dynamics. *Plant Species Biology*, 15:31–41.

[Jordano, 1991] Jordano, P. (1991). Gender variation and expression of monoecy in *Juniperus phoenicea* (L.) (Cupressaceae). *Botanical Gazette*, 152:476–485.

[Joseph et al., 2016] Joseph, T., Hickerson, M., and Alvarado-Serrano, D. (2016). Demographic inference under a spatially continuous coalescent model. *Heredity*, 117:94.

[Jouganous et al., 2017] Jouganous, J., Long, W., Ragsdale, A. P., and Gravel, S. (2017). Inferring the joint demographic history of multiple populations: beyond the diffusion approximation. *Genetics*, 206:1549–1567.

[Kacelnik et al., 1986] Kacelnik, A., Houston, A., and Schmid-Hempel, P. (1986). Central-place foraging in honey bees: the effect of travel time and nectar flow on crop filling. *Behavioral Ecology and Sociobiology*, 19:19–24.

[Kalinowski, 2005] Kalinowski, S. T. (2005). HP-RARE 1.0: a computer program for performing rarefaction on measures of allelic richness. *Molecular Ecology Notes*, 5:187–189.

[Karron and Mitchell, 2012] Karron, J. and Mitchell, R. (2012). Effects of floral display size on male and female reproductive success in *Mimulus ringens*. *Annals of Botany*, 109:563–570.

[Keitt, 2009] Keitt, T. H. (2009). Habitat conversion, extinction thresholds, and pollination services in agroecosystems. *Ecological Applications*, 19:1561–1573.

[Kennedy et al., 2013] Kennedy, C. M., Lonsdorf, E., Neel, C. M., Williams, N. M., Ricketts, T. H., Winfree, R., and Bommarco, R. (2013). A global quantitative synthesis of local and landscape effects on native bee pollinators in agroecosystems. *Ecology Letters*, 16:584–599.

[Kimura, 1964] Kimura, M. (1964). Diffusion models in population genetics. *Journal of Applied Probability*, 1:177–232.

[Kleijn et al., 2015] Kleijn, D., Winfree, R., Bartomeus, I., Carvalheiro, L. G., Henry, M., Isaacs, R., Klein, A.-M., Kremen, C., M'gonigle, L. K., Rader, R., et al. (2015). Delivery of crop pollination services is an insufficient argument for wild pollinator conservation. *Nature Communications*, 6:7414.

[Klein et al., 2007] Klein, A. M., Vaissiere, B. E., Cane, J. H., Steffan-Dewenter, I., Cunningham, S. A., Kremen, C., and Tscharntke, T. (2007). Importance of pollinators in changing landscapes for world crops. *Proceedings of the Royal Society B*, 274:303–313.

[Klein and Randić, 1993] Klein, D. J. and Randić, M. (1993). Resistance distance. *Journal of Mathematical Chemistry*, 12:81–95.

[Klinkhamer and De Jong, 1997] Klinkhamer, P. and De Jong, TJ an Metz, H. (1997). Sex and size in cosexual plants. *Trends in Ecology and Evolution*, 12:260–265.

[Klinkhamer and de Jong, 1993] Klinkhamer, P. and de Jong, T. (1993). Attractiveness to pollinators: a plant's dilemma. *Oikos*, 66:180–184.

[Knight et al., 2005] Knight, M., Martin, A., Bishop, S., Osborne, J. L., Hale, R., Sanderson, R. A., and Goulson, D. (2005). An interspecific comparison of foraging range and nest density of four bumblebee (*Bombus*) species. *Molecular Ecology*, 14:1811–1820.

[Knight, 2003] Knight, T. (2003). Floral density, pollen limitation, and reproductive success in *Trillium grandiflorum*. *Oecologia*, 137:557–563.

[Korbecka et al., 2002] Korbecka, G., Klinkhamer, P., and Vrieling, K. (2002). Selective embryo abortion hypothesis revisited - a molecular approach. *Plant Biology*, 4:298–310.

[Korneliussen et al., 2014] Korneliussen, T. S., Albrechtsen, A., and Nielsen, R. (2014). ANGSD: Analysis of next generation sequencing data. *BMC Bioinformatics*, 15:356.

[Kotler and Blaustein, 1995] Kotler, B. P. and Blaustein, L. (1995). Titrating food and safety in a heterogeneous environment: when are the risky and safe patches of equal value? *Oikos*, 74:251–258.

[Kremen, 2005] Kremen, C. (2005). Managing ecosystem services: What do we need to know about their ecology? *Ecology Letters*, 8:468–479.

[Kremen et al., 2007] Kremen, C., Williams, N. M., Aizen, M. A., Gemmill-Herren, B., LeBuhn, G., Minckley, R., Packer, L., Potts, S. G., Roulston, T., Steffan-Dewenter, I., et al. (2007). Pollination and other ecosystem services produced by mobile organisms: A conceptual framework for the effects of land-use change. *Ecology Letters*, 10:299–314.

[Kremen et al., 2002] Kremen, C., Williams, N. M., and Thorp, R. (2002). Crop pollination from native bees at risk from agricultural intensification. *Proceedings of the National Academy of Sciences*, 99:16182–16816.

[Kunin, 1997] Kunin, W. (1997). Population size and density effects in pollination: pollinator foraging and plant reproductive success in experimental

arrays of *Brassica kaber*. *Journal of Ecology*, 85:225–234.

[Laca et al., 2010] Laca, E. A., Sokolow, S., Galli, J. R., and Cangiano, C. A. (2010). Allometry and spatial scales of foraging in mammalian herbivores. *Ecology Letters*, 13:311–320.

[Larsen et al., 2005] Larsen, T., Williams, N., and C, K. (2005). Extinction order and altered community structure rapidly disrupt ecosystem functioning. *Ecology Letters*, 8:538–547.

[Latouche-Hall et al., 2004] Latouche-Hall, C., Ramboer, A., Bandou, E., Caron, H., and Kremer, A. (2004). Long-distance pollen flow and tolerance to selfing in a neotropical tree species. *Molecular Ecology*, 13:1055–1064.

[Laurance et al., 2014] Laurance, W., Sayer, J., and Cassman, K. (2014). Agricultural expansion and its impacts on tropical nature. *Trends in Ecology and Evolution*, 29:107–116.

[Lavorel, 2013] Lavorel, S. (2013). Plant functional effects on ecosystem services. *Journal of Ecology*, 101:4–8.

[Le Roux and Wieczorek, 2008] Le Roux, J. and Wieczorek, A. (2008). Isolation and characterization of polymorphic microsatellite markers from the velvet tree, *Miconia calvescens* DC. (Melastomataceae). *Molecular Ecology Resources*, 8:961–964.

[Lee and Bazzaz, 1982] Lee, T. and Bazzaz, F. (1982). Regulation of fruit and seed production in an annual legume, *Cassia fasciculata*. *Ecology*, 63:1363–1373.

[Legendre and Fortin, 2010] Legendre, P. and Fortin, M.-J. (2010). Comparison of the Mantel test and alternative approaches for detecting complex multivariate relationships in the spatial analysis of genetic data. *Molecular Ecology Resources*, 10:831–844.

[Levin and Kerster, 1969] Levin, D. and Kerster, H. (1969). Density dependent gene dispersal in *Liatris*. *American Naturalist*, 103:61–74.

[Li, 2011] Li, H. (2011). A statistical framework for SNP calling, mutation discovery, association mapping and population genetical parameter estimation from sequencing data. *Bioinformatics*, 27:2987–2993.

[Li et al., 2009] Li, H., Handsaker, B., Wysoker, A., Fennell, T., Ruan, J., Homer, N., Marth, G., Abecasis, G., and Durbin, R. (2009). The sequence alignment/map format and SAMtools. *Bioinformatics*, 25:2078–2079.

[Liebhold and Bascompte, 2003] Liebhold, A. and Bascompte, J. (2003). The Allee effect, stochastic dynamics and the eradication of alien species. *Ecology Letters*, 6:133–140.

[Lihoreau et al., 2010] Lihoreau, M., Chittka, L., and Raine, N. (2010). Travel optimization by foraging bumblebees through re-adjustments of traplines after discovery of new feeding locations. *American Naturalist*, 176:744–757.

[Lihoreau et al., 2012] Lihoreau, M., Raine, N. E., Reynolds, A. M., Stelzer, R. J., Lim, K. S., Smith, A. D., Osborne, J. L., and Chittka, L. (2012). Radar tracking and motion-sensitive cameras on flowers reveal the development of pollinator multi-destination routes over large spatial scales. *PLoS Biology*, 10:e1001392.

[Lloyd and Bawa, 1984] Lloyd, D. and Bawa, K. (1984). Modification of the gender of seed plants in varying conditions. *Evolutionary Biology*, 17:255–338.

[Loiselle et al., 1995] Loiselle, B., Sork, V., Nason, J., and Graham, K. (1995). Spatial genetic structure of a neotropical understory shrub, *Psychotria officinalis*. *American Journal of Botany*, 82:1420–1425.

[Lonsdorf et al., 2009] Lonsdorf, E., Kremen, C., Ricketts, T., Winfree, R., Williams, N., and Greenleaf, S. (2009). Modelling pollination services across agricultural landscapes. *Annals of Botany*, 103:1589–1600.

[Luck and Daily, 2003] Luck, G. and Daily, G. (2003). Tropical countryside bird assemblages: richness, composition, and foraging differ by landscape context. *Ecological Applications*, 13:235–247.

[Mace et al., 2012] Mace, G., Norris, K., and Fitter, A. (2012). Biodiversity and ecosystem services: A multilayered relationship. *Trends in Ecology and Evolution*, 27:19–26.

[Makino et al., 2007] Makino, T., Ohashi, K., and Sakai, S. (2007). How do floral display size and the density of surrounding flowers influence the likelihood of bumble bee revisitation to a plant? *Functional Ecology*, 21:87–95.

[Marshall et al., 1998] Marshall, T., Slate, J., Kruuk, L., and Pemberton, J. (1998). Statistical confidence for likelihood-based paternity inference in natural populations. *Molecular Ecology*, 7:639–655.

[Mazer, 1992] Mazer, S. (1992). Environmental modifications of gender allocation in wild radish: consequences for sexual and natural selection. In Wyatt, R., editor, *Ecology and evolution of plant reproduction: new approaches*, pages 181–225. Chapman and Hall, New York.

[McNamara and Houston, 1997] McNamara, J. M. and Houston, A. I. (1997). Currencies for foraging based on energetic gain. *American Naturalist*, 150:603–617.

[McRae, 2006] McRae, B. H. (2006). Isolation by resistance. *Evolution*, 60:1551–1561.

[McRae and Beier, 2007] McRae, B. H. and Beier, P. (2007). Circuit theory predicts gene flow in plant and animal populations. *Proceedings of the National Academy of Sciences*, 104:19885–19890.

[McRae et al., 2008] McRae, B. H., Dickson, B. G., Keitt, T. H., and Shah,

V. B. (2008). Using circuit theory to model connectivity in ecology, evolution, and conservation. *Ecology*, 89:2712–2724.

[McVean and Cardin, 2005] McVean, G. A. and Cardin, N. J. (2005). Approximating the coalescent with recombination. *Philosophical Transactions of the Royal Society B*, 360:1387–1393.

[Mead, 1965] Mead, R. (1965). A generalised logit-normal distribution. *Biometrics*, 21:721–732.

[Memmott et al., 2007] Memmott, J., Craze, P. G., Waser, N. M., and Price, M. V. (2007). Global warming and the disruption of plant-pollinator interactions. *Ecology Letters*, 10:710–717.

[Memmott et al., 2004] Memmott, J., Waser, N. M., and Price, M. V. (2004). Tolerance of pollination networks to species extinctions. *Proceedings of the Royal Society B*, 271:2605–2611.

[Michener, 2000] Michener, C. D. (2000). *The bees of the world*, volume 1. JHU Press, Baltimore.

[Miller et al., 2005] Miller, C. R., Joyce, P., and Waits, L. P. (2005). A new method for estimating the size of small populations from genetic mark-recapture data. *Molecular Ecology*, 14:1991–2005.

[Moorcroft, 2012] Moorcroft, P. R. (2012). Mechanistic approaches to understanding and predicting mammalian space use: recent advances, future directions. *Journal of Mammalogy*, 93:903–916.

[Moorcroft and Barnett, 2008] Moorcroft, P. R. and Barnett, A. (2008). Mechanistic home range models and resource selection analysis: a reconciliation and unification. *Ecology*, 89:1112–1119.

[Morellet et al., 2013] Morellet, C., Bonenfant, L., Börger, F., Ossi, F., Cagnacci, M., Heurich, P., and Kjellander (2013). Seasonality, weather and climate affect home range size in roe deer across a wide latitudinal gradient within Europe. *Journal of Animal Ecology*, 82:1326–1339.

[Mugabo et al., 2014] Mugabo, M., Perret, B., Meylan, S., and Le Galliard, J. (2014). Density-dependent immunity and parasitism risk in experimental populations of lizards naturally infested by ixodid ticks. *Ecology*, 96:450–460.

[Nason et al., 1996] Nason, J., Herre, E., and Hamrick, J. (1996). Paternity analysis of the breeding structure of strangler fig populations: Evidence for substantial long-distance wasp dispersal. *Journal of Biogeography*, 23:501–512.

[Ne'eman et al., 2010] Ne'eman, G., Jurgens, A., Newstrom-Lloyd, L., Potts, S., and Dafni, A. (2010). A framework for comparing pollinator performance: Effectiveness and efficiency. *Biological Reviews*, 85:435–451.

[Nei and Kumar, 2000] Nei, M. and Kumar, S. (2000). *Molecular evolution and phylogenetics*. Oxford University Press, Oxford.

[Nelson and Demas, 1996] Nelson, R. J. and Demas, G. E. (1996). Seasonal changes in immune function. *Quarterly Review of Biology*, 71:511–548.

[Nielsen et al., 2012] Nielsen, R., Korneliussen, T., Albrechtsen, A., Li, Y., and Wang, J. (2012). SNP calling, genotype calling, and sample allele frequency estimation from new-generation sequencing data. *PloS One*, 7:e37558.

[Obeso and Herrera, 1994] Obeso, J. and Herrera, C. (1994). Inter- and intraspecific variation in fruit traits in co-occurring vertebrate-dispersed plants. *International Journal of Plant Sciences*, 155:382–387.

[O'Connell et al., 2006] O'Connell, O., Mosseler, L., and Rajora, A. (2006). Impacts of forest fragmentation on the mating system and genetic diversity of white spruce (*Picea glauca*) at the landscape level. *Heredity*, 97:418–426.

[Ohashi et al., 2007] Ohashi, K., Thomson, J., and D'Souza, D. (2007). Trapline foraging by bumble bees: IV. optimization of route geometry in the absence of competition. *Behavioral Ecology*, 18:1–11.

[Ollerton et al., 2011] Ollerton, J., Winfree, R., and Tarrant, S. (2011). How many flowering plants are pollinated by animals. *Oikos*, 120:321–326.

[Osborne et al., 1999] Osborne, J., Clark, S., Morris, R., Williams, I., Riley, J., Smith, A., Reynolds, D., and Edwards, A. (1999). A landscape-scale study of bumble bee foraging range and constancy, using harmonic radar. *Journal of Applied Ecology*, 36:519–533.

[Osborne et al., 2008] Osborne, J. L., Martin, A. P., Carreck, N. L., Swain, J. L., Knight, M. E., Goulson, D., Hale, R. J., and Sanderson, R. A. (2008). Bumblebee flight distances in relation to the forage landscape. *Journal of Animal Ecology*, 77:406–415.

[Parmenter et al., 2003] Parmenter, R. R., Yates, T. L., Anderson, D. R., Burnham, K. P., Dunnum, J. L., Franklin, A. B., Friggens, M. T., Lubow, B. C., Miller, M., Olson, G. S., et al. (2003). Small-mammal density estimation: a field comparison of grid-based vs. web-based density estimators. *Ecological Monographs*, 73:1–26.

[Peakall and Smouse, 2012] Peakall, R. and Smouse, P. (2012). GENALEX 6.5: genetic analysis in Excel. population genetic software for teaching and research - an update. *Bioinformatics*, 28:2537–2539.

[Pearson and Ruggiero, 2003] Pearson, D. E. and Ruggiero, L. F. (2003). Transect versus grid trapping arrangements for sampling small-mammal communities. *Wildlife Society Bulletin*, 31:454–459.

[Perez-Mendez et al., 2015] Perez-Mendez, N., Jordano, P., and Valido, A. (2015). Downsized mutualisms: Consequences of seed dispersers' body-size reduction for early plant recruitment. *Perspectives in Plant Ecology, Evolution and Systematics*, 17:151–159.

[Peterman et al., 2014] Peterman, W. E., Connette, G. M., Semlitsch, R. D., and Eggert, L. S. (2014). Ecological resistance surfaces predict fine-scale

genetic differentiation in a terrestrial woodland salamander. *Molecular Ecology*, 23:2402–2413.

[Peters, 2003] Peters, H. (2003). Neighbourhood-regulated mortality: the influence of positive and negative density dependence on tree populations in species-rich tropical forests. *Ecology Letters*, 6:757–765.

[Philpott, 2009] Philpott, S. (2009). Functional richness and ecosystem services: bird predation on arthropods in tropical agroecosystems. *Ecological Applications*, 19:1858–1867.

[Pirotte et al., 2007] Pirotte, A., Renders, J.-M., Saerens, M., et al. (2007). Random-walk computation of similarities between nodes of a graph with application to collaborative recommendation. *IEEE Transactions on Knowledge and Data Engineering*, 3:355–369.

[Plummer, 2003] Plummer, M. (2003). Jags: A program for analysis of bayesian graphical models using gibbs sampling. In *Proceedings of the 3rd International Workshop on Distributed Statistical Computing*, volume 124.

[Pollinator Health Task Force, 2015] Pollinator Health Task Force (2015). *National strategy to promote the health of honey bees and other pollinators*. The White House.

[Pope and Jha, 2017] Pope, N. S. and Jha, S. (2017). Inferring the foraging

ranges of social bees from sibling genotypes sampled across discrete locations. *Conservation Genetics*, 18:645–658.

[Pope and Jha, 2018] Pope, N. S. and Jha, S. (2018). Seasonal food scarcity prompts long-distance foraging by a wild social bee. *American Naturalist*, 191:45–57.

[Pothen et al., 1990] Pothen, A., Simon, H. D., and Liou, K.-P. (1990). Partitioning sparse matrices with eigenvectors of graphs. *SIAM Journal on Matrix Analysis and Applications*, 11:430–452.

[Prỳs-Jones and Corbet, 1991] Prỳs-Jones, O. and Corbet, S. (1991). *Bumblebees*. Slough: The Richmond Publishing Co., Slough.

[R Development Core Team, 2011] R Development Core Team (2011). R: A language and environment for statistical computing.

[Raine and Chittka, 2008] Raine, N. E. and Chittka, L. (2008). The correlation of learning speed and natural foraging success in bumble-bees. *Proceedings of the Royal Society B*, 275:803–808.

[Rao and Strange, 2012] Rao, S. and Strange, J. P. (2012). Bumble bee (Hymenoptera: Apidae) foraging distance and colony density associated with a late-season mass flowering crop. *Environmental Entomology*, 41:905–915.

[Rathcke and Lacey, 1985] Rathcke, B. and Lacey, E. P. (1985). Phenological patterns of terrestrial plants. *Annual Review of Ecology and Systematics*, 16:179–214.

[Raubenheimer and Simpson, 2012] Raubenheimer, S. J. and Simpson, Tait, A. H. (2012). Match-mismatch: Conservation physiology, nutritional ecology, and the timescales of biological adaptation. *Philosophical Transactions of the Royal Society B*, 367:1628–1646.

[Ray et al., 2010] Ray, N., Currat, M., Foll, M., and Excoffier, L. (2010). SPLATCHE2: a spatially explicit simulation framework for complex demography, genetic admixture and recombination. *Bioinformatics*, 26:2993–2994.

[Raymond and Rousset, 1995] Raymond, M. and Rousset, F. (1995). GENEPOP version 1.2: a population genetics software for exact test and ecumenicism. *Journal of Heredity*, 86:248–249.

[Redhead et al., 2016] Redhead, J. W., Dreier, S., Bourke, A. G. H., Heard, M. S., Jordan, W. C., Sumner, S., Wang, J., and Carvell, C. (2016). Effects of habitat composition and landscape structure on worker foraging distances of five bumblebee species. *Ecological Applications*, 26:726–739.

[Reiss, 1988] Reiss, M. (1988). Scaling of home range size: Body size, metabolic needs and ecology. *Trends in Ecology and Evolution*, 3:85–86.

[Richards, 2000] Richards, M. H. (2000). Evidence for geographic variation in colony social organization in an obligately social sweat bee, *Lasioglossum malachurum* Kirby (Hymenoptera: Halictidae). *Canadian Journal of Zoology*, 78:1259–1266.

[Ritland, 2002] Ritland, K. (2002). Extensions of models for the estimation of mating systems using N independent loci. *Heredity*, 88:221–228.

[Robertson et al., 1999] Robertson, A. W., Mountjoy, C., Faulkner, B. E., Roberts, M. V., and Macnair, M. R. (1999). Bumble bee selection of *Mimulus guttatus* flowers: the effects of pollen quality and reward depletion. *Ecology*, 80:2594–2606.

[Rodriguez and Hawkins, 2000] Rodriguez, M. and Hawkins, B. (2000). Diversity, function and stability in parasitoid communities. *Ecology Letters*, 3:35–40.

[Roubik and Aluja, 1983] Roubik, D. and Aluja, M. (1983). Flight ranges of *Melipona* and *Trigona* in tropical forest. *Journal of the Kansas Entomological Society*, 56:217–222.

[Roubik and Wolda, 2001] Roubik, D. and Wolda, H. (2001). Do competing honey bees matter? dynamics and abundance of native bees before and after honey bee invasion. *Population Ecology*, 43:53–62.

[Royle et al., 2009] Royle, J., Karanth, K., Gopalaswamy, A., and Kumar, N. (2009). Bayesian inference in camera trapping studies for a class of spatial capturerecapture models. *Ecology*, 90:3233–3244.

[Royle et al., 2013a] Royle, J. A., Chandler, R. B., Gazenski, K. D., and Graves, T. A. (2013a). Spatial capture-recapture models for jointly estimating population density and landscape connectivity. *Ecology*, 94:287–294.

[Royle et al., 2013b] Royle, J. A., Chandler, R. B., Sollmann, R., and Gardner, B. (2013b). *Spatial capture-recapture*. Academic Press, Cambridge.

[Rue et al., 2009] Rue, H., Martino, S., and Chopin, N. (2009). Approximate Bayesian inference for latent Gaussian models by using integrated nested Laplace approximations. *Journal of the Royal Statistical Society B*, 71:319–392.

[Sahli and Conner, 2007] Sahli, H. and Conner, J. (2007). Visitation, effectiveness, and efficiency of 15 genera of visitors to wild radish, *Raphanus raphanistrum* (Brassicaceae). *American Journal of Botany*, 94:203–209.

[Sala et al., 2000] Sala, O., Chapin, F., and Armesto, J. (2000). Global biodiversity scenarios for the year 2100. *Science*, 287:1770–1774.

[Savolainen et al., 2013] Savolainen, O., Lascoux, M., and Merilä, J. (2013). Ecological genomics of local adaptation. *Nature Reviews Genetics*, 14:807.

[Schaal, 1978] Schaal, B. (1978). Density dependent foraging on *Liatris pycnostachya*. *Evolution*, 32:452–454.

[Schlather et al., 2015] Schlather, M., Malinowski, A., Menck, P. J., Oesting, M., and Strokorb, K. (2015). Analysis, simulation and prediction of multivariate random fields with package randomfields. *Journal of Statistical Software*, 63:1–25.

[Schmid-Hempel and Schmid-Hempel, 1990] Schmid-Hempel, P. and Schmid-Hempel, R. (1990). Endoparastic larvae of conopid flies alter pollination behavior of bumble bees. *Naturwissenschaften*, 77:450–452.

[Shirk et al., 2010] Shirk, A., Wallin, D., Cushman, S., Rice, C., and Warheit, K. (2010). Inferring landscape effects on gene flow: a new model selection framework. *Molecular Ecology*, 19:3603–3619.

[Shirk et al., 2018] Shirk, A. J., Landguth, E. L., and Cushman, S. A. (2018). A comparison of regression methods for model selection in individual-based landscape genetic analysis. *Molecular Ecology Resources*, 18:55–67.

[Siffczyk et al., 2003] Siffczyk, C., Brotons, L., Kangas, K., and Orell, M. (2003). Home range size of willow tits: a response to winter habitat loss. *Oecologia*, 136:635–642.

[Slaa et al., 2003] Slaa, E., Wassenberg, J., and Biesmeijer, J. (2003). The use of field-based social information in eusocial foragers: local enhancement among nestmates and heterospecifics in stingless bees. *Ecological Entomology*, 28:369–379.

[Solis-Montero et al., 2015] Solis-Montero, L., Vergara, C., and Vallejo-Marin, M. (2015). High incidence of pollen theft in natural populations of a buzz-pollinated plant. *Arthropod-Plant Interactions*, 9:599–611.

[Sork et al., 1999] Sork, V. L., Nason, J., Campbell, D. R., and Fernandez, J. F. (1999). Landscape approaches to historical and contemporary gene

flow in plants. *Trends in Ecology and Evolution*, 14:219–224.

[Souto et al., 2002] Souto, C., Aizen, M., and Premoli, A. (2002). Effects of crossing distance and genetic relatedness on pollen performance in *Alstroemeria aurea* (Alstroemeriaceae). *American Journal of Botany*, 89:427–432.

[Spear et al., 2010] Spear, S. F., Balkenhol, N., Fortin, M.-J., McRae, B. H., and Scribner, K. (2010). Use of resistance surfaces for landscape genetic studies: considerations for parameterization and analysis. *Molecular Ecology*, 19:3576–3591.

[Srivastava and Vellend, 2005] Srivastava, D. and Vellend, M. (2005). Biodiversity-ecosystem function research: Is it relevant to conservation? *Annual Review of Ecology Evolution and Systematics*, 36:267–294.

[Stacy et al., 1996] Stacy, E., Hamrick, J., Nason, J., Hubbell, S., Foster, R., and Condit, R. (1996). Pollen dispersal in low-density populations of three neotropical tree species. *American Naturalist*, 148:275–298.

[Steffan-Dewenter et al., 2002] Steffan-Dewenter, I., Münzenberg, U., Bürger, C., Thies, C., and Tscharntke, T. (2002). Scale-dependent effects of landscape context on three pollinator guilds. *Ecology*, 83:1421–1432.

[Steinbeiss et al., 2008] Steinbeiss, S., Beßler, H., Engels, C., Temperton, V. M., Buchmann, N., Roscher, C., Kreutziger, Y., Baade, J., Habekost, M., and Gleixner, G. (2008). Plant diversity positively affects short-term soil carbon storage in experimental grasslands. *Global Change Biology*, 14:2937–2949.

[Stephens and Charnov, 1982] Stephens, D. W. and Charnov, E. L. (1982). Optimal foraging: some simple stochastic models. *Behavioral Ecology and Sociobiology*, 10:251–263.

[Stephens and Krebs, 1986] Stephens, D. W. and Krebs, J. R. (1986). *Foraging theory*. Princeton University Press, Princeton.

[Stephens et al., 1999] Stephens, P., Sutherland, W., and Freckleton, R. (1999). What is the Allee effect? *Oikos*, 87:185–190.

[Stolle et al., 2009] Stolle, E., Rohde, M., Vautrin, D., Solignac, M., Schmid-Hempel, P., Schmid-Hempel, R., and Moritz, R. F. A. (2009). Novel microsatellite DNA loci for *Bombus terrestris* (Linnaeus 1758). *Molecular Ecology Resources*, 9:1345–1352.

[Stolle et al., 2011] Stolle, E., Wilfert, L., Schmid-Hempel, R., Schmid-Hempel, P., Kube, M., Reinhardt, R., and Moritz, R. F. A. (2011). A second generation genetic map of the bumblebee *Bombus terrestris* (Linnaeus 1758) reveals slow genome chromosome evolution in the Apidae. *BMC Genomics*, 12:48.

[Stout, 2000] Stout, J. (2000). Does size matter? Bumblebee behaviour and the pollination of *Cytisus scoparius* L. (Fabaceae). *Apidologie*, 31:129–139.

[Sun et al., 2014] Sun, C. C., Fuller, A. K., and Royle, J. A. (2014). Trap configuration and spacing influences parameter estimates in spatial capture-recapture models. *PloS One*, 9:e88025.

[Tani et al., 2012] Tani, N., Tsumura, Y., and Fukasawa, K. (2012). Male fecundity and pollen dispersal in hill dipterocarps: significance of mass synchronized flowering and implications for conservation. *Journal of Ecology*, 100:405–415.

[Tepedino et al., 1999] Tepedino, V., Sipes, S., and Griswold, T. (1999). The reproductive biology and effective pollinators of the endangered beardtongue *Penstemon penlandii* (Scrophulariaceae). *Plant Systematics and Evolution*, 219:39–54.

[Thomson and Eisenhart, 2003] Thomson, J. and Eisenhart, K. (2003). Rescue of stranded pollen grains by secondary transfer. *Plant Species Biology*, 18:67–74.

[Tierney and Kadane, 1986] Tierney, L. and Kadane, J. B. (1986). Accurate approximations for posterior moments and marginal densities. *Journal of the American Statistical Association*, 81:82–86.

[Urban and Keitt, 2001] Urban, D. and Keitt, T. (2001). Landscape connectivity: a graph-theoretic perspective. *Ecology*, 82:1205–1218.

[Urban et al., 2009] Urban, D. L., Minor, E. S., Treml, E. A., and Schick, R. S. (2009). Graph models of habitat mosaics. *Ecology Letters*, 12:260–273.

[Utsumi et al., 2009] Utsumi, S. A., Cangiano, C. A., Galli, J. R., M. B. McEachern, M. W., Demment, E. A., and Laca (2009). Resource heterogeneity and foraging behaviour of cattle across spatial scales. *BMC Ecology*, 9:9.

[Van Oosterhout et al., 2004] Van Oosterhout, C., Hutchinson, W., Wills, D., and Shipley, P. (2004). MICROCHECKER: software for identifying and correcting genotyping errors in microsatellite data. *Molecular Ecology Notes*, 4:535–538.

[van Oosterhout et al., 2006] van Oosterhout, C., Weetman, D., and Hutchinson, W. F. (2006). Estimation and adjustment of microsatellite null alleles in nonequilibrium populations. *Molecular Ecology Notes*, 6:255–256.

[Vekemans and Hardy, 2004] Vekemans, X. and Hardy, O. (2004). New insights from fine-scale spatial genetic structure analyses in plant populations. *Molecular Ecology*, 13:921–935.

[Villeger et al., 2008] Villeger, S., Mason, N., and Mouillot, D. (2008). New multidimensional functional diversity indices for a multifaceted framework in functional ecology. *Ecology*, 89:2290–2301.

[Visscher and Seeley, 1982] Visscher, P. K. and Seeley, T. D. (1982). Foraging strategy of honeybee colonies in a temperate deciduous forest. *Ecology*, 63:1790–1801.

[Vivarelli et al., 2011] Vivarelli, D., Petanidou, T., Nielsen, A., and Cristofolini, G. (2011). Small-size bees reduce male fitness of the flowers of *Ononis masquillierii* (Fabaceae), a rare endemic plant in the northern Apennines. *Botanical Journal of the Linnean Society*, 165:267–277.

[Waal et al., 2014] Waal, C., Anderson, B., and Ellis, A. (2014). Relative density and dispersion pattern of two southern African Asteraceae affect fecundity through heterospecific interference and mate availability, not pollinator visitation rate. *Journal of Ecology*, 103:513–525.

[Wagenius, 2006] Wagenius, S. (2006). Scale dependence of reproductive failure in fragmented *Echinacea* populations. *Ecology*, 87:931–941.

[Wagenius et al., 2010] Wagenius, S., Hangelbroek, H., Ridley, C., and Shaw, R. (2010). Biparental inbreeding and interremnant mating in a perennial prairie plant: Fitness consequences for progeny in their first eight years. *Evolution*, 64:761–771.

[Waites, 2004] Waites, A. (2004). Pollinator visitation, stigmatic pollen loads and among-population variation in seed set in *Lythrum salicaria*. *Journal of Ecology*, 92:512–526.

[Wang, 2004] Wang, J. L. (2004). Sibship reconstruction from genetic data with typing errors. *Genetics*, 166:1963–1979.

[Waters et al., 2013] Waters, J., Fraser, C., and Hewitt, G. (2013). Founder takes all: density-dependent processes structure biodiversity. *Trends in Ecology and Evolution*, 28:78–85.

[Westphal et al., 2006] Westphal, C., I., T., and Tscharntke (2006). Foraging trip duration of bumblebees in relation to landscape-wide resource availability. *Ecological Entomology*, 31:389–394.

[Williams et al., 2012] Williams, N. M., Regetz, J., and Kremen, C. (2012). Landscape-scale resources promote colony growth but not reproductive performance of bumble bees. *Ecology*, 93:1049–1058.

[Worton, 1987] Worton, B. (1987). A review of models of home range for animal movement. *Ecological Modelling*, 38:277–298.

[Wright, 2002] Wright, J. (2002). Plant diversity in tropical forests: a review of mechanisms of species coexistence. *Oecologia*, 130:1–14.

[Wright and Barrett, 1999] Wright, S. and Barrett, S. (1999). Size-dependent gender modification in a hermaphroditic perennial herb. *Proceedings of the Royal Society B*, 266:225–232.

[Zeller et al., 2016] Zeller, K. A., Creech, T. G., Millette, K. L., Crowhurst, R. S., Long, R. A., Wagner, H. H., Balkenhol, N., and Landguth, E. L. (2016). Using simulations to evaluate Mantel-based methods for assessing landscape resistance to gene flow. *Ecology and Evolution*, 12:4115–4128.

[Zeller et al., 2012] Zeller, K. A., McGarigal, K., and Whiteley, A. R. (2012). Estimating landscape resistance to movement: a review. *Landscape Ecology*, 27:777–797.

[Zhao and Lu, 2009] Zhao, R. and Lu, B. (2009). Fine-scale genetic structure enhances biparental inbreeding by promoting mating events between more related individuals in wild soybean (*Glycine soja*; Fabaceae) populations. *American Journal of Botany*, 96:1138–1147.

[Zurbuchen et al., 2010a] Zurbuchen, A., Cheesman, S., Klaiber, J., Muller, A., Hein, S., and Dorn, S. (2010a). Long foraging distances impose high costs on offspring production in solitary bees. *Journal of Animal Ecology*, 79:674–681.

[Zurbuchen et al., 2010b] Zurbuchen, A., Landert, L., Klaiber, J., Müller, A., Hein, S., and Dorn, S. (2010b). Maximum foraging ranges in solitary bees: only few individuals have the capability to cover long foraging distances. *Biological Conservation*, 143:669–676.